THE UNIVERSITY OF CHICAGO

FUNCTIONAL EVOLUTION OF A MORPHOGENETIC GRADIENT

A DISSERTATION SUBMITTED TO

THE FACULTY OF THE DIVISION OF THE BIOLOGICAL SCIENCES

AND THE PRITZKER SCHOOL OF MEDICINE

IN CANDIDACY FOR THE DEGREE OF

DOCTOR OF PHILOSOPHY

DEPARTMENT OF ORGANISMAL BIOLOGY AND ANATOMY

BY

CHUN WAI KWAN

CHICAGO, ILLINOIS

MARCH 2017

Table of Contents

List of Figures

Abstract[1]

Bone Morphogenetic Proteins (BMPs) pattern the dorsal-ventral axis of bilaterian embryos; however, their roles in the evolution of body plan are largely unknown. We examined their functional evolution in fly embryos. BMP signaling specifies two extraembryonic tissues, the serosa and amnion, in basal-branching flies such as *Megaselia abdita*, but only one, the amnioserosa, in *Drosophila melanogaster*. The BMP signaling dynamics are similar in both species until the beginning of gastrulation, when BMP signaling broadens and intensifies at the edge of the germ rudiment in Megaselia, while remaining static in Drosophila. Here we show that the differences in gradient dynamics and tissue specification result from evolutionary changes in the gene regulatory network that controls the activity of a positive feedback circuit on BMP signaling, involving the *tumor necrosis factor alpha* homolog *eiger*. These data illustrate an evolutionary mechanism by which spatiotemporal changes in morphogen gradients can guide tissue complexity.

[1] Parts of the work presented here are modified from the paper: Kwan, C.W., Gavin-Smyth, J., Ferguson, E.L. and Schmidt-Ott, U. (2016). Functional evolution of a morphogenetic gradient. eLife *5*, e20894.

Acknowledgements

I would like to take this opportunity to thank all of those who had supported and helped me during the six years of my PhD research. First of all, I would like to express my gratitude to Dr. Urs Schmidt-Ott. He is an outstanding scientist and supervisor. During my study, he has given me many valuable and insightful opinions and taught me much about research. He has substantially helped me in overcoming the numerous hurdles that I encountered during research. Secondly, I would to thank CheeHyurng Park and Matteen Rafiqi for their patient guidance. They have taught me how to work with *Megaselia abdita* and helped me tremendously in mastering the necessary techniques in my projects. A special thanks to my collaborators, Edwin Ferguson and Jackie Gavin-Symth, who provide helpful comments and teach me a lot in doing quantification experiments. This thesis would not be possible without them.

Also, I would like to thank the University and my supervisor for providing the generous financial support for my projects and also thank the members of my dissertation committee, Dr. Manyuan Long, Dr. Robert Ho, and Dr. Edwin Ferguson who have helped to oversee my project. Furthermore, I like to express my gratitude to the former and current staff in the Darwinian Sciences Cluster, especially Audrey Aronowsky and Alison Anastasio, who help me a lot in dealing with the administration.

I would also like to give thanks to all my former and current lab mates, including Steffen Lemke, Mijung Kim, Jeff Klomp, Derek Athy, and Yoseop Yoon for their support and advice during these six years of my study. The life of PhD can sometimes be a daunting and frustrating experience, but this lab has provided a warm and friendly atmosphere for me to accomplish this project. I am really grateful to all my colleagues for their support.

1) Introduction

1.1) Morphogenetic gradient

An important question in developmental biology is how the embryo is patterned, and how identical cells are specified in different parts of the embryo over time to become distinctive morphological structures. The mechanism of patterning, in turn, is important to understand evolution as morphologies evolve through changing the patterning mechanism. Two major theories have been proposed to address the problem of patterning. One theory proposes that patterning is achieved by positional information carried by the concentration gradient of a chemical that acts on a field within which cells have their positional information specified with respect to the same set of reference points. Known as the French flag model proposed by Lewis Wolpert (Wolpert, 1968, 1969, 1971), it states that patterning occurs by a two-step process: initially, a chemical diffuses from a source over a field of cells toward a "sink" to establish a concentration gradient that provides positional information. Secondly, this gradient is interpreted by cells in the field, which adopt different fates according to the chemical concentration. Another model is the reaction-diffusion (RD) model proposed by Alan Turing, published in a landmark paper in 1952, entitled 'The chemical basis of morphogenesis " (Turing, 1952), in which Turing coined the term "morphogen" to indicate chemical substances that diffuse between cells and induce specific responses at different concentrations. In his model, different morphogens diffuse and react with each other in a concentration-dependent manner to break symmetry in a homogenous cell field subjected only to minor random fluctuations. Turing was able to show that such "reaction-diffusion" (RD) systems can converge to six different stable states, including oscillations, travelling waves and spatial patterns (reviewed by Kondo and Miura,

2010; Turing, 1952). Unlike Wolpert's model, which gained wide popularity initially due to its conceptual simplicity, Turing's model was largely ignored. Its revival began in the 1970s with the work of Gierer and Meinhardt (Gierer and Meinhardt, 1972), which shows that self-organized patterns can be formed by RD models composed of a short-range self-enhancing activator and a long-range inhibitor. As later shown by others (Marcon et al., 2016), modified RD networks do not necessarily require differential diffusivity of the activator and inhibitor to generate stable pattern. RD networks have been used to describe different biological systems including spacing of nitrogen fixing heterocysts in filamentous bacteria (Callahan and Buikema, 2001; Huang et al., 2004; Risser and Callahan, 2009; Yoon and Golden, 1998), the hair follicles and feather buds in the skin of mammals and birds, respectively (Harris et al., 2005; Michon et al., 2008; Mou et al., 2006; Painter et al., 2012; Sick et al., 2006; Zhang et al., 2009), the pigment pattern in the skin of zebrafish (Hamada et al., 2014; Inaba et al., 2012; Nakamasu et al., 2009; Yamanaka and Kondo, 2014), germ layer specification in zebrafish (Chen and Schier, 2002; Müller et al., 2012; Schier, 2009), left-right patterning in mouse (Nakamura et al., 2006; Shiratori and Hamada, 2006), palatal ridges of mammals (Economou et al., 2012) and patterning of digits in limb buds (Newman and Frisch, 1979; Raspopovic et al., 2014; Sheth et al., 2012). These studies serve as examples of how RD models can produce complex pattern during development.

The French flag model and RD model are different in several aspects. In the French flag model, morphogens do not interact and as a result, morphogen gradients are static, while in the RD model, morphogens interact with each other and can produce dynamic gradients in space and time. The French flag model also presupposes an initial source of asymmetry, namely the source from which a morphogen diffuses, while the RD model does

not make such presupposition and is more concerned with breaking symmetry in an initially uniform environment.

In terms of evolution, these two theories have different implications. In the French flag model, since the morphogen gradient is static, evolution occurs through change in the threshold response of the target cells. For example, through increasing or decreasing the sensitivity of threshold responses of target cells, tissue boundaries can be altered. In contrast, morphogen gradients in the RD model are dynamic and the resulting patterns can be altered through changing model parameters such as strengths and types of interactions between morphogens, diffusion rates, boundary conditions, etc. Thus, RD models suggest that change in the dynamic of morphogen gradients can guide morphological evolution. While this mechanism is theoretically possible, there is only limited direct experimental evidence for the role of morphogen gradient dynamics in leading evolutionary change. For example, the tube-like structures (called dorsal appendages) in the eggshells of various Drosophila species differs considerably in position, shape and number, and their diversification has been correlated with the spatial patterns of Bone Morphogenetic Protein (BMP) signaling, which are attributed to the expression pattern of BMP receptors in different species (Niepielko et al., 2011, 2012). Another example is the evolution of beak shape in Darwin's finches. Darwin's finches different in beak size and shape; the beak length for example correlating with the level of BMP gene expression (Abzhanov et al., 2004). While these studies suggest a direct role of BMP signaling in guiding morphological evolution, they did not measure the BMP signaling gradient and did not provide evidence that change in the shape or dynamic of the BMP gradient can guide the evolution of morphology and tissue complexity. Thus, it has remained unclear whether evolving

morphogen gradient dynamics can guide morphological evolution and if that is the case, what kind of mechanisms are responsible for altering the gradient dynamics.

To address these questions, I have functionally compared the embryonic BMP gradients of two fly species, *Megaselia abdita* and *Drosophila melanogaster*. My main goal has been to understand how these two species specify distinct extraembryonic tissue complements downstream of BMP signaling. The result of this study provides general insight into how a morphogen gradient can guide morphological evolution and tissue complexity. In the reminder of this introduction, I provide the context in which I conducted this study, namely, a brief summary of BMP signaling in *Drosophila melanogaster* and how it patterns the extaembryonic tissue (part 1.2), the evolution and function of extraembryonic tissue (part 1.3), and features of my experimental system, *Megaselia abdita* (part 1.4), and introduce different hypothetical models of BMP–dependent extraembryonic tissue specification in *Megaselia abdita* (part 1.5).

1.2) BMP signaling in Drosophila as a model for morphogen gradients

BMP belongs to the Transforming Growth Factor beta (TGF-β) family of signaling molecules, and has morphogen properties such as spatially restricted expression, long-range activity and ability to activate genes at different thresholds (Ferguson and Anderson, 1992; Lecuit et al., 1996; Nellen et al., 1996). BMP signaling has been shown to be involved in various developmental processes in Drosophila such as the maintenance of the germline stem cell niche (Casanueva and Ferguson, 2004; Kawase et al., 2004; Xie and Spradling, 1998, 2000), size control of the hematopoietic niche (Pennetier et al., 2012) and determining cell identity during regeneration of gastrointestinal tract (Li et al., 2013). Two

of the most thoroughly studied models in Drosophila are 1) the BMP gradient in the wing imaginal disc during larval development and 2) the BMP gradient in the dorsal ectoderm of the early embryo. These models have provided important insight into how morphogen gradients form and function. Below, I will discuss these two systems with special focus on amnioserosa specification.

1.2.1) Wing discs patterning in Drosophila by BMP signaling

The wing imaginal disc is an epithelial organ that grows during the larval stage and becomes the adult wing after metamorphosis. BMP signaling is important in patterning the wing imaginal disc by forming a morphogen gradient along the anterior-posterior axis (**Fig. 1.1**). The BMP ligand *decapentaplegic* (*dpp*) is secreted anterior to the boundary between anterior and posterior compartments of the wing discs and disperses to form a concentration gradient along the anterior-posterior axis. One important function of *dpp* is to repress the expression of the transcriptional repressor *brinker* (*brk*), which forms an opposing concentration gradient to *dpp* (Campbell and Tomlinson, 1999; Jazwinska et al., 1999; Minami et al., 1999). These two opposing gradients of *dpp* and *brk* then regulate a nested expression of target genes including *spalt* (*sal*) and *optomotor-blind* (*omb*), which patterns the wing disc and determines the location of the wing veins along the anterior-posterior axis. In addition to patterning, experiments also show that BMP signaling is important in regulating the size of the wing disc (Burke and Basler, 1996; Zecca et al., 1995); in *dpp* mutant clones, wing disc cells are reduced while ectopic expression of *dpp* induces cell proliferation in wing disc. Thus, the wing disc is an important model

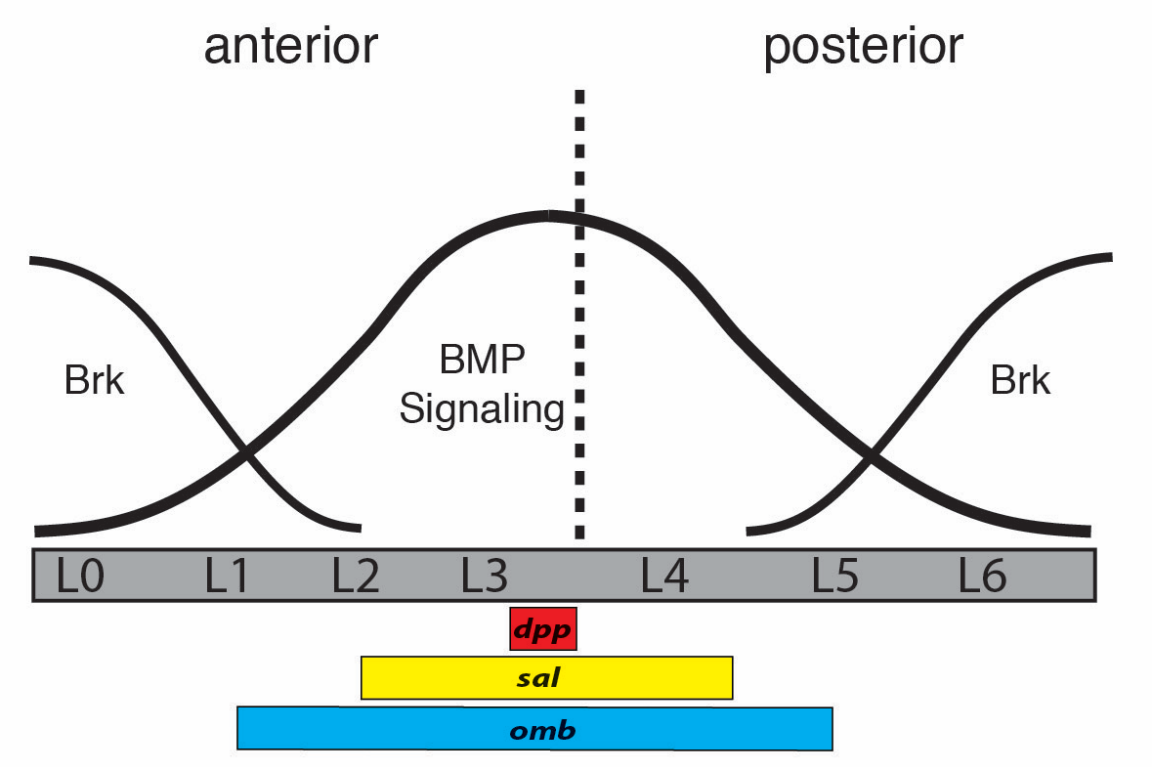

Figure 1.1: Wing disc development in Drosophila.

Simplified drawings of BMP signaling and Brinker (Brk) gradients (continuous lines) are depicted above sketches of the wing imaginal disc (grey) in cross section along the anterior-posterior axis. Wing veins (L0-6) are specified by the BMP signaling gradient and combinations of transcription factors. Dotted line represents the border between anterior and posterior compartment of the wing disc. *dpp*: *decapentaplegic*; *sal*: *spalt*; *omb*: *optomotor-blind*.

to study how patterning and growth are coordinated by the morphogen gradient.

1.2.2) Specification of amnioserosa in Drosophila by BMP signaling

Besides wing patterning, BMP signaling is also important for dorsal ventral axis patterning in Drosophila. The molecular mechanism of BMP signaling in Drosophila embryos is very well known and this facilitates molecular comparison with other species. Furthermore, the function of the BMP gradient in dorsal ventral patterning is well conserved throughout the animal kingdom (Bier and De Robertis, 2015). I therefore chose this model for comparing the BMP gradients in different species and to study how morphogen gradients evolve.

BMP signaling in the early Drosophila embryo involves two types of ligands: Decapentaplegic (Dpp) and Screw (Scw). Dpp is expressed in the dorsal 40% of the embryo circumference while Scw is expressed ubiquitously. The BMP ligand binds to a receptor complex consisting of serine/threonine kinases- type 1 receptors, Thickens (Tkv) and Saxophone (Sax), which are specific to Dpp and Scw respectively, and type 2 receptor Punt (Put). Upon ligand binding, Put phosphorylates Tkv and Sax and the activated Tkv and Sax receptors phosphorylate a downstream transducer called Mothers against Dpp (Mad). Mad belongs to the Smad family of signal transduction proteins. Phosphorylated Mad (pMad) then binds another Smad protein Medea (Med) and the resulting complex Mad/Med translocates into the nucleus where it binds to DNA and regulates the transcription of BMP target genes. High level of Dpp and Scw activity is necessary for amnioserosa specification.

BMP signaling is highly dynamic in Drosophila embryos at the blastoderm stage (**Fig. 1.2**). Initially, a shallow gradient of BMP signaling is formed in the dorsal domain during the blastoderm stage, which is refined into a sharp peak along the dorsal midline at the start of gastrulation (Dorfman and Shilo, 2001; Ross et al., 2001). Peak BMP signaling specifies the dorsal most tissue, which in *Drosophila melanogaster*, becomes an extraembryonic tissue called amnioserosa, while the rest of the embryo, which is exposed to low or no BMP siognaling, become embryonic tissue. The dynamic change of the BMP signaling gradient is driven by two main processes: extracellular movement of the ligand and positive feedback.

During extracellular movement, the BMP ligands Dpp and Scw are transported in the extracellular space toward the dorsal midline. This involves the binding of the ligands to Short gastrulation (Sog) (Biehs et al., 1996; Decotto and Ferguson, 2001) and Twisted gastrulation (Tsg) (Ross et al., 2001). The resulting complex then diffuses through the space between embryo and eggshell (perivitelline space). At the dorsal side, the metalloprotease Tolloid (Tld) is expressed and cleaves Sog (Marques et al., 1997; Shimell et al., 1991; Srinivasan et al., 2002). This releases Dpp and Scw and allows signaling on the dorsal side, thus creating a shallow gradient of BMP signaling during blastoderm cellularization.

This shallow gradient is then transformed by positive feedback into a sharp peak at the onset of gastrulation (Wang and Ferguson, 2005). This feedback is promoted by the homeobox gene *zerknüllt* (*zen*), which is broadly activated on the dorsal side independently of BMP signaling (Doyle et al., 1989; Liang et al., 2008; Rushlow et al., 1987a, 2001; Xu et al., 2005). This early phase of *zen* expression is critical for the activation of two regulators

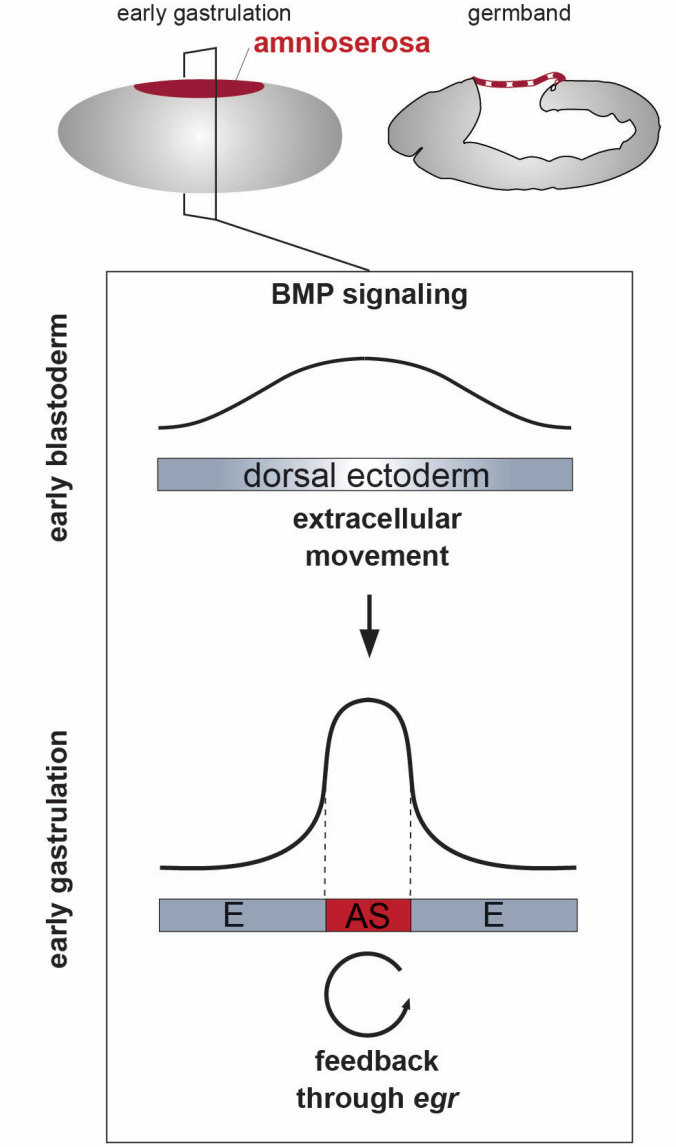

Figure 1.2: BMP-depend amnioserosa specification in Drosophila.

Embryo sketches (anterior left, dorsal up) depicting amnioserosa (AS, maroon) development in Drosophila. Schematic of BMP gradient profile above the dorsal ectoderm (E, grey). The midpoint of ectoderm represents the dorsal midline.

of BMP signaling (Gavin-Smyth et al., 2013): the *tumor necrosis factor alpha* homologue *eiger* (*egr*) (Igaki and Miura, 2014; Igaki et al., 2002), which promotes BMP signaling by positive feedback, and the cell-surface BMP binding protein *crossveinless-2* (*cv-2*), which antagonizes BMP signaling in the dorsal ectoderm but also promotes signaling in other contexts (Conley et al., 2000; Serpe et al., 2008). e*gr cv2* double mutant embryos have a similar average pMad peak intensity compared to wild type but exhibit increased variability in pMad and amnioserosa cell number (Gavin-Smyth et al., 2013), suggesting that both genes function in a genetic network that confers robustness to the BMP gradient. Drosophila species lacking the early phase of broad *zen* activity exhibit decanalized, variable pMad intensities in the blastoderm as well as decanalized amnioserosa cell numbers (Gavin-Smyth et al., 2013).

1.3) Introduction to the extraembryonic tissues

The BMP gradient also specifies the extraembryonic tissue on the dorsal side in other insects. However, instead of amnioserosa, most other insects including lower dipterans develop two distinct extraembryonic epithelia, called serosa and amnion (Panfilio, 2008; Schmidt-Ott and Kwan, 2016). The serosa is formed from blastoderm cells that do not contribute to the germ rudiment (prospective embryo and amnion), lines the inner side of the eggshell and surrounds the whole embryo. The amnion originates from the edge of the germ rudiment and in most insects, it closes over the ventral side of the embryo to form a fluid-filled cavity between the embryo and amnion, called "amniotic cavity". This ancestral condition is found in the early branching lineages in Diptera (indicated by black square in **Fig. 1.3**). In basal-branching lineages of cyclorrhaphan flies

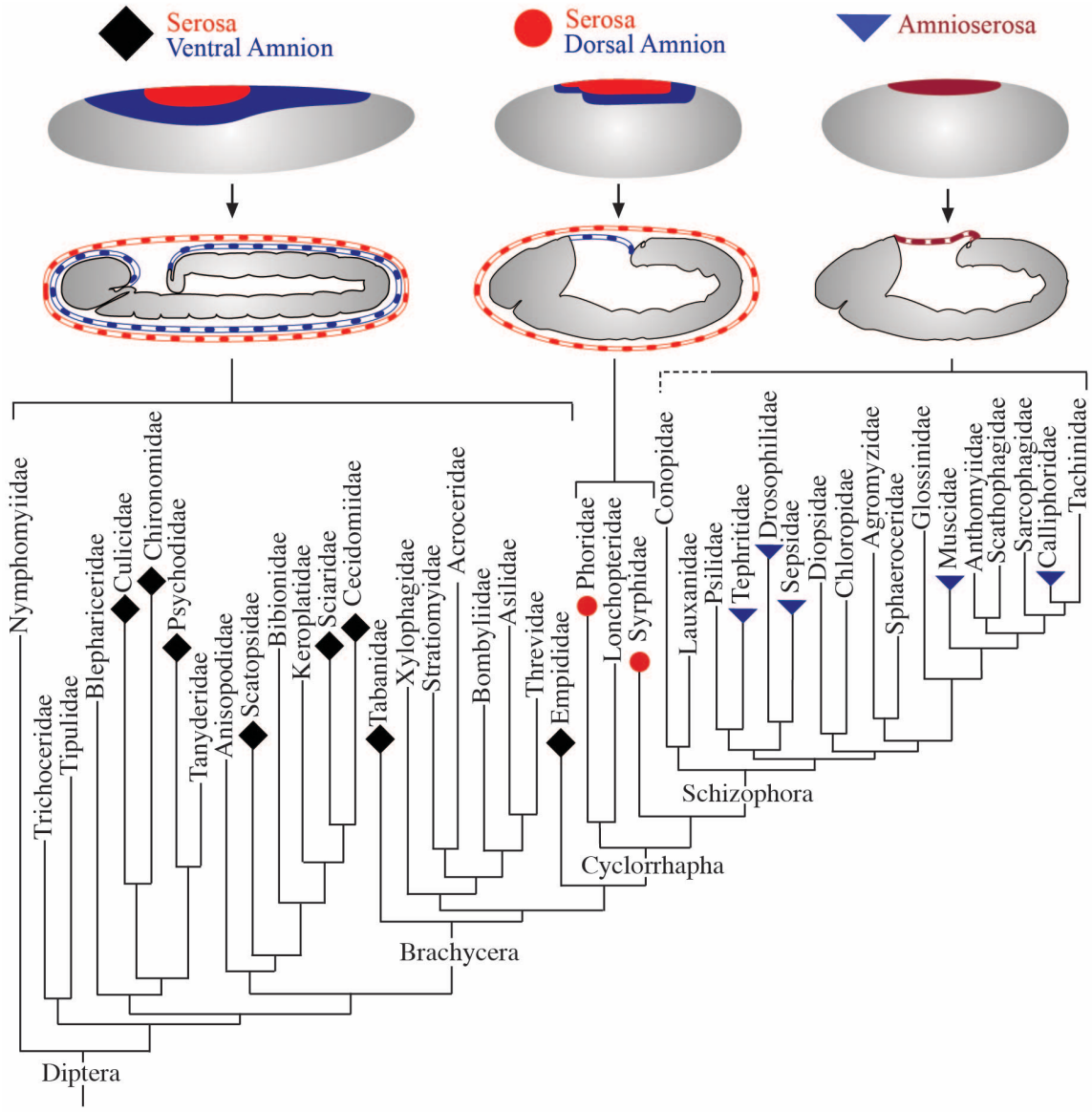

Figure 1.3: Evolution of extraembryonic tissues in Diptera

(indicated by red circle in **Fig. 1.3**), the serosa and amnion are retained, but the amnion closes over the dorsal side instead of the ventral side, covering the yolk sack, thus forming a dorsal amnion. In higher cyclorrhaphan flies (Schizophora) like Drosophila, no distinct serosa and amnion exists (indicated by blue triangle in **Fig. 1.3**). Instead, a single epithelium called amnioserosa develops on the dorsal side of the embryo. Thus, Diptera underwent two dramatic rearrangements of extraembryonic tissues during evolution.

The serosa has been shown to play several important functions in embryos. Firstly, it secretes a cuticle underneath the eggshell to provide desiccation resistance (Goltsev and Papatsenko, 2009; Jacobs et al., 2013, 2015; Rezende et al., 2008; Vargas et al., 2014). Secondly, it can mount a strong immune reaction to protect against pathogens (Gorman et al., 2004; Jacobs and van der Zee, 2013; Jacobs et al., 2014). Furthermore, many non-holometabolous insects undergo longitudinal axis inversion, and the serosa helps to realign the axis of the embryo to that of the egg (Panfilio, 2009). Compared to serosa functions, amnion functions are less well known. Recently, it has been shown that in Tribolium, amnion plays an important role in initiating the rupture and withdrawal of the extraembryonic tissues, a process that is essential for development (Hilbrant et al., 2016). In Drosophila, the amnioserosa is proposed to be homologous to the amnion, mainly supported by the expression and function of the gene *zen* in different species (Rafiqi et al., 2008, 2010; Rushlow and Levine, 1990; van der Zee et al., 2005). The amnioserosa is required for germ band retraction and dorsal closure (Flores-Benitez and Knust, 2015; Frank and Rushlow, 1996; Lamka and Lipshitz, 1999; Scuderi and Letsou, 2005; Shen et al., 2013; Yip et al., 1997). During development, the germ band elongates and folds into a u-shape tissue. Germ band retraction shortens this u-shaped germ band and aligns the

embryo with the anterior posterior axis of the egg. After germ band retraction, there is an opening on the dorsal side of the embryo, which is covered by the amnioserosa. During dorsal closure this opening is sealed by the dorsal epidermis while the amnioserosa cells are taken up into the yolk and disintegrate. The amnion is believed to play a similar role in other species like Megaselia but this is less well-supported (Rafiqi et al., 2010).

1.4) Introduction to the experimental system

The primary goal of my dissertation research has been to better understand how BMP signaling specifies serosa and amnion in basal-branching dipterans. While amnioserosa specification in Drosophila is a well-known process, how other flies specify serosa and amnion was so far largely unknown. I choose the scuttle fly *Megaselia abdita* as my experimnetal model. Megaselia belongs to the Phoridae family and develops a serosa and a dorsal amnion. This condition is also found in syrphid flies (Rafiqi et al., 2008), which represent another branch of lower cyclorrhaphan flies (Wiegmann et al., 2011) and may thus have been present in the last common ancestor of Megaselia and Drosophila. The rather close relationship of Megaselia and Drosophila also facilitates the comparison of developmental mechanisms of extraembryonic tissue specification between these species. Furthermore, Megaselia is a well-established experimental system for comparative studies (Rafiqi et al., 2011; Wotton et al., 2014) and various embryological techniques have been developed for this species, such as embryo fixation, in situ hybridization, immunostaining, and microinjection to study gene expression and function. An draft genome assembly and embryonic transcriptome data (Jiménez-Guri et al., 2013) are available and transgenic techniques have been developed to express fluorescent reporters in the nuclei ubiquitously

in this species (Caroti et al., 2015). Throughout this thesis, the staging scheme for Megaselia is based on (Wotton et al., 2014), which divides the development of Megaselia according to the staging scheme for *Drosophila melanogaster* (Campos-Ortega and Hartenstein, 1997).

1.5) Different models for serosa and amnion specification in Megaselia

BMP signaling is essential for extraembryonic tissue specification in flies, including Drosophila and Megaselia, but the mechanism by which the BMP gradient specifies two distinct extraembryonic tissues in Megaselia, or any other insect, is poorly understood. Theoretically, serosa and amnion could be specified by two different thresholds of a single BMP signaling gradient (**Fig. 1.4A**). Alternatively, they could be specified by two gradients of different BMP ligands, the threshold of each gradient specifying serosa or amnion, respectively (**Fig. 1.4B**). It is also conceivable that BMP signaling alone may not be enough to specify two distinct extraembryonic tissues. Instead, a second dorsal-ventral signaling center could be required to subdivide an undifferentiated BMP-created extraembryonic tissue into amnion and serosa (**Fig. 1.4C**). Finally, the BMP signaling gradient could be dynamic, specifying serosa during the blastoderm stage and amnion during early gastrulation (**Fig. 1.4D**). These four models are not mutually exclusively and could occur in combination with each other to specify serosa and amnion. In this thesis, I tested the fourth model by examining the specification of extraembryonic tissues using different genetic markers (Part 2.1), monitoring the dynamic change of BMP signaling and functionally testing its temporal requirement (Part 2.2), and dissecting the genetic circuit that underlies the dynamic BMP signaling gradient (Part 2.3).

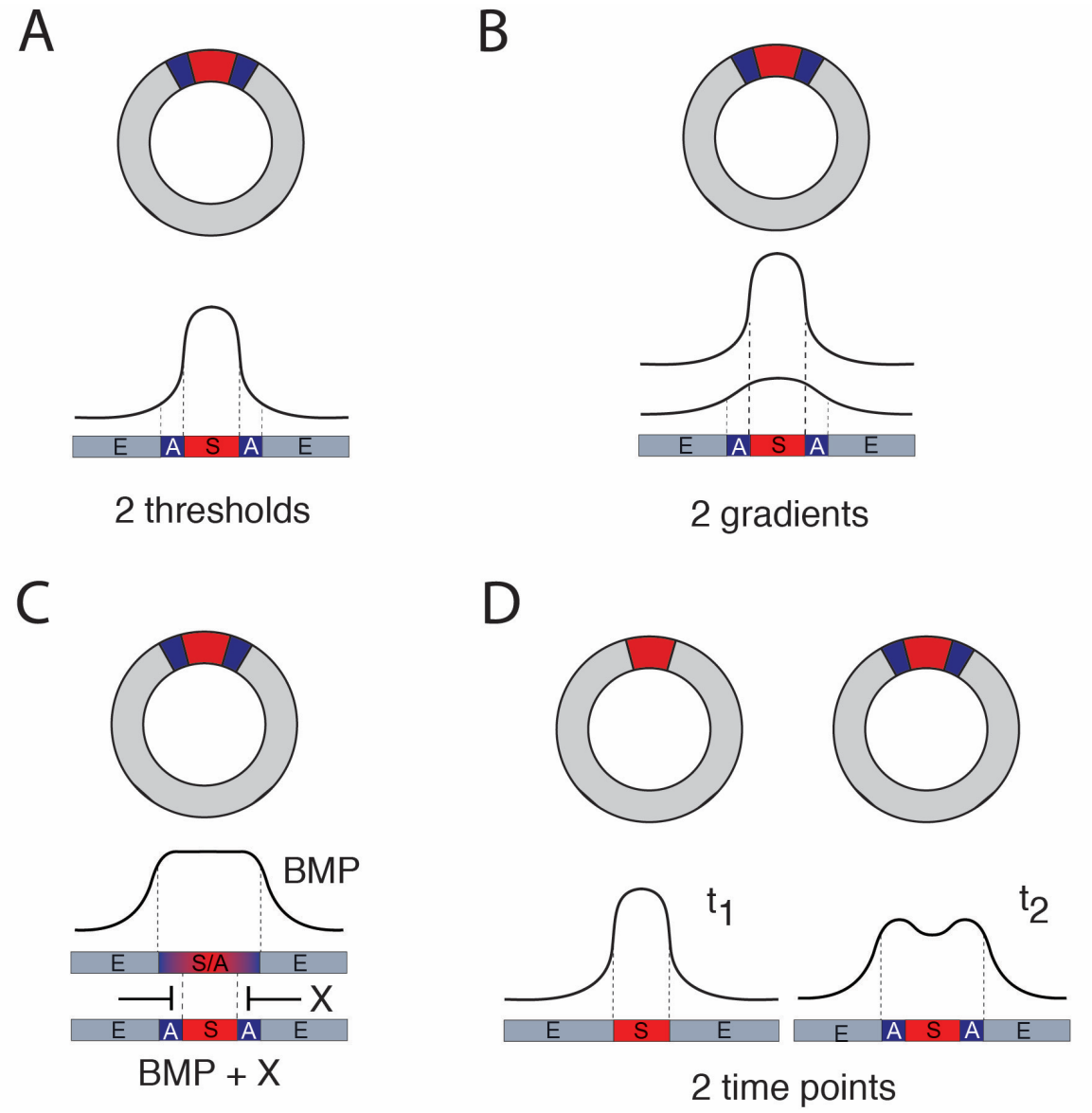

Figure 1.4: Four different models of serosa and amnion specification in Megaselia.

A-D, Cross sections of the cellular blastoderm with prospective serosa (red), amnion (blue) and dorsal ectoderm (grey) are depicted below BMP gradient profiles. S: serosal tissue; A: amnioic tissue; E: embryonic tissue; X: Unknown signaling factor.

2) Results

2.1) Markers of extraembryonic tissue in Megaselia

In Megaselia, serosa and amnion specification can be visualized with a combination of genetic markers. Here, I review markers that I used to examine the mechanism of serosa and amnion specification in Megaselia.

Mab-zen (Stauber et al., 1999) is a homolog of *zerknüllt*, which encodes a homeodomain protein required for amnioserosa specification in *Drosophila melanogaster* (Rushlow and Levine, 1990; Rushlow et al., 1987a, 1987b). *Mab-zen* marks and specifies serosa cells in blastoderm (stage 5) and gastrula embryos (stage 6) (Rafiqi et al., 2008). Knockdown of *Mab-zen* by RNAi changes the fate of serosa cells to amnion cells (Rafiqi et al., 2008), while overexpression of *Mab-zen* promotes expression of a downstream serosa marker (*Mab-ddc*) and represses genes that are expressed in the amnion, such as *Mab-doc* (Rafiqi et al., 2010). In the present study, I use *Mab-zen* as a specific serosa marker.

Mab-hnt (Rafiqi et al., 2010) is a homologue of *hindsight/pebbled* (*hnt*), which encodes a zinc finger protein required for maintaining amnioserosa tissue after gastrulation (Frank and Rushlow, 1996; Yip et al., 1997). *Mab-hnt* is expressed in stage 5 and 6 embryos in a slightly wider domain than *Mab-zen,* encompassing both the prospective serosa and amnion (Rafiqi et al., 2010, 2012). Additionally, *Mab-hnt* is expressed in the anterior and posterior midgut primordia and in ectodermal cells at germ band retraction stage (Rafiqi et al., 2010).

Mab-doc (Rafiqi et al., 2010) is a homologue of the three *Dorsocross* (*Doc*) paralogues of Drosophila, which encode T-box proteins that are required for folding and maintaining amnioserosa tissue (Reim et al., 2003). The three *Doc* paralogs of Drosophila

are expressed in amnioserosa during cellular blastoderm, in a metameric pattern in the dorsal ectodermal and mesodermal cells during germ band extension. *Mab-doc* is expressed in prospective serosa and amnion cells, in a metameric pattern of mesodermal and epidermal cells, prospective optic lobes and medial patch of head blastoderm (Rafiqi et al., 2010). In stage 5 and 6 embryos, the extraembryonic domains of *Mab-do*c and *Mab-hnt* overlap (**Fig. 2.1.1**). I also identified a paralogue of *Mab-doc*, named *Mab-doc2*, which is expressed similarly (**Fig. 2.1.2A-B**). Sequence alignment shows that *Mab-doc* and *Mab-doc2* share 55.7% protein similarity (**Fig. 2.1.2C**) and protein tree analysis suggests that the gene duplication resulting in *Mab-doc* and *Mab-doc2* occurred independently of the two *Doc* duplications in the Drosophila lineage (**Fig. 2.1.2D**).

Mab-eve (Bullock et al., 2004) is a homologue of the pair-rule segmentation gene *even-skipped* (*eve*) of Drosophila, which is expressed in stage 5 and 6 embryos in seven transverse stripes with double segment periodicity. While in Drosophila these stripes are circumferentially closed in stage 5 and 6 embryos, in Megaselia they split along the dorsal midline, beginning in stage 5 (Rafiqi et al., 2012). The time course of serosa and amnion specification is suggested by the dorsal repression of *Mab-eve*. Initially, the *Mab-eve* stripes are circumferential and overlap with the dorsal domains of *Mab-zen* and *Mab-doc/hnt* (**Fig. 2.1.3A**). During late blastoderm, as a result of repression by BMP signaling (Rafiqi et al., 2012), *Mab-eve* is down-regulated at the dorsal midline and abuts the *Mab-zen* domain (**Fig. 2.1.3B**), but withdraws further to abut the *Mab-doc/hnt* domain after gastrulation begins (**Fig. 2.1.3C**). This time course suggests that amnion specification finishes after the onset of gastrulation when *Mab-eve* is no longer expressed in prospective amnion cells.

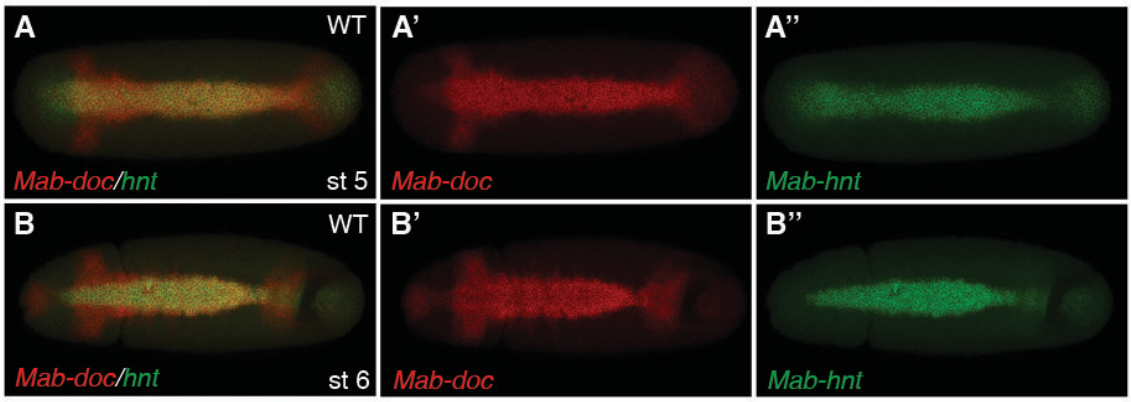

Figure 2.1.1: *Mab-hnt* and *Mab-doc* expression.

A-B, *Mab-hnt* and *Mab-doc* expression at the late blastoderm (**A**) and early gastrulation stage (**B**). Dorsal views with anterior left.

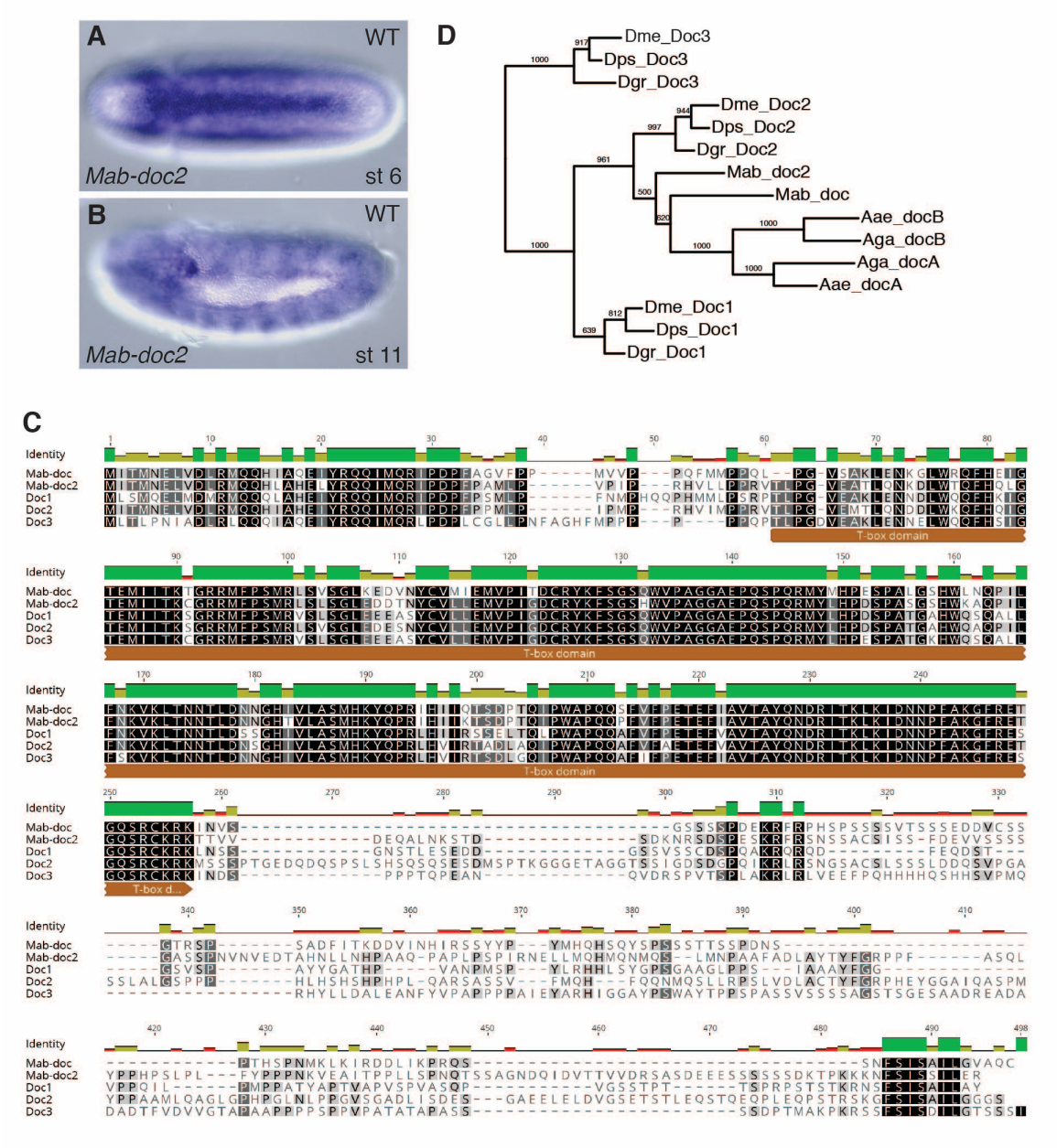

Figure 2.1.2: *Mab-doc2* expression.

A-B, *Mab-doc2* expression at early gastrulation (**A**) and the extended germ band stage (**B**).

C, MUSCLE-generated alignment of T-box genes from *Megaselia abdita* and *Drosophila melanogaster*. The T-box domain highlighted above contains T-box core sequence extended N- and C-terminally according to (Reim et al., 2003).

Figure 2.1.2 continued

D, Maximum likelihood gene tree based on full-length Doc protein homologues. Aae (*Aedes aegypti*), Aga (*Anopheles gambiae*), Mab (*Megaselia abdita*), Dme (*Drosophila melanogaster*), Dps (*Drosophila pseudoobscura*), Dgr (*Drosophila grimshawi*). Bootstrap values, based on 1000 replicas, are shown.

A, Dorsal views with anterior left. **B**, Lateral views with dorsal up and anterior left.

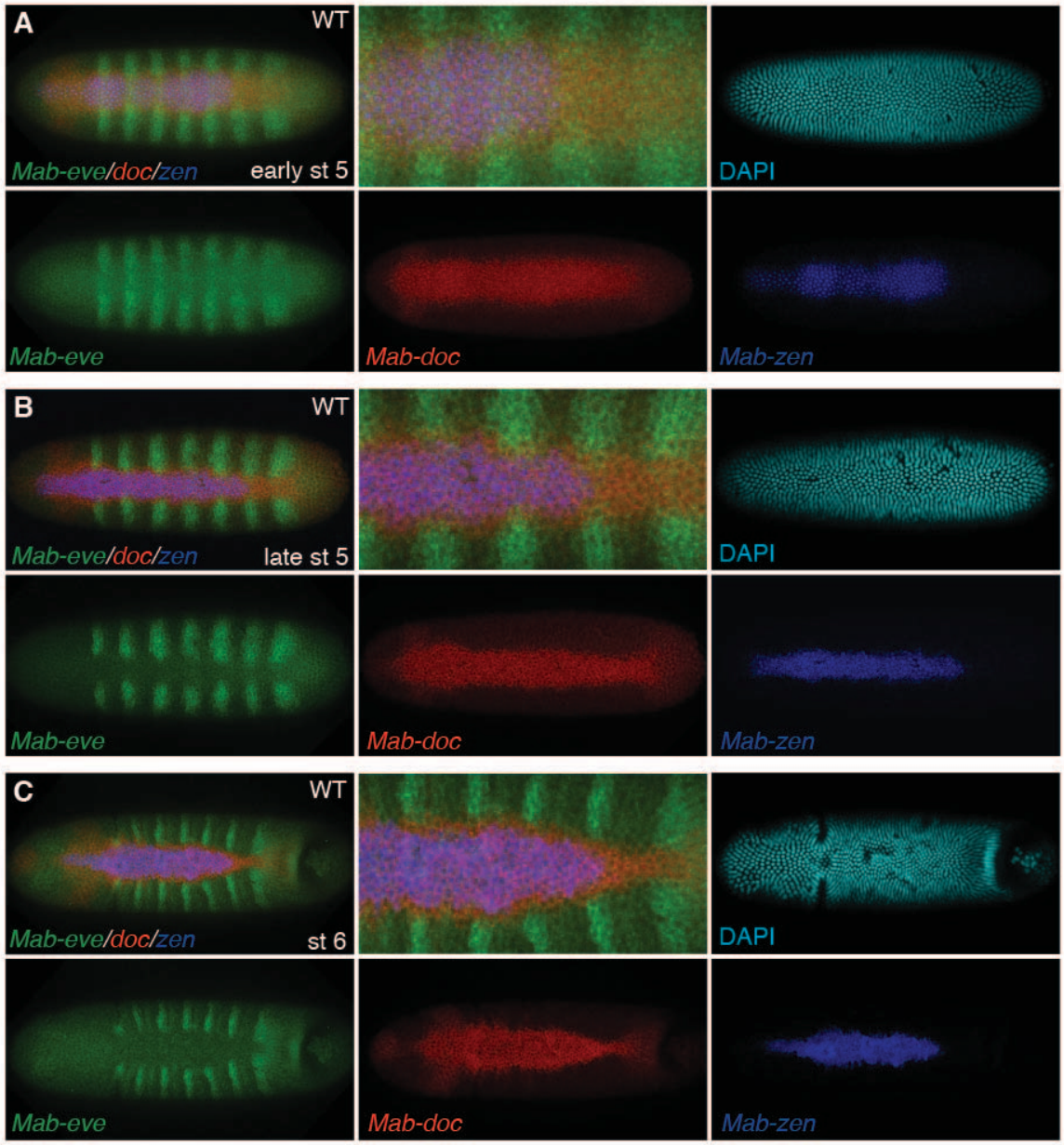

Figure 2.1.3: *Mab-zen*, *Mab-doc* and *Mab-eve* expression.

A-C, *Mab-zen*, *Mab-doc* and *Mab-eve* expression at early blastoderm (**A**), late blastoderm (**B**) and early gastrulation (**C**) stage, indicating amnion specification occurs at early gastrulation. Dorsal views with anterior left.

Mab-egr, a homologue of *tumor necrosis factor alpha* gene, *eiger* (*egr*) (Igaki et al., 2002), was examined because *egr* promotes BMP signaling in Drosophila embryos (Gavin-Smyth et al., 2013). In Drosophila, *egr* is broadly expressed dorsally during the blastoderm stage (stage 5), restricted to the dorsal most cells at early gastrulation (stage 6), and after germ band extension (stage 10) (Gavin-Smyth et al., 2013), expressed primarily in the nervous system (Igaki et al., 2002). In Megaselia, *Mab-egr* begins weakly in prospective serosa and amnion cells at the end of the blastoderm stage (late stage 5), and increases in these cells during gastrulation (stage 6). After germ band extension (stage 11) until dorsal closure (end of stage 15), *Mab-egr* is expressed in amnion cells but not in serosa cells, and after dorsal closure (stage 16), *Mab-egr* is detected in the central nervous system (**Figs. 2.1.4 and 2.1.5A-B**).

In the following, I will discern prospective serosa and amnion cells in stage 5 and 6 embryos using *Mab-zen* as serosa marker and *Mab-doc* and *Mab-hnt* as serosa and amnion markers. In addition, I will use *Mab-eve* repression as a marker for the completion of serosa specification during stage 5 and amnion specification during stage 6. Differentiated amnion cells, which are polyploid and much larger than the adjacent embryonic cells (**Fig. 2.1.5C-D**), will be identified after germ band extension (stage 11) using amnion specific *Mab-egr* expression.

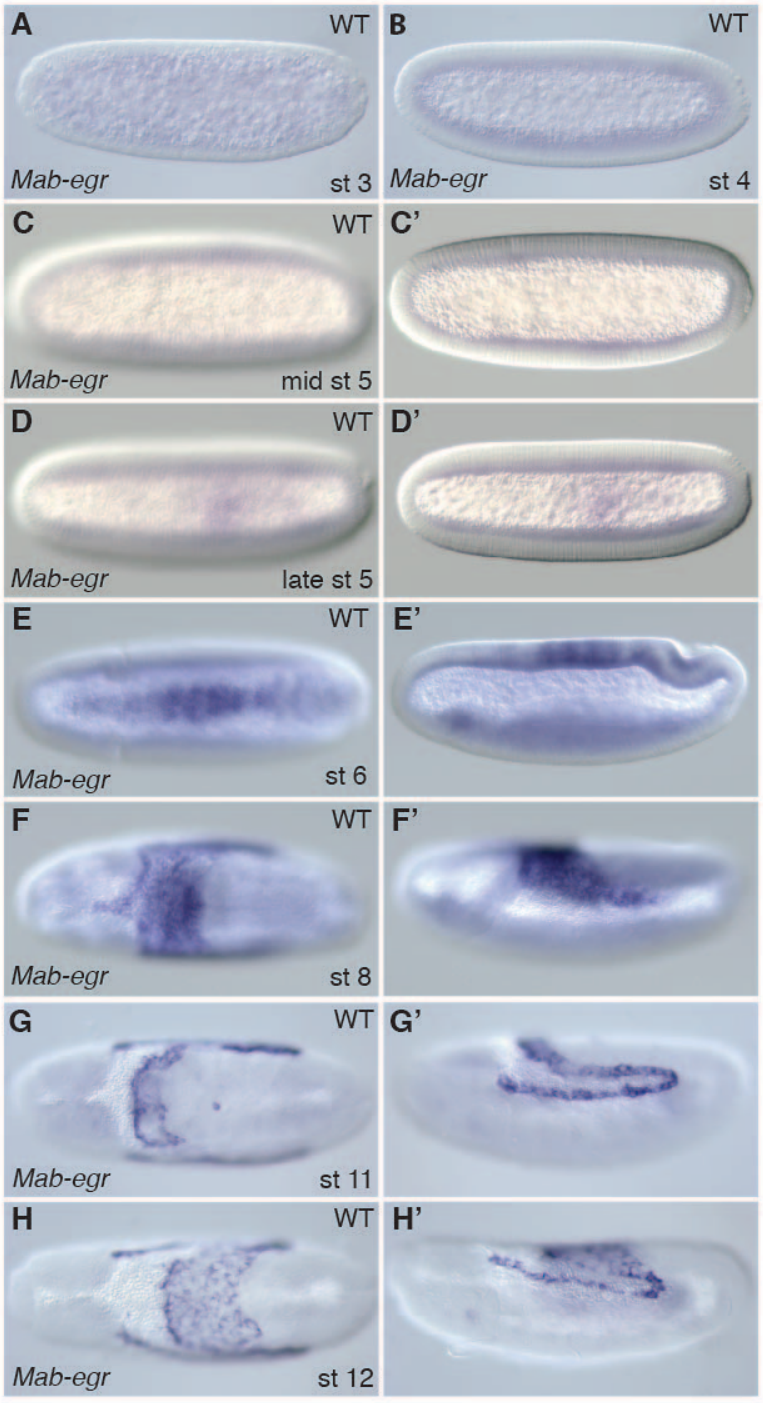

Figure 2.1.4: Expression profile of *Mab-egr*.

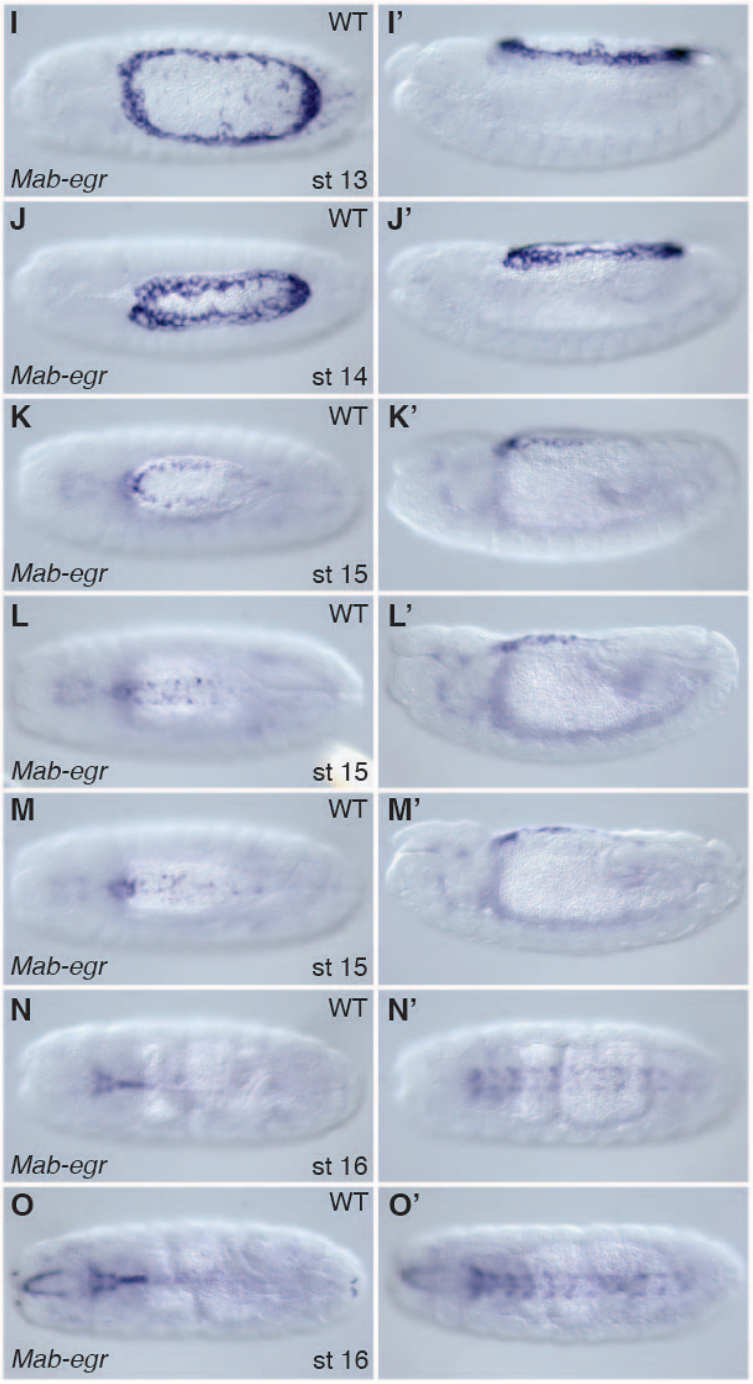

Figure 2.1.4 continued

A-O, *Mab-egr* expression in Megaselia embryos before blastoderm formation (**A**), at syncytial blastoderm (**B**), during blastoderm cellularization (**C**), at cellular blastoderm (**D**), early gastrulation (**E**), early and late germ band extension (**F**, **G**), during germ band

Figure 2.1.4 continued

retraction (**H**), at the end of germ band retraction (**I**), dorsal closure stages (**J-M**) and after dorsal closure (**N**, **O**).

C-O, Dorsal views with anterior left. **A**, **B**, **C'-M'**, Lateral views with dorsal up and anterior left. **N'-O'**, Ventral views with anterior left.

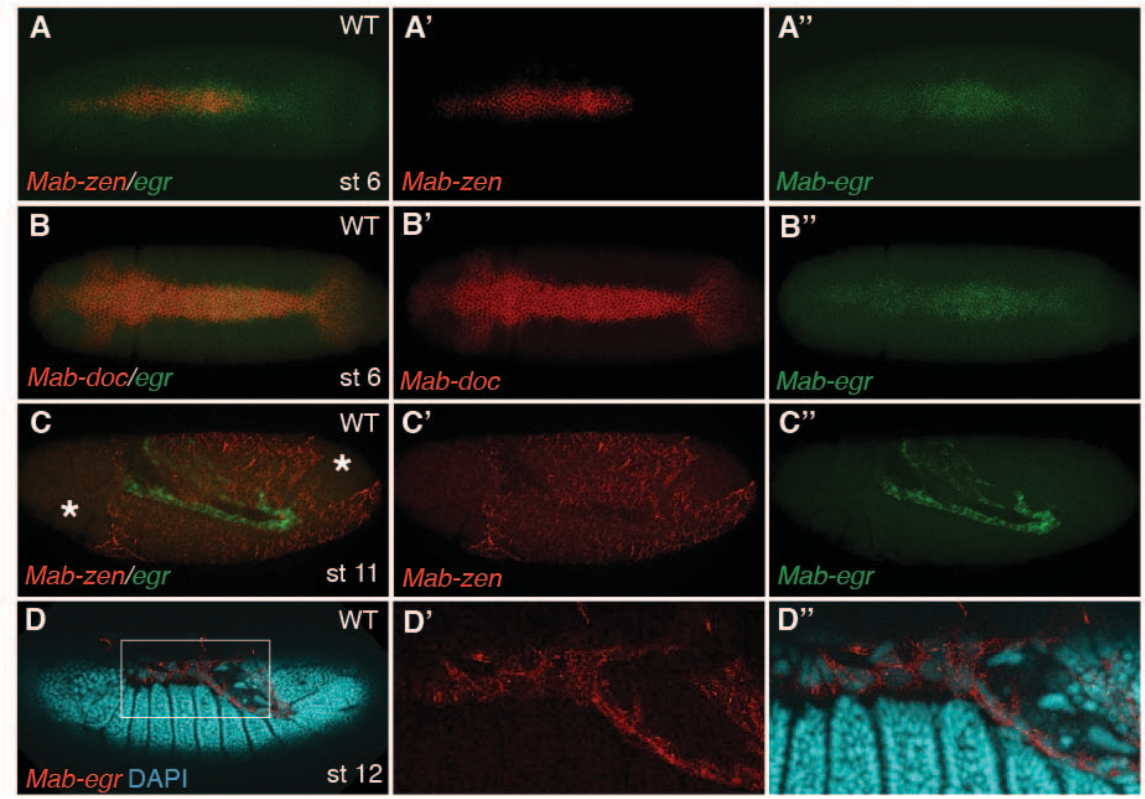

Figure 2.1.5: *Mab-egr* expression in relation to *Mab-zen*, *Mab-doc* and DAPI.

A-B, *Mab-zen* and *Mab-egr* expression (**A**), *Mab-doc* and *Mab-egr* expression (**B**) at early gastrulation.

C-D, *Mab-zen* and *Mab-egr* expression at the late germ band (**C**) and *Mab-egr* expression with nuclei labeled with DAPI at germ band retraction (**D**). Asterisks denote tears in the serosa during sample preparation. Boxed region enlarged (**D'-D''**).

A-B, Dorsal views with anterior left. **C-D**, Lateral views with dorsal up and anterior left.

2.2) Temporal requirement of BMP signaling in extraembryonic tissue specification

In Megaselia and Drosophila, BMP signaling specifies extraembryonic epithelia and can be quantified by staining with an antibody specific to the activated phosphorylated form of Mad (pMad), an essential transcriptional effector of the BMP pathway (Dorfman and Shilo, 2001). During early blastoderm stages in both species, BMP signaling is initially low and broadly distributed over the dorsal regions of the embryo but refines into a narrow dorsal stripe of high activity by the onset of gastrulation (**Fig. 2.2.1A', C'**). However, during early gastrulation in Megaselia, the BMP signaling domain broadens to encompass the edge of the germ rudiment comprising the presumptive amnion (**Fig. 2.2.1B'**), while the pattern in Drosophila remains static (**Fig. 2.2.1D'**). In order to determine how the BMP signaling domain relates to the extraembryonic tissues, embryos were co-stained with pMad and extraembryonic tissue markers (*Mab-zen* and *Mab-eve*). In late blastoderm embryos of Megaselia, the pMad domain overlaps with the expression domain of *Mab-zen* (**Fig. 2.2.1A**), but at the beginning of gastrulation, when a gap appears between the *Mab-zen* and *Mab-eve* expression domains, the pMad domain expands beyond the *Mab-zen* domain (**Fig. 2.2.1B**). In contrast, the lateral limits of the pMad and *zen* domains always match during both stages in Drosophila (**Fig. 2.2.1C-D**). Thus, during early gastrulation, broadening of the BMP signaling domain is unique to Megaselia and correlates with the completion of amnion specification both temporally and spatially.

These findings raise the question of whether temporal changes in the pMad gradient are required for the specification of distinct serosa and amnion tissues. To examine the temporal requirement of BMP signaling for serosa and amnion specification, I compared

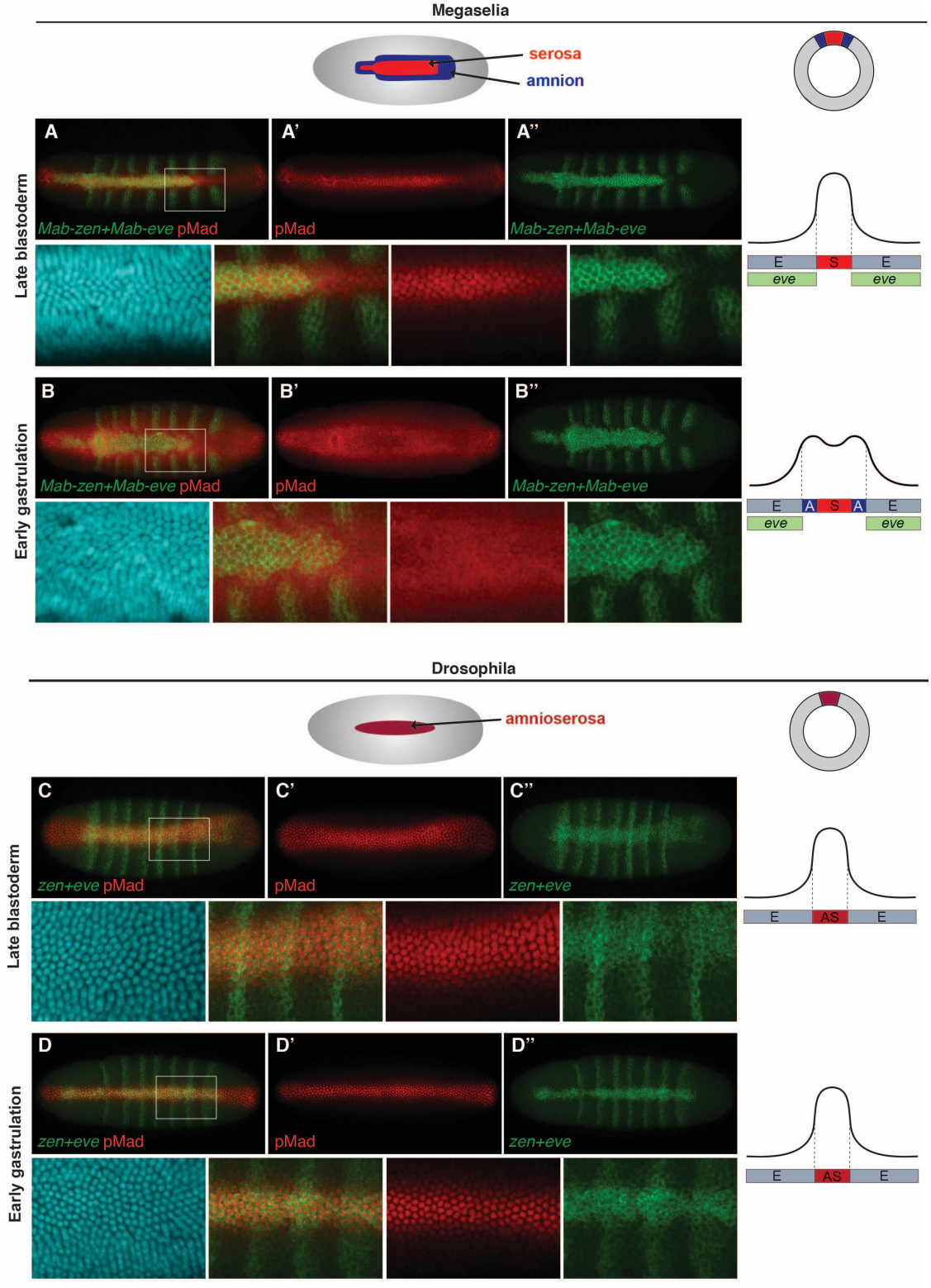

Figure 2.2.1: *zen* and *eve* homolog expression, and pMad staining in Megaselia and Drosophila.

Figure 2.2.1 continued

A-D, Mab-zen, Mab-eve expression in relation to pMad in Megaselia (**A-B**) and Drosophila (**C-D**) at late blastoderm (**A,C**) and early gastrulation (**B,D**). Dorsal views with anterior left.

the effect *Mab-dpp* RNAi induced before blastoderm formation and after 50% blastoderm cellularization. While knockdown of BMP signaling before blastoderm formation by *Mab-dpp* RNAi suppresses serosa and amnion specification completely, resulting in loss of *Mab-zen* expression and circumferential *Mab-eve* stripes at stages 5 and 6 (Rafiqi et al., 2012), *Mab-dpp* knockdown at the end of the blastoderm stage did not affect expression of *Mab-zen*; however, in five of the thirteen embryos analyzed repression of *Mab-eve* in the amnion anlage was incomplete (**Fig. 2.2.2A-B**). *Mab-dpp* knockdown at the end of stage 5 also reduced *Mab-egr* expression in a majority of stage 11/12 embryos (55%, n=40). Conversely, injection of *Mab-dpp* mRNA at the end of stage 5 caused an expansion of the *Mab-egr* domain in at least 35% of the embryos (n=57) (**Fig. 2.2.2C-E**). Taken together, these data provide evidence that BMP signaling during gastrulation is necessary and sufficient for amnion specification.

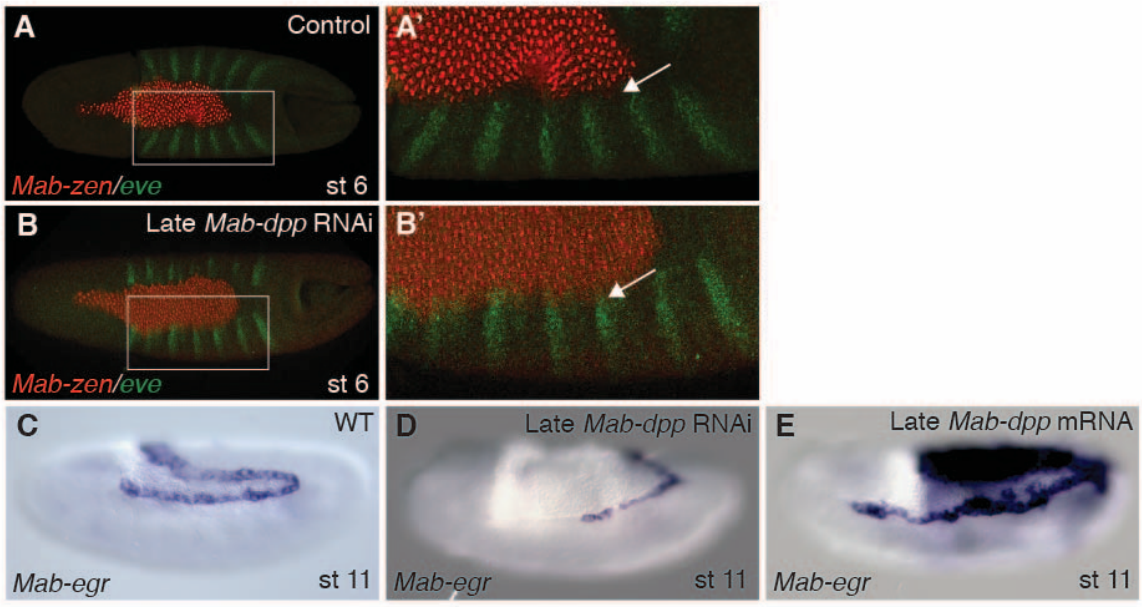

Figure 2.2.2: Gastrular BMP signaling is required for amnion but not sersoa development.

A-B, *Mab-zen* and *Mab-eve* expression in early gastrula control embryo (**A**, enlargement **A'**) and following *Mab-dpp* knockdown after 50% blastoderm cellularization (**B**. enlargement **B'**). Arrows, gap between the *Mab-eve* and *Mab-zen* domains (**A'**) that is suppressed in the knockdown embryo (**B**).

C-E, *Mab-egr* expression at germ band extension in wild-type embryo (**C**), after *Mab-dpp* knockdown (**D**) or *Mab-dpp* overexpression (**E**) after 50% blastoderm cellularization.

A-B, Dorsal views with anterior left. **C-E**, Lateral views with dorsal up and anterior left.

2.3) A positive feedback loop of the BMP gradient is important for amnion specification during gastrulation

2.3.1) *Mab-hnt* and *Mab-doc* are essential for amnion specification

In Drosophila, both BMP signaling and *zen* are necessary at the blastoderm stage for expression of the three *Doc* paralogs and *hnt* in the amnioserosa anlage, even though the essential function of these genes in amnioserosa maintenance becomes apparent only after gastrulation (Reim et al., 2003; Yip et al., 1997). In Megaselia, knockdown of BMP signaling by *Mab-dpp* RNAi represses the expression of both *Mab-hnt* (Rafiqi et al., 2012) and *Mab-doc* (**Fig. 2.3.1A-C**). However, *Mab-zen* knockdown does not affect *Mab-hnt* and *Mab-doc* expression (**Fig. 2.3.1D-I**), and *Mab-doc* and *Mab-hnt* do not regulate each other's expressions (**Fig. 2.3.1J-K**). Thus, in Megaselia, BMP signaling activates *Mab-doc* and *Mab-hnt* independently from *Mab-zen*, suggesting *Mab-doc* and *Mab-hnt* could play a role in amnion specification.

To test this possibility, I examined amnion specification in *Mab-hnt* and *Mab-doc/doc2* RNAi embryos. Following knockdown of *Mab-hnt, Mab-doc/doc2* or *Mab-doc/hnt* activity, I observed confluent expression domains of *Mab-zen* and *Mab-eve* during early gastrulation (5/11, 4/9 and 8/9 embryos, respectively; **Fig. 2.3.2**). I also observed *Mab-eve* stripes penetrating and repressing the expression domain of *Mab-zen* in four severe cases following *Mab-doc/hnt* knockdown, consistent with the observation that ectopic *Mab-eve* can inhibit *Mab-zen* (**Fig. 6.2**). Knockdown of these genes also reduced *Mab-egr* expression at stage 11/12 (**Fig. 2.3.3A-F**). This effect was strongest when *Mab-doc/doc2* and *Mab-hnt* were repressed simultaneously, indicating that *Mab-doc/doc2* and *Mab-hnt* complement each other are essential for amnion specification in Megaselia. Conversely, overexpression

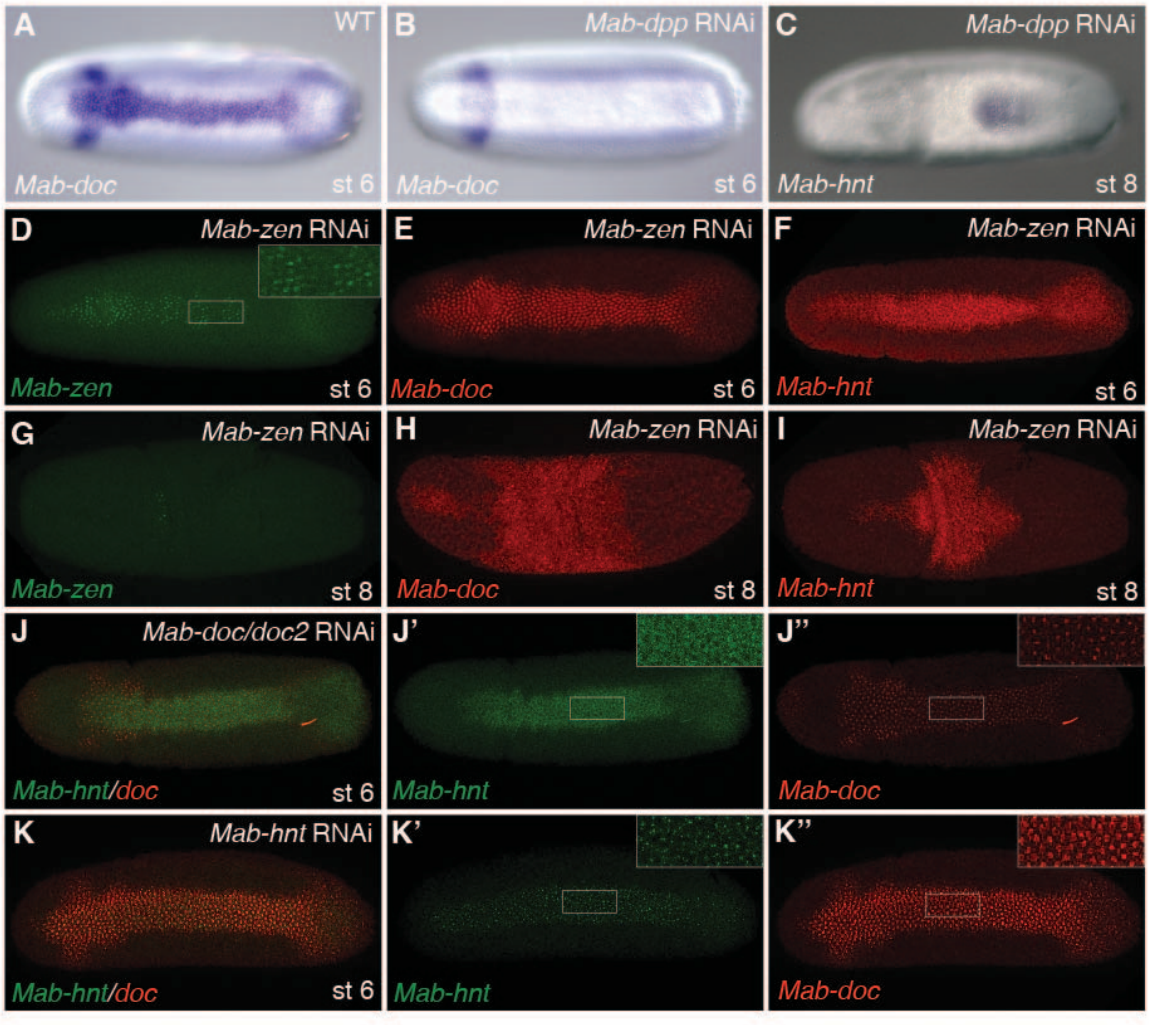

Figure 2.3.1: *Mab-hnt* and *Mab-doc* are regulated by BMP signaling but independent of each other and *Mab-zen*.

A-C, *Mab-doc* expression at early gastrulation in wild type (**A**) and after *Mab-dpp* knockdown (**B**). *Mab-hnt* expression at early gastrulation after *Mab-dpp* knockdown (**C**) (image from Rafiqi).

D-I, *Mab-zen* (**D**, **G**), *Mab-doc* (**E**, **H**), and *Mab-hnt* (**F**, **I**) expression at early gastrulation (**D-F**) and early germ band extension (**G-I**) following *Mab-zen* knockdown.

J-K, *Mab-hnt* and *Mab-doc* expression at early gastrulation following *Mab-doc/doc2* knockdown (**J**) or *Mab-hnt* knockdown (**K**). Dorsal views with anterior left.

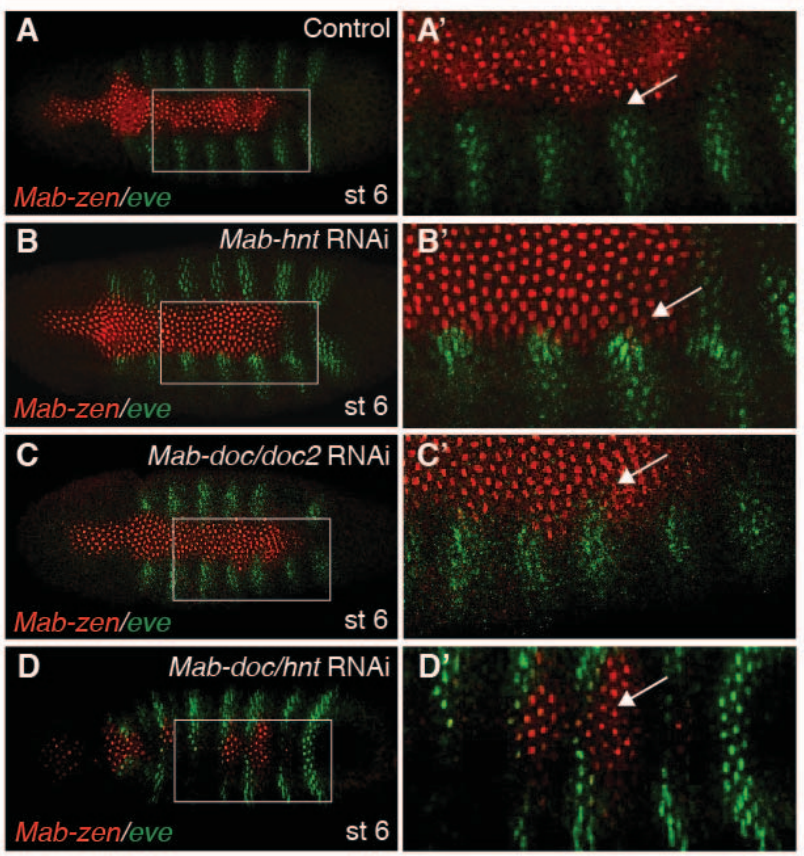

Figure 2.3.2: *Mab-hnt* and *Mab-doc* are essential for amnion specification.

A-D, *Mab-zen* and *Mab-eve* expression in early gastrula control embryo (**A**, enlargement **A'**) and after *Mab-hnt* knockdown (**B**, enlargement **B'**), *Mab-doc*/*doc2* knockdown (**C**, enlargement **C'**) or *Mab-doc*/*hnt* knockdown (**D**, enlargement **D'**). Arrows, gap between the *Mab-eve* and *Mab-zen* domains (**A**) that is suppressed in the knockdown embryos (**B-D**). In severe case of *Mab-doc*/*hnt* knockdown, *Mab-eve* strips penetrate into the *Mab-zen* domain (**D**). Dorsal views with anterior left.

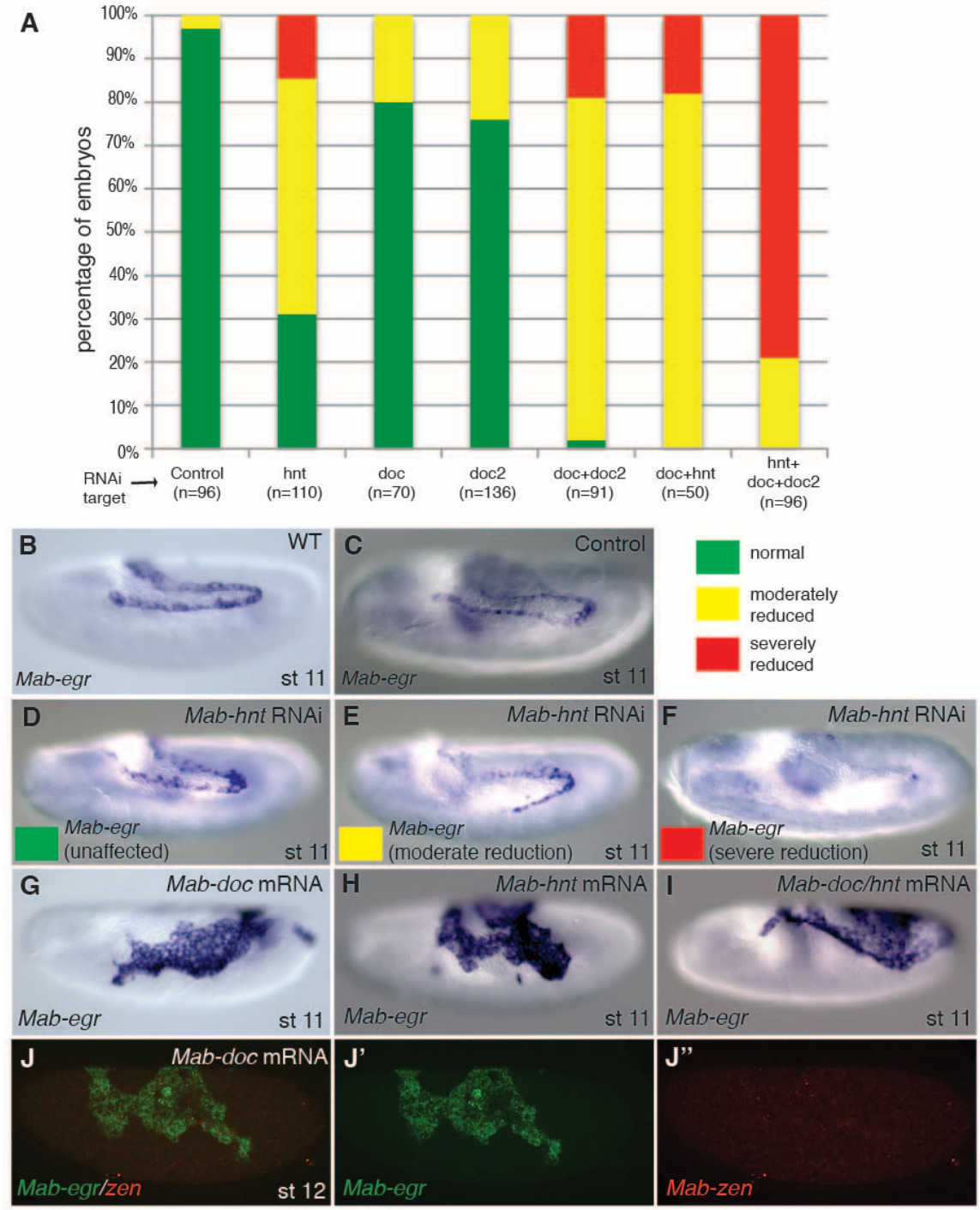

Figure 2.3.3: Mab-hnt and Mab-doc/doc2 are essential and sufficient for amnion differentiation.

A-F, Bar chart (**A**) quantifying the reduction of *Mab-egr* expression at germ band extension after *Mab-hnt* and/or *Mab-doc/doc2* knockdown and representative embryos of wild-type

Figure 2.3.3 continued

(**B**), control (**C**), normal (green, **D**), moderately reduced (yellow, **E**), or severely reduced (red, **F**) phenotypes.

G-J, *Mab-egr* expression at germ band extension following *Mab-doc* overexpression (**G**), *Mab-hnt* overexpression (**H**) and *Mab-doc/hnt* overexpression (**I**). *Mab-egr* and *Mab-zen* expression at stage 12 following *Mab-doc* overexpression (**J**).

Lateral views with dorsal up and anterior left.

of *Mab-doc*, *Mab-hnt* or *Mab-doc/hnt* induced ectopic amnion, as evidenced by an enlargement of the *Mab-egr* domain at stage 11/12 (**Fig. 2.3.3G-I**). *Mab-egr* positive cells of such embryos did not express *Mab-zen* (**Fig. 2.3.3J**), consistent with their amniotic identity. Theses results show that *Mab-doc/doc2* and *Mab-hnt* are important for the development of amniotic tissue.

2.3.2) *Mab-doc and Mab-hnt* may specify amnion indirectly by regulating BMP signaling

To test whether *Mab-doc* and *Mab-hnt* can induce amnion development independently of each other, I injected *Mab-hnt* mRNA into *Mab-doc/doc2* RNAi embryos or *Mab-doc* mRNA into *Mab-hnt* RNAi embryos, and examined *Mab-egr* expression in stage 11/12 embryos. Overexpression of *Mab-hnt* in *Mab-doc/doc2* RNAi embryos failed to induce ectopic *Mab-egr* expression while overexpression of *Mab-doc* in *Mab-hnt* RNAi embryos resulted in ectopic *Mab-egr* expression at stage 11/12 (**Fig. 2.3.4**). Thus, overexpression of *Mab-doc* could bypass the requirement for *Mab-hnt* in amnion specification, while overexpression of *Mab-hnt* could not bypass the requirement for *Mab-doc,* consistent with the hypothesis that *Mab-doc* and *Mab-hnt* share a common target necessary for amnion formation that is primarily dependent upon *doc* activity.

Overexpression of *Mab-doc* could promote amnion formation in an instructive manner, by activating ectopically the amnion gene network of Megaselia, or might promote amnion formation in a permissive manner, e.g., by elevating BMP signaling. I tested this possibility by injecting *Mab-doc* mRNA into *Mab-dpp* RNAi embryos. Overexpression of *Mab-doc* in *Mab-dpp* knockdown embryos resulted in the complete elimination of *Mab-egr*

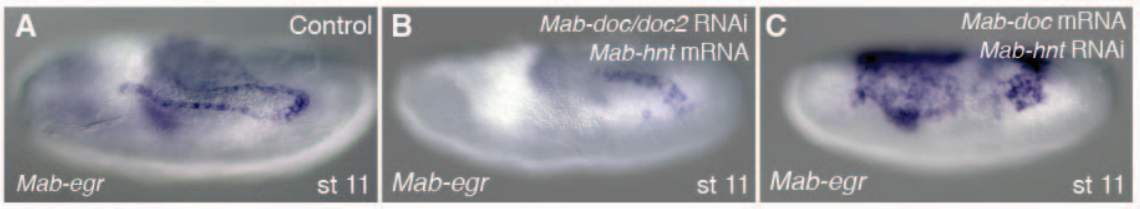

Figure 2.3.4: *Mab-hnt* and *Mab-doc* partially compensate each other in amnion development.

A-C, *Mab-egr* expression at stage 11/12 in control (**A**), following *Mab-hnt* overexpression and *Mab-doc*/*doc2* knockdown (**B**) or *Mab-doc* overexpression and *Mab-hnt* knockdown (**C**).

Lateral views with dorsal up and anterior left.

expression at stage 11/12 embryos (n=44) (**Fig. 2.3.5A-B**). Conversely, overexpression of *Mab-dpp* in *Mab-doc/doc2* knockdown embryos resulted in ectopic expression of *Mab-egr* at stage 11/12 (36%, n=47) (**Fig. 2.3.5C**). Thus, BMP signaling is sufficient to direct the expression of amnion specific genes in the absence of *Mab-doc/doc2* activity. To confirm that this result was not due to an excessive non-physiological level of Mab-Dpp produced by the injected mRNA, I asked whether the endogenous level of BMP signaling at the dorsal midline in the blastoderm embryo would be sufficient to specify amnion in the absence of both *Mab-doc/doc2* and the serosal determinant *Mab-zen*. Knockdown of *Mab-zen* partially restored amnion in *Mab-doc/doc2* knockdown embryos (**Fig. 2.3.5E-G**). This result shows that endogenous levels of *Mab-doc/doc2* are not essential for amnion specification.

To directly test whether *Mab-doc* can promote amnion formation by elevating BMP signaling, I quantified pMad staining intensity in embryos after *Mab-doc/doc2* knockdown. While *Mab-doc/doc2* knockdown had little effect on pMad levels during the late blastoderm stage compared to control embryos (one-sided Wilcoxon rank sum test, p= 0.3697; **Fig. 2.3.6A**), in early gastrula stage embryos, knockdown of *Mab-doc/doc2* resulted in significantly reduced pMad levels compared to control embryos (one-sided Wilcoxon rank sum test, p= 0.01165; **Fig. 2.3.6B**). In contrast, knockdown of *Mab-zen* did not alter the average level of pMad at the beginning of gastrulation (one-sided Wilcoxon rank sum test, p= 0.2367; **Fig. 2.3.6C**). The observation that *Mab-doc/doc2* is dispensable for amnion cell fate specification but necessary for wild-type levels of BMP signaling at the early gastrula stage strongly supports the model that amnion formation is driven by a *Mab-doc*-dependent elevation of BMP signaling in the amnion anlage at the onset of gastrulation.

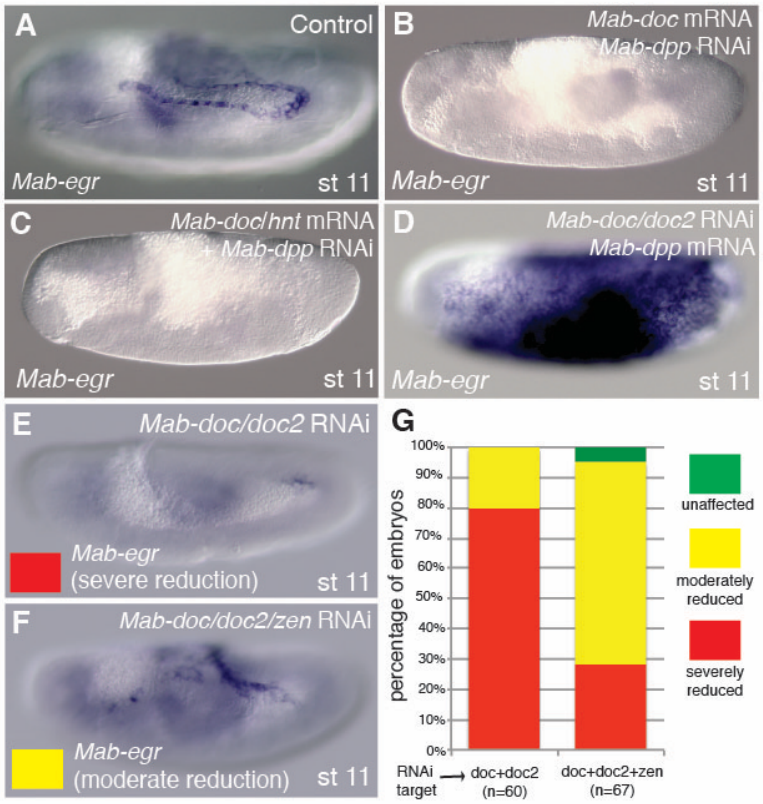

Figure 2.3.5: *Mab-doc* requires BMP signaling for amnion specification.

A-D, *Mab-egr* expression at germ band extension in control (**A**), *Mab-doc* overexpression and *Mab-dpp* knockdown (**B**), *Mab-doc*/*hnt* overexpression and *Mab-dpp* knockdown (**C**), and *Mab-dpp* overexpression and *Mab-doc*/*doc2* knockdown (**D**).

E-G, *Mab-egr* expression at stage 11/12 following *Mab-doc*/*doc2* knockdown (**E**), and *Mab-doc*/*doc2*/*zen* knockdown (**F**). Bar chart (**G**) showing the percentages of embryos with normal (green), moderately (yellow) or severely reduced (red) *Mab-egr* expression at stage 11/12 following *Mab-doc*/*doc2* knockdown or *Mab-doc*/*doc2*/*zen* knockdown.

Lateral views with dorsal up and anterior left.

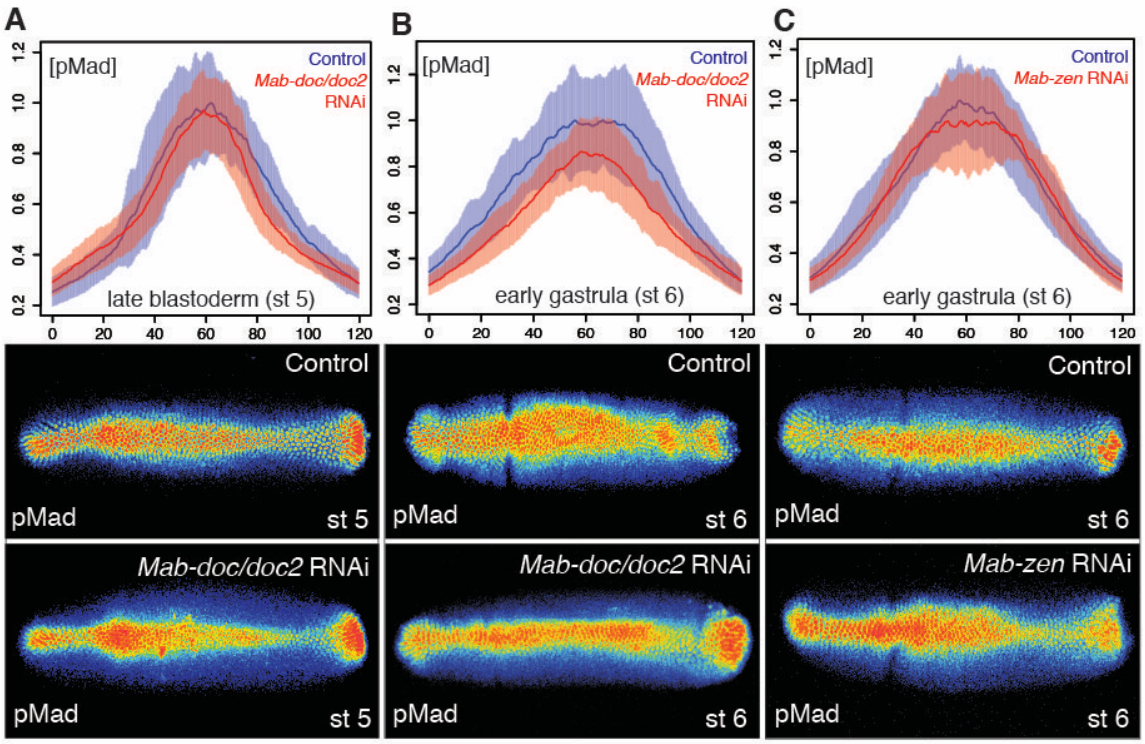

Figure 2.3.6: *Mab-doc* but not *Mab-zen* promotes gastrular BMP signaling.

A-C, Mean and shaded standard deviation of pMad intensities plotted across 120 µm of the D/V axis in control injected embryos (blue) and in *Mab-doc/doc2* knockdown embryos (red) at the cellular blastoderm stage (n=10, control n=10) (**A**), at early gastrulation (n=11, control n=11) (**B**), and in *Mab-zen* knockdown embryos (red) at early gastrulation (n=10, control n=17) (**C**) with representative embryos stained for pMad underneath each plot. Dorsal views with anterior left.

2.3.3) *Mab-doc* promotes BMP signaling partly through *Mab-egr*

I then explored the mechanism by which *Mab-doc* promotes BMP signaling at the gastrula stage. Embryos injected with *Mab-doc* mRNA displayed a local expansion of the pMad domain during gastrulation (15/15) that was typically coupled with a depletion of endogenous pMad in adjacent regions (12/15) (**Fig. 2.3.7A-B**). This result parallels a phenotype observed in Drosophila where injection of mRNA encoding activated BMP receptors into the blastoderm embryo causes an increase in BMP ligand-receptor interactions coupled with a decrease in BMP ligand-receptor binding in nearby regions (Wang and Ferguson, 2005). These data indicate that a positive feedback circuit downstream of BMP signaling increases local receptor-ligand interactions and that, due to a limiting amount of BMP ligand, ligand-receptor interactions decrease in nearby regions (Wang and Ferguson, 2005). Conversely, Megaselia embryos injected with *Mab-zen* mRNA (n=11) had a similar pMad domain to injected control embryos (n=12) (**Fig. 2.3.8A-B**) and developed a reduced or abnormal amnion (44/51) (**Fig. 2.3.8C-D**). These results suggest *Mab-doc*, but not *Mab-zen*, locally activates a positive feedback circuit in the Megaselia embryo, where BMP ligands are limiting.

Recent experiments in Drosophila identified *egr* activity as a component of a positive feedback circuit (Gavin-Smyth et al., 2013). To determine whether *Mab-egr* could be a component of this positive feedback circuit, we asked whether knockdown of *Mab-egr* could modify the phenotype caused by injection of *Mab-doc* mRNA. While the pMad domains in all these embryos were locally expanded (14/14) (**Fig. 2.3.7C**), only a few embryos (2/14) displayed a depletion of endogenous pMad in adjacent regions. These data

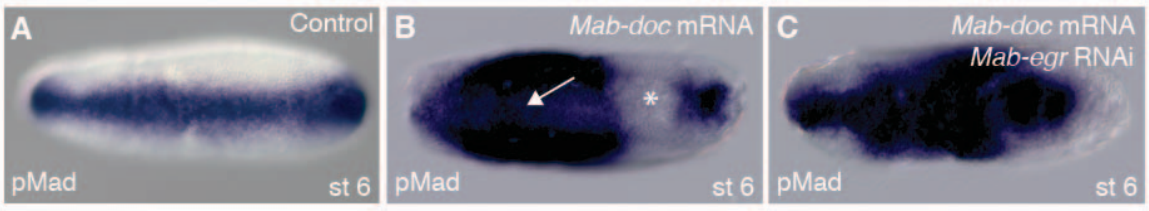

Figure 2.3.7: *Mab-doc* promotes BMP signaling partly through *Mab-egr*.

A-C, pMad in control (**A**), following *Mab-doc* overexpression at site of injection (arrow) (**B**) or *Mab-doc* overexpression and *Mab-egr* knockdown (**C**). The asterisk marks site of endogenous pMad depletion.

Dorsal views with anterior left.

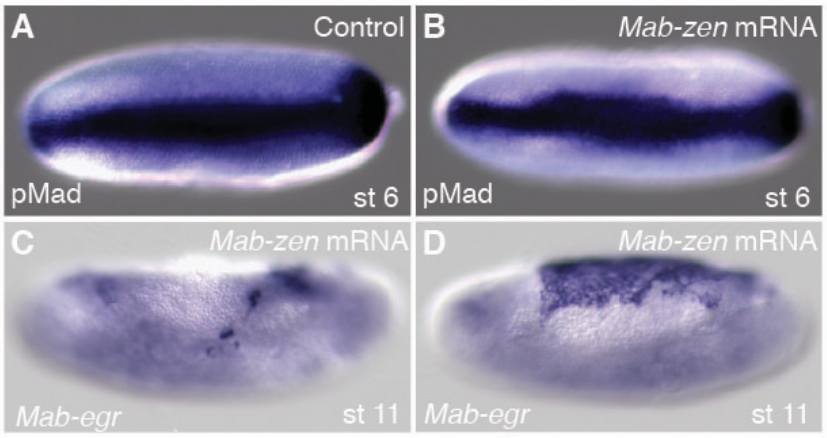

Figure 2.3.8: Effect of *Mab-zen* overexpression on BMP signaling.

A-B, pMad staining at early gastrulation in control (**A**) and after *Mab-zen* overexpression (**B**).

C-**D**, *Mab-egr* expression at late germband extension after *Mab-zen* overexpression. The majority of embryos showed reduced *Mab-egr* expression (37/51) (**C**) while a minority of embryos showed either expanded *Mab-egr* expression (7/51) (**D**), possibly as a consequence of premature serosa-amnion disruption, or were indistinguishable from wild type (7/51) (not shown).

A, **B**, Dorsal views with anterior left. **C**, **D**, Lateral views with dorsal up and anterior left.

indicate that *Mab-egr* increases the ability of cells overexpressing *Mab-doc* to compete for BMP ligands during early gastrulation.

In Drosophila, loss of *egr* reduces intensity of pMad staining by 50% (Gavin-Smyth et al., 2013). Similarly, we found that, at the onset of gastrulation, pMad levels in *Mab-egr* knockdown embryos were reduced by about 50% on average (one-sided Wilcoxon rank sum test, p= 0.00381) (**Fig. 2.3.9**). The efficiency of *Mab-egr* knockdown was confirmed by the absence of *Mab-egr* expression in *Mab-egr* RNAi (**Fig. 2.3.10**). Confluent expression domains of *Mab-eve* and *Mab-zen* could also be observed (3/10) in *Mab-egr* knockdown embryos (**Fig. 2.3.11**). As *Mab-egr* expression extends to the edge of the gastrulating germ rudiment, these observations suggest that *Mab-egr* promotes amnion specification downstream of *Mab-doc/doc2* by elevating BMP signaling during gastrulation in prospective amnion cells.

The expansion of the pMad domain in *Mab-egr* RNAi embryos injected with *Mab-doc* mRNA suggests that *Mab-doc* promotes BMP signaling not only by *Mab-egr* but also one or more other factors. One of the potential candidates is the BMP ligand *Mab-dpp*. While *Mab-doc/doc2* RNAi did not affect the expression of *Mab-dpp* in an obvious manner (**Fig. 2.3.12A-B**), preliminary data suggest that *Mab-doc* overexpression can increase the level of *Mab-dpp* (**Fig. 2.3.12C**). However, a quantitative method, such as qPCR, might be necessary to validate this finding.

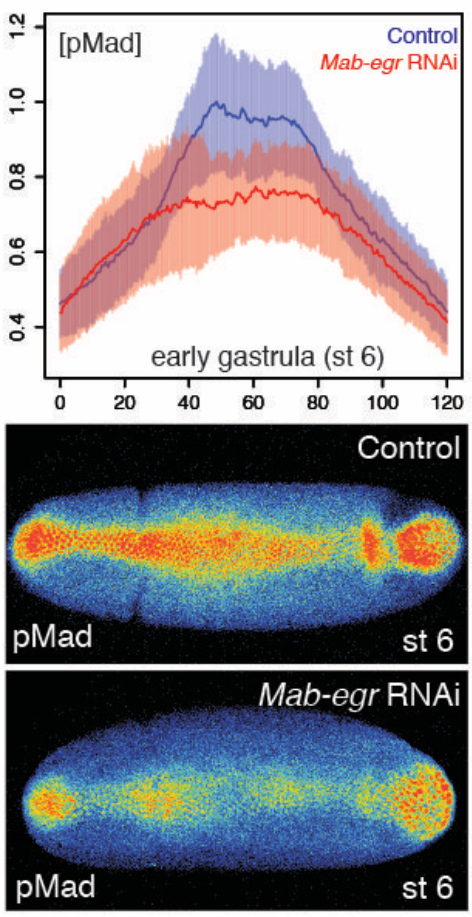

Figure 2.3.9: *Mab-egr* promotes BMP signaling.

Mean intensity and standard deviation of pMad staining plotted across 120 μm of the D/V axis in control embryos (blue, n=10) and *Mab-egr* knockdown embryos (red, n=9) at early gastrulation with representative embryos stained for pMad underneath the plot.

Dorsal views with anterior left.

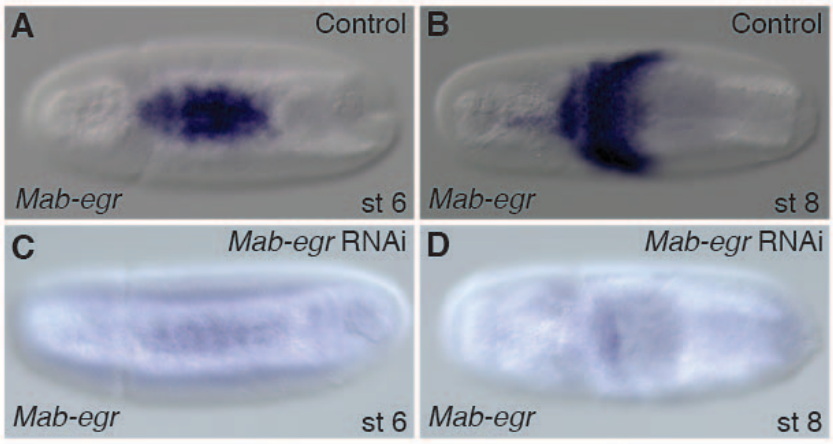

Figure 2.3.10: Efficiency of *Mab-egr* RNAi.

A-D, *Mab-egr* expression in control (**A, B**) and *Mab-egr* knockdown embryos (**C**, **D**) at early gastrulation and during germ band extension, respectively.

Dorsal views with anterior left.

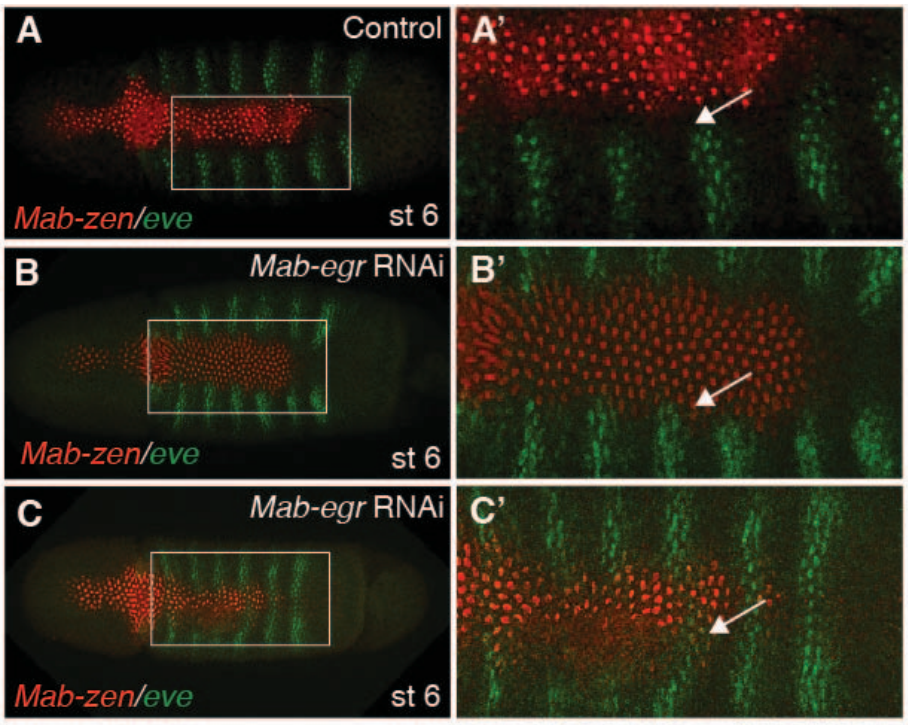

Figure 2.3.11: *Mab-egr* is essential for amnion specification.

A-C, *Mab-zen* and *Mab-eve* expression at early gastrulation in control (**A**, enlargement **A'**), and after *Mab-egr* knockdown with arrow indicating suppressed gap between the *Mab-eve* and *Mab-zen* domains (**B** and **C**, enlargement **B'** and **C'**, respectively). In severe case, *Mab-eve* strips pentrate into *Mab-zen* domain (**C**).

Dorsal views with anterior left.

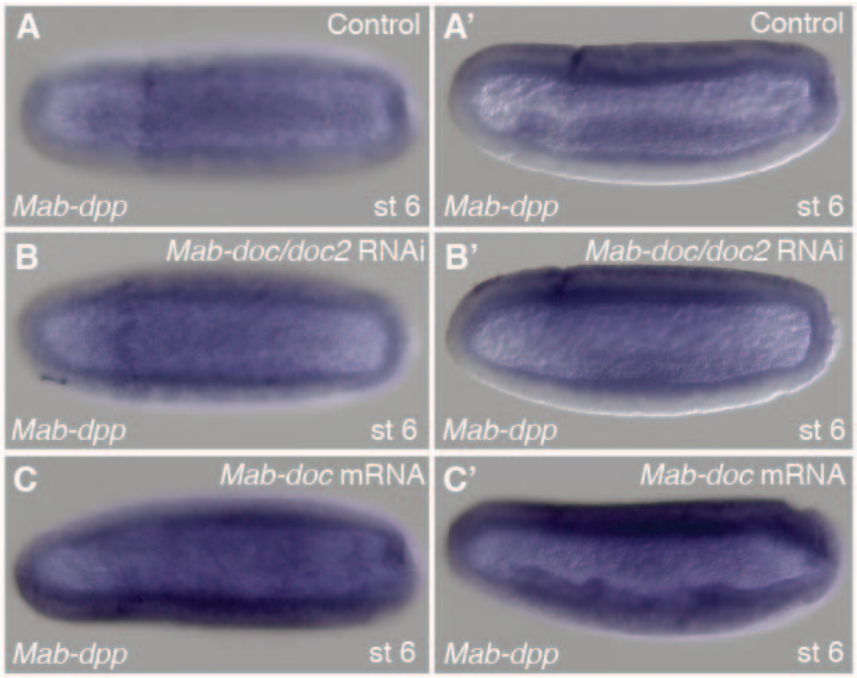

Figure 2.3.12: *Mab-doc* might promote BMP signaling through *Mab-dpp*.

A, **B**, *Mab-dpp* expression in early gastrula control embryo (**A**), following *Mab-doc*/*doc2* knockdown (**B**), or *Mab-doc* overexpression (**C**).

A, **B**, **C**, Dorsal views with anterior left. **A'**, **B'**, **C'**, Lateral views with dorsal up and anterior left.

2.3.4) *Mab-egr* is regulated by BMP signaling and *Mab-doc*, and partly by *Mab-zen*

In Drosophila, *egr* expression begins at the syncytial blastoderm stage under the control of both BMP signaling and *zen,* whereas in Megaselia, *Mab-egr* expression begins at the onset of gastrulation. To study the regulation of *Mab-egr* in Megaselia, I examined the expression of *Mab-egr* in *Mab-dpp* RNAi embryos, *Mab-doc/doc2* RNAi embryos, *Mab-doc/doc2/hnt* RNAi embryos, and *Mab-zen* RNAi embryos at stage 6. In *Mab-dpp* knockdown embryos, *Mab-egr* expression was completely absent (**Fig. 2.3.13A-B**). In *Mab-doc/doc2* knockdown embryos, *Mab-egr* expression was greatly reduced (**Fig. 2.3.13C-D**). *Mab-doc/doc2/hnt* triple knockdown did not further reduce *Mab-egr* expression during gastrulation. Finally, *Mab-zen* knockdown embryos displayed only a slight reduction in *Mab-egr* expression during gastrulation (**Fig. 2.3.13E**). This slight reduction was stage specific because at germ band extension, *Mab-zen* knockdown embryos displayed an increase in the number of *Mab-egr* expressing cells due to the transformation of serosa into amnion (**Fig. 2.3.13F**). Taken together, my results suggest that until stage 6, *Mab-egr* is primarily under the control of BMP signaling and *Mab-doc*, and partly under the control of *Mab-zen*.

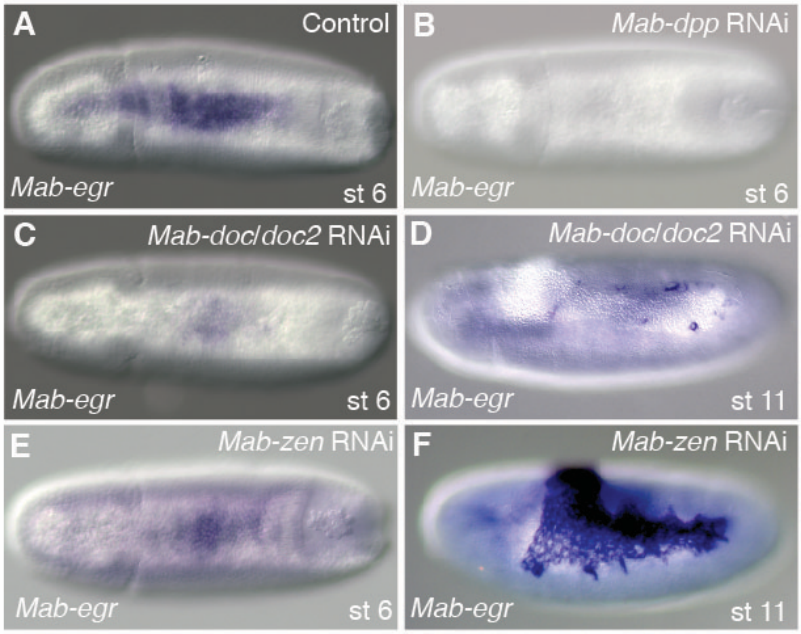

Figure 2.3.13: *Mab-egr* is regulated by BMP signaling and *Mab-doc*, and partly by *Mab-zen*.

A-F, *Mab-egr* expression in control at early garstulation (**A**), after *Mab-dpp* knockdown at early garstulation (**B**), after *Mab-doc*/*doc2* knockdown at early garstulation (**C**) and at germ band extension (**D**), and after *Mab-zen* knockdown at early gastrulation (**E**) and at germ band extension (**F**).

A-C, **E**, Dorsal views with anterior left. **D**, **F**, Lateral views with dorsal up and anterior left.

3) Discussions

3.1) Summary of the Megaselia model of extraembryonic tissue specification

I have shown that Megaselia achieves serosa and amnion specification by the dynamic change of the BMP signaling gradient, which is driven by a positive feedback loop involving *Mab-doc* and *Mab-egr* (**Fig. 3.1**). During the early blastoderm stage, Megaselia forms a shallow gradient of BMP signaling on the dorsal side of the embryo (**Fig. 3.1A**). This initial gradient may form in response to *sog*, like in Drosophila, because the expression of this gene is conserved in both species (Rafiqi et al., 2012). By the end of the blastoderm stage, the shallow pMad gradient has refined into a sharp peak that represses the *Mab-eve* expression along the dorsal midline (**Fig. 3.1B**). This transformation is likely promoted by a positive feedback mechanism, like in Drosophila, but may occur independently of *egr*, given that *Mab-egr* expression begins at the end of stage 5. Hence, the underlying mechanism for sharpening the BMP signaling gradient in Megaselia embryos during the blastoderm stage remains unknown. In Megaslia, the blastodermal BMP gradient might be solely responsible for establishing the nested expression of *Mab-zen* in prospective serosa and *Mab-doc/doc2* and *Mab-hnt* in prospective serosa and amnion tissues, respectively, but the temporally distinct requirement of BMP signaling for serosa and amnion specification that I demonstrated in this study shows that nested expression of these genes is not sufficient for the differential specification of serosa and amnion. Activation of *Mab-zen* and repression of *Mab-eve* ensures serosa specification during the late blastoderm stage. While this patterning phase is not sufficient to specify amnion tissue, it sets the stage for *Mab-doc/doc2*-dependent *Mab-egr* expression during gastrulation. After the onset of

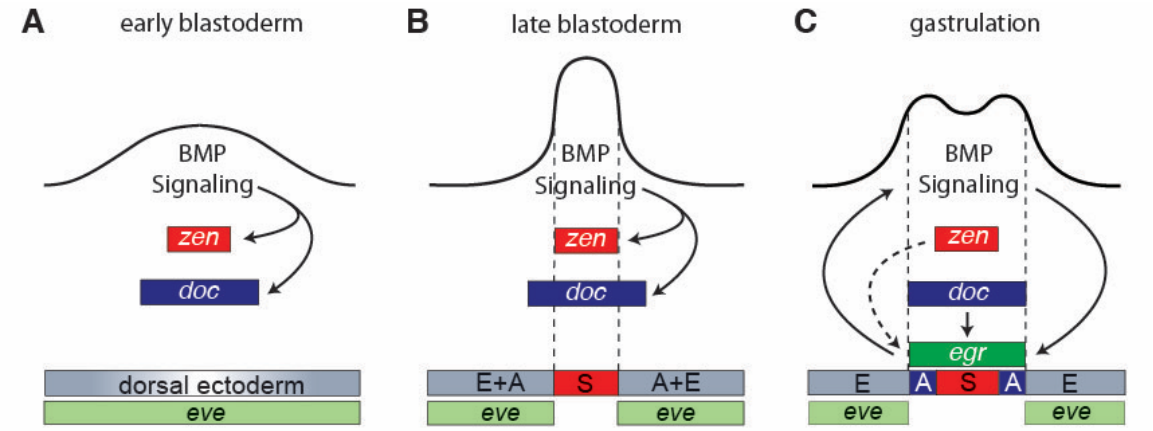

Figure 3.1: Model of extraembryonic tissue specification in Megaselia.

Consecutive BMP signaling profiles (continuous lines) are depicted above sketches of the developing dorsal ectoderm (grey) in cross section, illustrating BMP-dependent steps of sequential serosa (red) and amnion (blue) specification at early blastoderm (A), late blastoderm (B) and early gastrulation (C). The midpoint of ectoderm represents the dorsal midline. S: serosal tissue; A: amniotic tissue; E: embryonic tissue.

gastrulation, *Mab-doc/doc2* and BMP signaling, with additional input from *Mab-zen*, activates *Mab-egr* expression (**Fig. 3.1C**). While *Mab-doc/doc2* expression begins during early blastoderm, *Mab-egr* expression is delayed, beginning just before the onset of gastrulation. The reason for this delay remains unknown. Here I propose that the *Mab-doc/doc2*-dependent *Mab-egr* expression in the serosa and amnion promotes BMP signaling in these tissues and guides the broadening of BMP signaling during gastrulation. Gastrular BMP signaling at the edge of the germ rudiment may finalize the specification of amnion by repressing regulators of embryonic development such as *Mab-eve*.

3.2) Comparison between Megaselia and Drosophila model

Megaselia and Drosophila have different BMP gradient dynamics (**Fig. 3.2**). Specifically, while both species show refinement of a shallow BMP gradient into a sharp peak during blastoderm, during early gastrulation, BMP signaling broadens and intensifies at the edge of the germ rudiment in Megaselia, but remains static in Drosophila. This Megaselia-specific gradient broadening is important for amnion specification. Drosophila may have lost the ability to specify amnion cells during gastrulation at the edge of the germ rudiment because it no longer exposes these cells to high BMP signaling. Interestingly, three-dimensional mathematical modeling of BMP activity predicts that broadening of BMP activity can also occur in Drosophila when there is an increase in embryo size or highly active positive BMP signaling feedback (Umulis and Othmer, 2012; Umulis et al., 2010). This occurs due to an imbalance between the transport of BMP-ligands and the rate at which they are being captured by receptors. The dynamics of BMP activity observed in

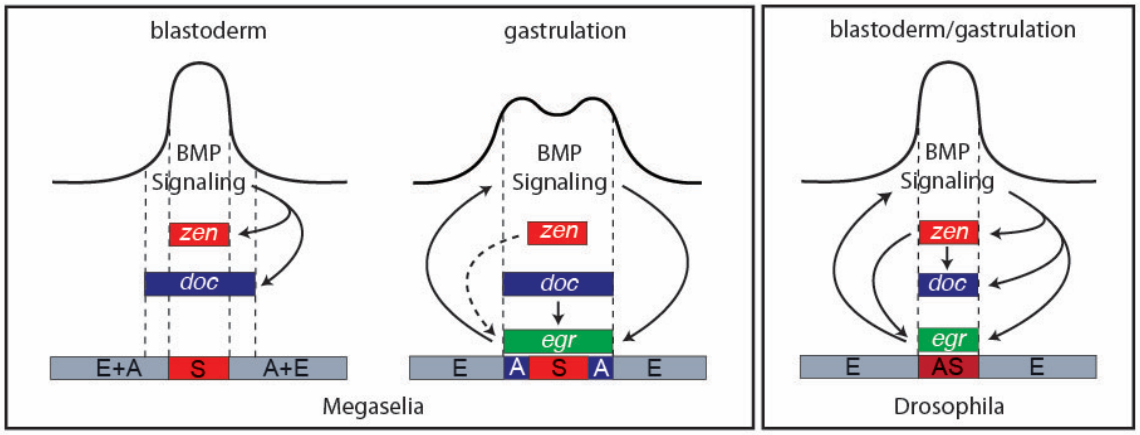

Figure 3.2: Comparison of extraembryonic tissue specification between Megaselia and Drosophila.

Consecutive BMP signaling profiles (continuous lines) are depicted above sketches of the developing dorsal ectoderm (grey) in cross section, illustrating BMP-dependent steps of sequential serosa (red) and amnion (blue) specification in Megaselia and amnioserosa (maroon) specification in Drosophila. The midpoint of ectoderm represents the dorsal midline. S: serosal tissue; A: amniotic tissue; E: embryonic tissue; AS: amnioserosa.

these simulations are remarkably similar to sequential changes of pMad distribution in the dorsal ectoderm of Megaselia. The embryo sizes of Drosophila and Megaselia are similar and therefore probably not the cause for the observed differences in the spatiotemporal pMad profiles of these species (Rafiqi et al., 2012). However, modification of the positive feedback loop could have altered the pMad profile in the Drosophila lineage.

I propose that the distinct BMP gradients of Megaselia and Drosophila are primarily the result of spatial changes in an *egr*-dependent positive feedback circuit during gastrulation. In Drosophila, *Doc* (along with *hnt*) is expressed downstream of *zen* and their expression domains in the amnioserosa match. In Megaselia, *Mab-doc* and *Mab-hnt* are expressed independent of *Mab-zen* and overlap with edge of the germ rudiment, which gives rise to the amnion. The shifted control of *egr* expression from *Doc* to *zen* in the Drosophila lineage is sufficient to explain the difference of *egr* expression between the two species during gastrulation, and hence also the difference in BMP signaling and tissue specification at this developmental stage. I therefore propose that this change led the evolutionary transition of the BMP gradient. Once *Doc* was downstream of *zen*, the latter might have gradually gained direct control of *egr* expression. This scenario is consistent with the observation that even in Megaselia, *Mab-zen* slightly promotes *Mab-egr* expression.

The data presented in this study seem to suggest that Drosophila only develops a reduced amnion. However, as suggested previously (Rafiqi et al., 2008, 2010), downregulation of *zen* in the amnioserosa after gastrulation might transform the amnioserosa cells into amnion cells. In Megaselia, *Mab-zen* expression continues in the serosa throughout the process of serosa formation. This suggests that the repression of *zen*

enables Drosophila embryos to specify amnion at a later stage, such that amnion functions in germ band retraction and dorsal closure can be executed. Since these processes are vital, the change of *zen* expression should have preceded the change in the positive feedback network in the lineage of flies with amnioserosa (Schizophora) to avoid an evolutionary stage without amnion. Thus, based on previous studies and my results, a possible evolutionary scenario of how amnioserosa arose can be reconstructed: first, repression of postgastrular *zen* expression was gained which led to loss of sersoa maintenance and expansion after gastrulation; second, the broadening of BMP gradient during early gastrulation was lost to reduce extraembryonic tissue types being initially specified from two to one.

Drosophila also acquired a BMP-independent broad *zen* expression domain in the syncytial blastoderm, which is not observed in other dipterans (Goltsev et al., 2007; Rafiqi et al., 2008). The acquisition of this early *zen* domain promotes *egr* expression in the syncytial blastoderm of Drosophila, where *egr* is part of a *zen*-dependent network that confers robustness to the BMP gradient (Gavin-Smyth et al., 2013). This early phase of *zen* expression is likely a derived feature that is not related to extraembryonic tissue evolution.

While the identity of regulatory factors of the positive feedback circuit may be evolutionarily labile (in Tribolium *Doc* and *hnt* appear to be dispensable for amnion specification (Horn and Panfilio, 2016)), the mechanism of amnion specification through feedback-driven spatiotemporal change in BMP signaling could apply to a wide range of insects, because in Tribolium the pMad domain also gradually shifts from the serosa to the presumptive amnion during early gastrula stages (Nunes da Fonseca et al., 2008; Sharma et al., 2013; van der Zee et al., 2006). The principle of evolving tissue complexity through

changes in positive feedback circuits of morphogen gradients has not yet been documented in other developmental contexts, but might also apply to unrelated traits, such as eyespots on butterfly wings (Monteiro, 2015).

4) Future directions

4.1) Role of *crossveinless-2* in Megaselia

In Drosophila, robustness of the BMP gradient requires a genetic network that involves *egr* and *cv-2* (Gavin-Smyth et al., 2013). The *egr cv-2* double mutant has more variability in the BMP gradient and amnioserosa cell number than the wild type. In contrast to *egr*, *cv-2* negatively regulates BMP signaling, and *cv-2* mutants show elevated BMP signaling. In Drosophila, *cv-2* is expressed in a broad dorsal domain and activated by the early phase of *zen* expression, together with *egr*. *cv-2* encodes a cell surface BMP binding protein that can either enhance or inhibit BMP signaling depending on the dosage and context (Conley et al., 2000; Serpe et al., 2008). At high concentration, *cv-2* sequesters BMP ligand and suppress the signaling while at low concentration facilitates the transfer of the ligand to the BMP receptor and promoting signaling (Serpe et al., 2008). The effect of *cv-2* also depends on the type of ligands. While in cell culture assay, *cv-2* only inhibits *dpp* signaling, it has biphasic effect on *gbb* signaling as it can both inhibit and promote signaling, depending on the concentration (Serpe et al., 2008). Interestingly, while *gbb* is not expressed in wild-type Drosophila blastoderm embryos, *Mab-gbb* is expressed in Megaselia blastoderm embryos and is required for dorsal-ventral patterning (Rafiqi et al., 2012). Therefore, the effect of cv-2 on BMP signaling in Megaselia is difficult to predict. One possibility is that the dorsal-most region with high *Mab-cv-2* concentration inhibits *Mab-gbb* signaling whereas slightly lateral region with moderate *Mab-cv-2* concentration will enhance *Mab-gbb* signaling. My preliminary analysis of *Mab-cv-2* is consistent with this hypothesis. In Megaselia, *Mab-cv-2* expression begins after the onset of gastrulation and, while occurring broadly, is slightly increased in extraembryonic region (**Fig. 4.1.1**).

Like *Mab-egr* (**Fig. 2.3.10**), *Mab-cv-2* and *Mab-egr/Mab-cv-2* knockdown also produced confluent expression domains of *Mab-zen* and *Mab-eve* (3/9 and 2/9, respectively) (**Fig. 4.1.2**), suggesting that *Mab-cv-2* is required for normal BMP patterning in Megaselia. However, *Mab-cv-2* in *Mab-doc/doc2* RNAi embryos was similar to its expression in wild-type embryos (**Fig. 4.1.3**), unlike *Mab-egr*. In order to determine whether *Mab-cv-2* enhance or inhibit BMP signaling in Megaselia, one can examine how *Mab-cv-2* RNAi affect the pMad profile. A reduction in pMad level will suggest that *Mab-cv-2* is BMP enhancer while elevation of pMad level will suggest BMP inhibition.

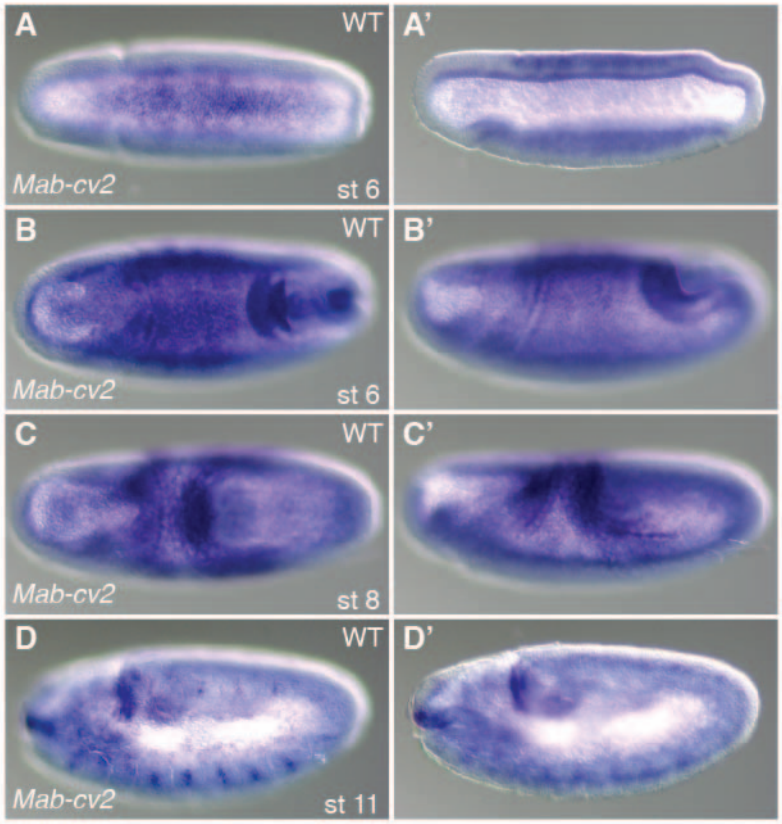

Figure 4.1.1: Expression profile of *Mab-cv-2*.

A-D, *Mab-cv-2* expression in Megaselia embryos at early gastrulation (**A**), late gastrulation (**B**), during germ band retraction (**C**), and at the end of germ band retraction (**D**).

A, **B**, **C**, Dorsal views with anterior left. **A', B'**, **C'**, **D**, **D'**, Lateral views with dorsal up and anterior left.

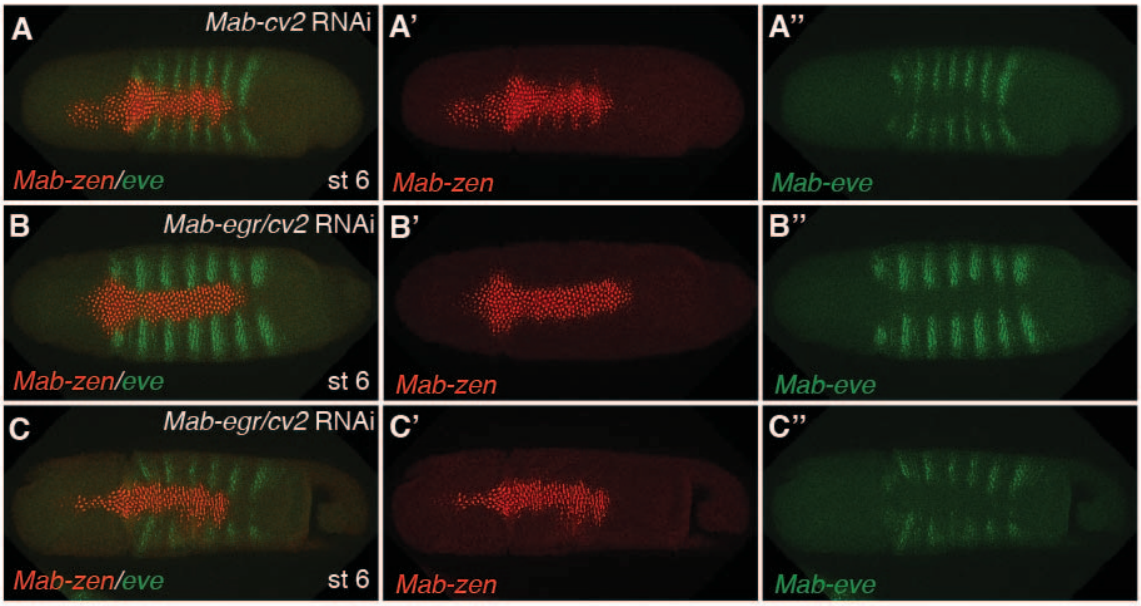

Figure 4.1.2: *Mab-cv-2* is essential for amnion specification.

A-C, *Mab-zen* and *Mab-eve* expression at early gastrulation after *Mab-cv-2* knockdown (**A**), and after *Mab-egr/cv-2* knockdown (**B-C**).

Dorsal views with anterior left.

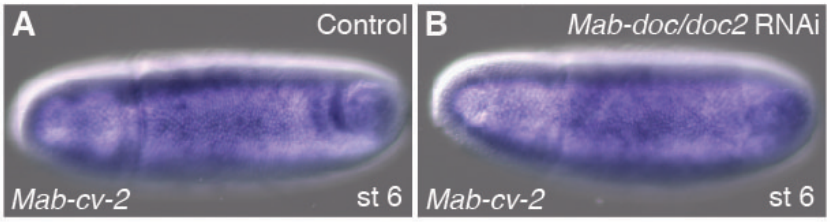

Figure 4.1.3: Regulation of *Mab-cv-2* is largely independent of *Mab-doc/doc2*.

A-B, *Mab-cv-2* expression at early gastrulation in control (**A**) and after *Mab-doc/doc2* knockdown (**B**). Dorsal views with anterior left.

4.2) Role of the JNK pathway in positive feedback of BMP signaling

egr promotes BMP signaling via the JNK pathway in Drosophila. *egr* encodes the ligand for the JNK pathway which transduces via the effector JNK homolog *basket (bsk)*. *egr* and *bsk* mutant embryos show reduction in BMP signaling intensity (Gavin-Smyth et al., 2013). To explore the possibility that *Mab-egr* also activates the JNK pathway to promote BMP signaling, one can monitor the effect on BMP signaling following knockdown of different JNK components. Two possible candidates would be homologs of *bsk* and JNK kinase *hemipterous (hep)*. In the case of *Mab-bsk*, knockdown should be feasible because this gene might not be expressed maternally (**Fig. 4.2A**). One potential obstacle could be the maternal *hep* expression in Megaselia, which is suggested by our transcriptome data (**Fig. 4.2B**). Since embryonic injection of dsRNA would be ineffective against maternally translated Hep protein, other techniques such as transgenic or CRISPR/Cas9 may need to be developed in order to disrupt the activity of this gene. Another interesting pathway component is the JNK receptor. So far only two JNK receptors have been found in Drosophila: *wengen* (*wgn*) (Kanda et al., 2002) and *grindelwald* (*grnd*) (Andersen et al., 2015), both of which mediate the activity of *egr*. In the blastoderm embryo, *wgn* is expressed on the ventral side while *grnd* has a broad dorsal expression domain (Berkeley Drosophila Genome Project), suggesting that *grnd* is likely the receptor to mediate *egr*-dependent positive feedback. Our Megaselia transcriptome suggest *Mab-grnd* expresssion begins at stage 5 and peaks during gastrulation (**Fig. 4.2C**), suggesting that *Mab-grnd* could also mediate the function of *Mab-egr* in Megaselia to promote BMP signaling and amnion specification. To test this hypothesis, one can examine the expression of *Mab-grnd* to determine whether it is expressed on the dorsal side during early gastrulation. If *Mab-grnd*

is required for BMP signaling and amnion specification, pMad level and *Mab-egr* expression at stage 11/12 would be reduced following *Mab-grnd* RNAi.

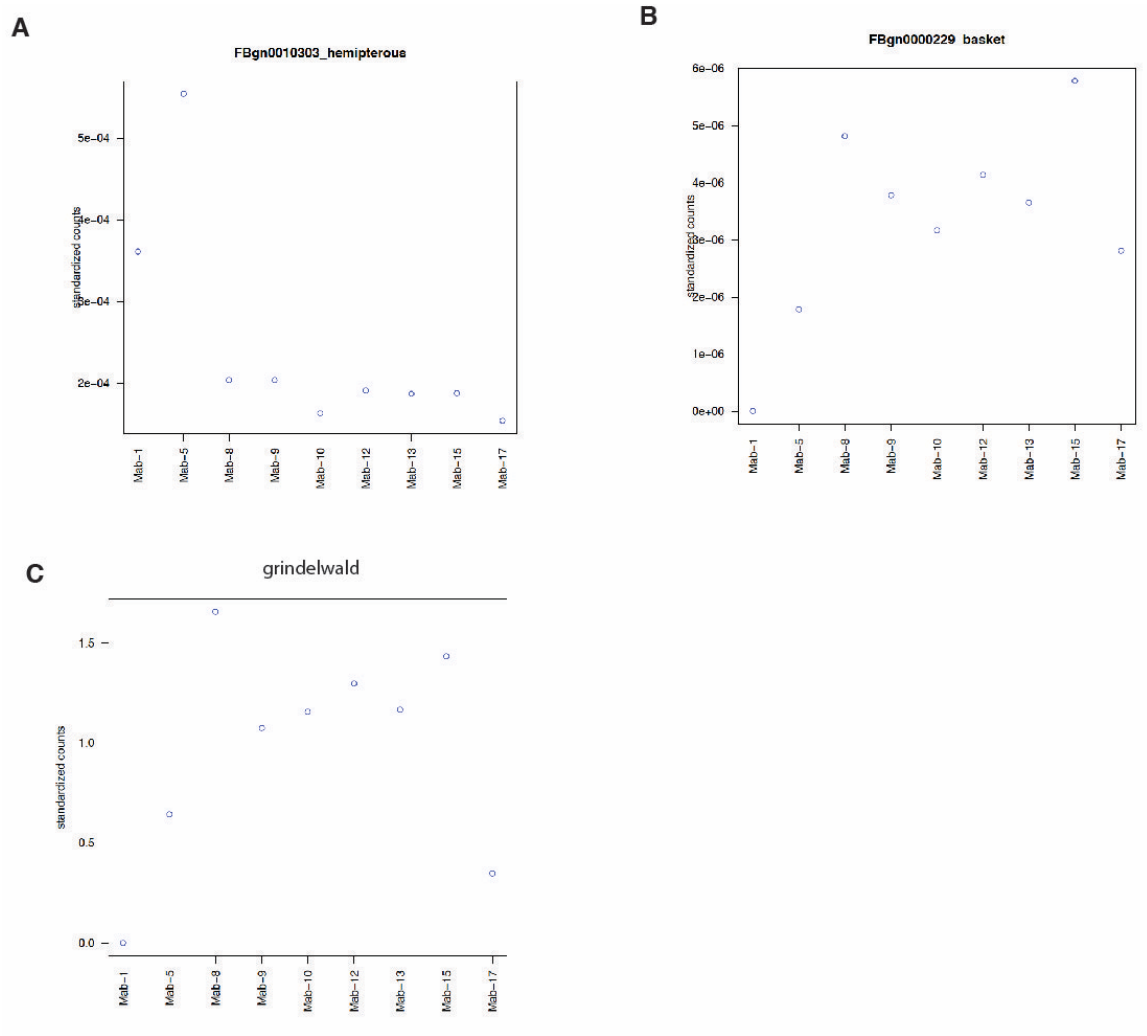

Figure 4.2: Transcriptome profile of JNK pathway gene in Megaselia.

A-E, Expression profile of JNK pathway genes, *hemipterous* (A), *basket* (B) and *grindelwald* (C) in Megaselia. For images of the embryonic stages, please refer to figure 5.

4.3) Role of *CG6234* in extraembryonic tissue specification

The gene *CG6234* encodes a putative transmembrane protein that was shown to be upregulated at gastrulation stage compared to syncytial blastoderm (Zúñiga et al., 2009). *CG6234* is first expressed on the dorsal side during blastoderm stage and its expression continues in the amnioserosa until germ band extension (Zúñiga et al., 2009). Following *CG6234* knockdown, the number of amnioserosa cells is reduced and defects in germ band retraction are observed, suggesting that *CG6234* is important for amnioserosa development. Interestingly, its homolog in Megaselia, *Mab-CG6234* is also expressed on the dorsal side (**Fig. 4.3**), suggesting a conserved role in control extraembryonic tissue development. However, unlike Drosophila, *Mab-CG6234* is only weakly detected at stage 5 and only becomes strongly expressed after the onset of gastrulation. Functional studies can be conducted on *Mab-CG6234* to explore its role in serosa and amnion development. The development of these two tissues can be followed in *Mab-CG6234* RNAi using *Mab-zen* and *Mab-egr* as serosa and amnion markers, respectively. *Mab-CG6234* may also be involved in positive feedback of the BMP signaling gradient, which can be tested by quantification of pMad level following *Mab-CG6234* knockdown and monitoring *Mab-CG6234* expression following *Mab-dpp* RNAi.

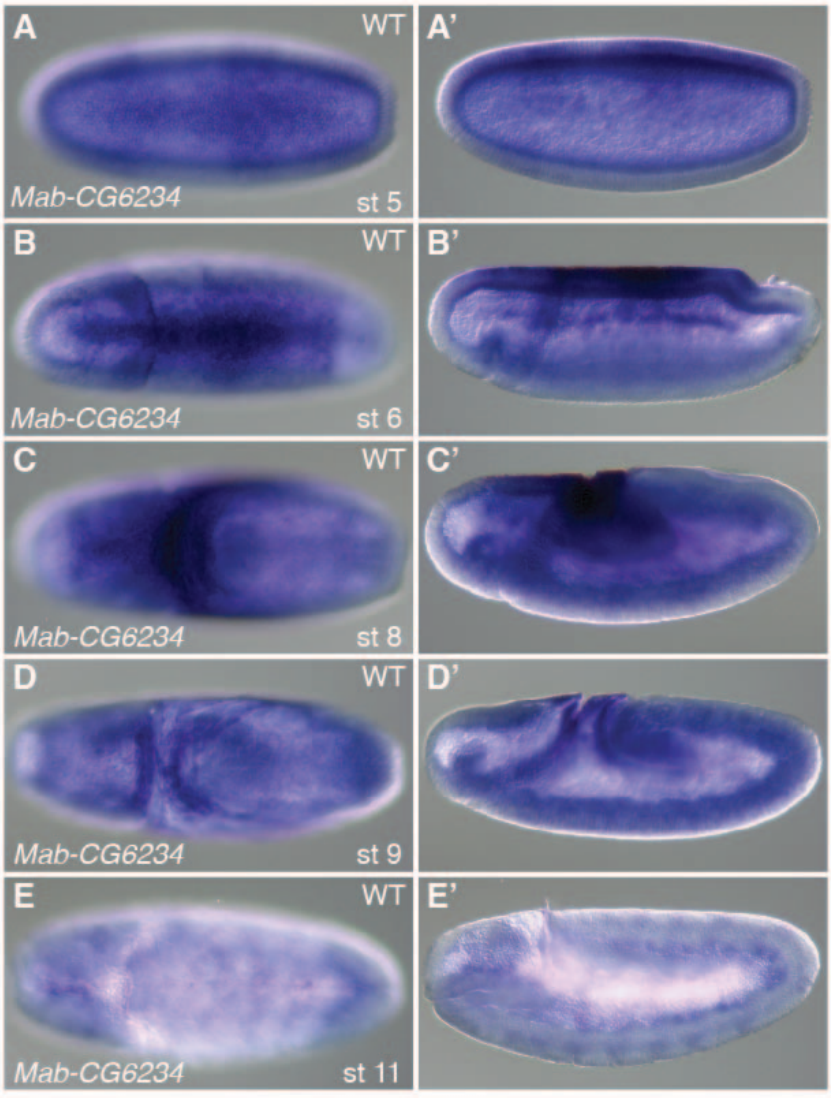

Figure 4.3: Expression profile of *Mab-CG6234*.

A-E, *Mab-CG6234* expression in Megaselia embryos at blastoderm (**A**), early gastrulation (**B**), early germ band extension (**C**), late germ band extension (**D**), and end of germ band extension (**E**).

A-D, Dorsal views with anterior left. **A'-E'**, Lateral views with dorsal up and anterior left. **E**, Ventral views with anterior left.

4.4) Mechanism of BMP gradient refinement during blastoderm stage in Megaselia

In section 2.3.2, I showed that *Mab-doc* elevates BMP signaling during early gastrulation but is dispensable during late blastoderm stage. How Megaselia refines the BMP gradient during blastoderm stages remains unknown. In Drosophila, the refinement of the BMP gradient during blastoderm stages is driven by *zen* and *egr*. Unlike *Mab-egr*, *Mab-zen* is expressed and coincides with the pMad domain during the blastoderm stage in Megaselia, suggesting that *Mab-zen,* while dispensable for promoting gastrular BMP signaling, may be required for BMP gradient refinement during the late blastoderm. This hypothesis can be tested by monitoring how pMad level is affected at the late blastoderm stage following *Mab-zen* knockdown and overexpression. Reduction of the pMad level after knockdown and an expansion of the pMad domain after overexpression would suggest that *Mab-zen,* similar to its Drosophila homolog, plays a conserved role in boosting BMP signaling, probably also via intracellular positive feedback. Other potential candidates are homologs of u-shaped group genes including *u-shaped (ush), serpent (srp), hnt, Doc,* and *tail-up (tup)*, which in Drosophila are important for the maintenance of amnioserosa and required for germ band retraction and dorsal closure (Frank and Rushlow, 1996; Reim et al., 2003; Yip et al., 1997). Except for *srp* (**appendix 6.1**)*, ush, hnt* and *tup* are also expressed on the dorsal side in Meagselia blastoderm embryos and required for germ band retraction and dorsal closure (Rafiqi et al., 2010), suggesting that they may be required for elevating BMP signaling. To test these hypotheses, I would quantify the pMad level in late blastoderm embryos following knockdown of u-shaped group genes.

Recently, it has been shown that the BMP peak of Drosophila embryos also depends on a positive feedback loop involving integrin (Sawala et al., 2015). This study shows that

integrin, which is an extracellular matrix receptor, is activated by the extracellular matrix protein collagen IV. The activated integrin then interacts with BMP receptors and stimulates the phosphorylation of Mad protein. BMP signaling, on the other head, activates integrin expression, thus forming a positive feedback loop that is required for the refinement of BMP peak gradient. Transcriptome data did not show expressions of the different copies of integrin genes in blastoderm stage in Megaselia (**Fig. 4.4**), however this finding needs to be confirmed by in situ hybridization.

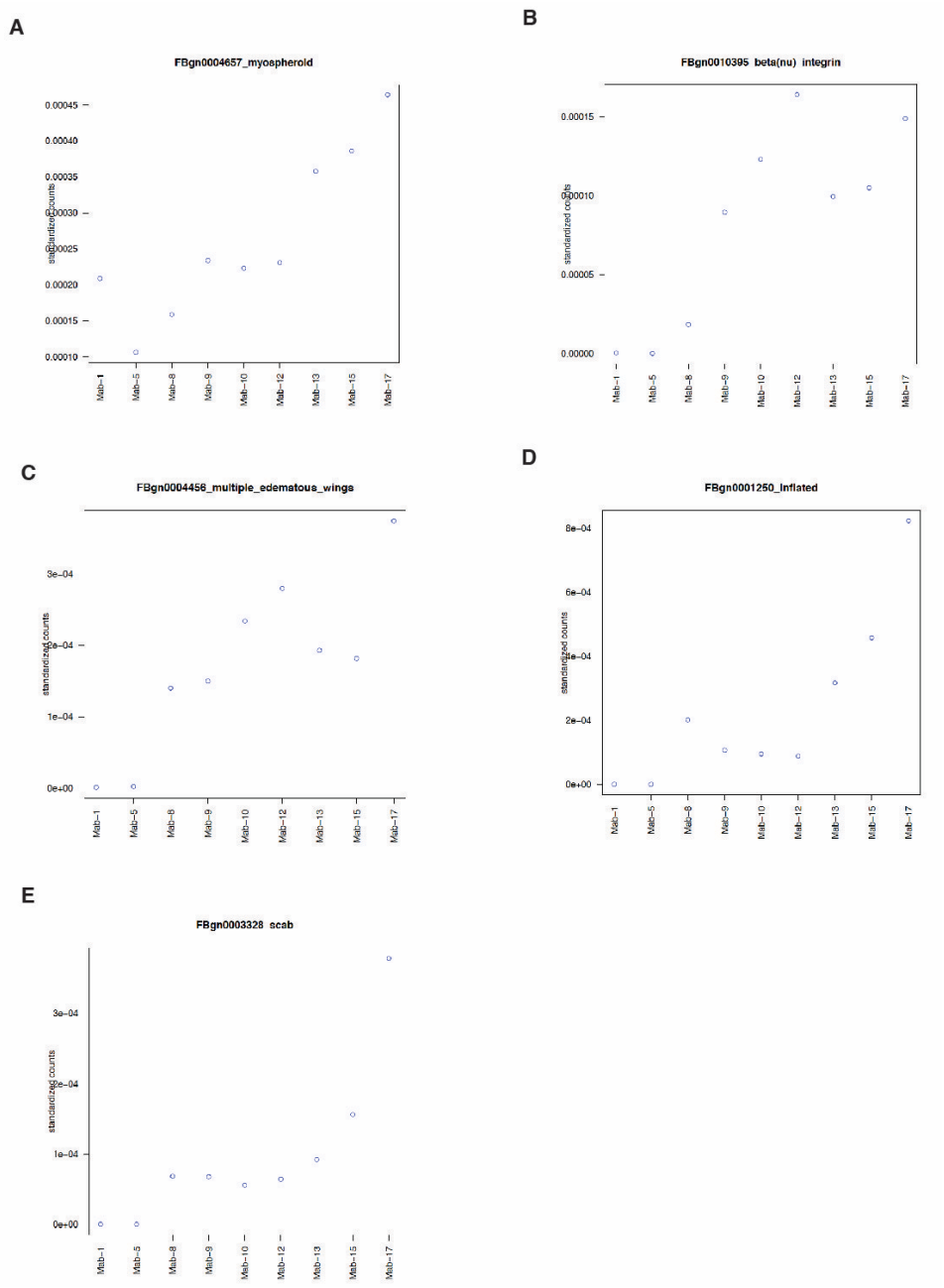

Figure 4.4: Transcriptome profile of integrin gene in Megaselia.

A-E, Expression profile of two beta-integrin genes, *myospheroid* (A) and *Integrin betanu subunit* (B) and three alpha-integrin genes, *multiple edematous wings* (C), *inflated* (D) and *scab* (E) in Megaselia. For images of the embryonic stages, please refer to figure 5.

4.5) Mechanism of ventral amnion development

The dorsal amnion in Megaselia represents an intermediate condition that is found in lower Cyclorrhapha flies while non-cyclorrhaphan flies and most other insects have a ventral amnion, which represents the ancestral condition (**Fig. 1.1**). Despite the wide phylogenic occurrence of ventral amnion closure, it is not known how ventral instead of dorsal amnion closure is achieved. One can explore this question by taking advantage of two model dipteran species in our lab that close the amnion ventrally: the midge *Chironomus riparius* in the Chironomidae family and mothfly *Clogmia albipunctata* in the Psychodidae family, which have well-establish protocols and genomic resources (Caroti et al., 2015; Jiménez-Guri et al., 2013, 2014; Klomp et al., 2015). My preliminary studies in Chironomus show that the pMad domain narrowly straddles the dorsal midline during blastoderm stages, but is much broader during early gastrulation (**Fig. 4.5A-C**). To confirm whether Chironomus, similar to Megaselia, also shows a broadening of BMP gradient beyond serosal tissue during gastrulation, one would need to do a double staining of pMad with *Mab-zen*. The broadening in Chironomus seems to be much more extensive compared to Megaselia, which may relate to the larger ventral amniotic tissue compare to dorsal amnion. *Cri-zen* and *Cri-hnt* also show dorsal expression while *Mab-eve* stripes are repressed dorsally during the blastoderm and gastrulation stage (**Fig. 4.5D-K**). However, no *Cri-egr* expression was detected in the blastoderm embryo in preliminary in situ hybridization experiments. This result needs to be confirmed by testing other probes that bind to different regions of the *Cri-egr* gene. If this negative result will be confirmed, it would suggest that the positive feedback circuit for BMP signaling is evolutionarily labile in dipterans. Furthermore, if *Cri-egr* cannot be used to monitor amnion development, an

alternative amnion marker would have to be identified in Chironomus. Alternatively, one could explore *egr* expression in another well-established model, Clogmia. Another interesting option is the soldier fly, *Hermetia illucens* in the Stratiomyidae family, which is being developed as another model in our lab. Although not as well-established as the other two species with regard to protocols and genomic resources, being a member of Brachycera, Hermetia is more closely related to the Cyclorrhapa flies including Megaselia and Drosophila and thus may be a better comparative model.

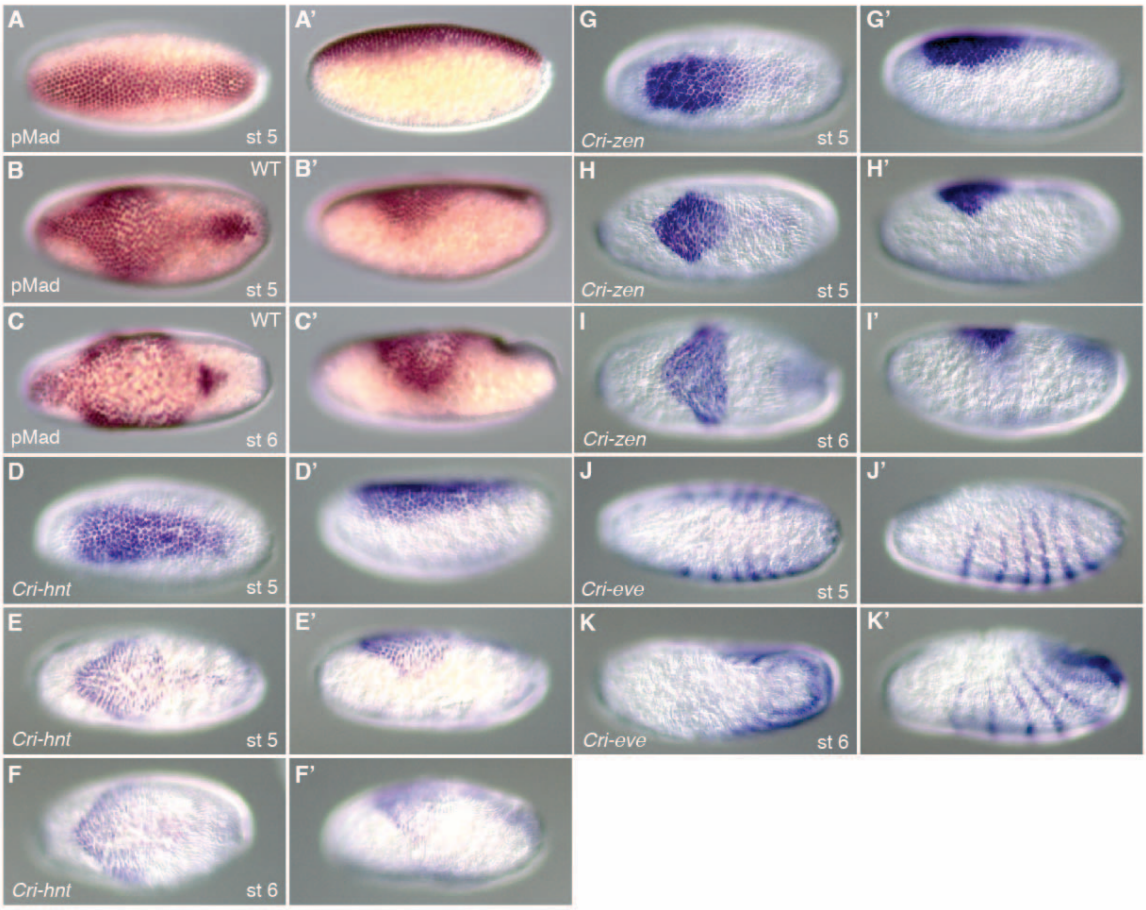

Figure 4.5: *Cri-zen*, *Cri-hnt* and *Cri-eve* expression, and pMad staining in *Chironomus riparius*.

A-C, pMad in Chironomus embryos at blastoderm (**A-B**), and early gastrulation (**C**).

D-F, *Cri-hnt* expression in Chironomus embryos at blastoderm (**D-E**), and early gastrulation (**F**).

G-I, *Cri-zen* expression in Chironomus embryos at blastoderm (**G-H**), and early gastrulation (**I**).

J-K, *Cri-eve* expression in Chironomus embryos at blastoderm (**J**), and early gastrulation (**K**). **A-K**, Dorsal views with anterior left. **A'-K'**, Lateral views with dorsal up and anterior left.

5) Materials and Methods

5.1) Megaselia culture, embryo collection, and fixation

Megaselia culture, embryo collection, and fixation are based on the standard protocols (Rafiqi et al., 2011). Briefly, cultures were maintained in three phase-shifted generations (each shifted by a week), each of which comprises 24 bottles. Megaselia was cultured in standard large Drosophila bottles (13 cm height x 5.5 cm diameter), supplemented with moist cotton and a protein-rich fish food mixture (Mix one part Spirulina Flake Food (Aquatic Eco-Systems, Inc., cat. no. ZSF5) with two parts Slow Sinking Powder (Aquatic Eco-Systems, Inc. cat. no. F1A) by weight. I maintained the cultures in an environmentally controlled chamber (BioCold Environmental Inc.) set at 25˚C and 50%–60% relative humidity on a 16/8-h day/night cycle, with the beginning of the dark cycle in the morning at 8-9 am. This setting for the light/dark transition allows egg collections in the morning because egg deposition peaks shortly (15–30 min) after the beginning of the dark cycle. Culture handling is described in the appendix (Protocol 1).

5.2) RNA probe, dsRNA and mRNA synthesis

RNA probes were labeled with digoxigenin (*Mab-egr, Mab-CG6234, Mab-cv-2, Mab-srp, Mab-CG7997, Mab-zen, Mab-cad, Mab-ftz, Mab-run, Mab-dpp,* and *Cri-hnt*), fluorescein (*Mab-doc*, *Mab-doc2, Mab-zen, Mab-hnt, Mab-h,* and *Cri-zen*) and biotin (*Mab-eve* and *Cri-eve*) as described (Kosman et al., 2004; Tautz and Pfeifle, 1989). Probe templates were synthesized from an embryonic cDNA library using the following primers:

Mab-CG6234 (#248)

5’-CAGAGATGCAATTAACCCTCACTAAAGGGAGAACCACCGAGCTCGATTGGAAGA-3’

5’-CCAAGCCTTCTAATACGACTCACTATAGGGAGATCCTCAAGCTCGTCATCGGCGT-3’

Mab-cv-2 (#250)

5’-CAGAGATGCAATTAACCCTCACTAAAGGGAGAACGGCGCAAATCCGACTGTTGT-3’

5’-CCAAGCCTTCTAATACGACTCACTATAGGGAGAAACGCAGAGTGGAGCCGCTT-3’

Mab-srp (#253)

5’-CAGAGATGCAATTAACCCTCACTAAAGGGAGATTCTTGCCGCTCCTCAGCCT-3’

5’-CCAAGCCTTCTAATACGACTCACTATAGGGAGAAGCCCGCAAGCATTGCACAC-3’

*Mab-egr*5’ (#256)

5’-CCAAGCCTTCTAATACGACTCACTATAGGGAGATGAGCTGCTGCCAGAGCGTT-3’

5’-CAGAGATGCAATTAACCCTCACTAAAGGGAGATGTGCATTTTGTGATTATTGAAAGT-3’

Mab-egr3’ (#255)

5’-CCAAGCCTTCTAATACGACTCACTATAGGGAGAAACTATGAGACAAATACTTAACGGA

-3’

5’-CAGAGATGCAATTAACCCTCACTAAAGGGAGATCGAGCGATTGACGTCTCAGT-3’

Mab-doc (#286)

5’-CCAAGCCTTCTAATACGACTCACTATAGGGAGAGACGAGGATGGCGAGTACTG-3’

5’-CAGAGATGCAATTAACCCTCACTAAAGGGAGAGTTCCCACCAATGGTTGTGC-3’

Mab-doc2 (#302)

5’-CCAAGCCTTCATTAACCCTCACTAAAGGGAGATGAGTGGTGTGGATATCGCG-3’

5’-CCAAGCCTTCTAATACGACTCACTATAGGGAGATGAGTGGTGTGGATATCGCG-3’

Mab-ftz (#291)

5’-CCAAGCCTTCATTAACCCTCACTAAAGGGAGAACGCCCAGCCAAAAGCAACT-3’

5’-CAGAGATGCATAATACGACTCACTATAGGGAGAGGTGTTTGGTTCGGGCATTGGGT-3’

Mab-run (#292)

5’-CCAAGCCTTCTAATACGACTCACTATAGGGAGATGGCCTCGATGATGCAGGAGA-3’

5’-CAGAGATGCAATTAACCCTCACTAAAGGGAGACGCCACCCCACCAGTTACCC-3’

Mab-dpp (#293)

5’-CCAAGCCTTCATTAACCCTCACTAAAGGGAGAGGATTGAAGAGGCGACCGAA-3’

5’-CAGAGATGCATAATACGACTCACTATAGGGAGAAATCGCTCCAGCCAACTTCA-3’

Cri-hnt (#249)

5’-CAGAGATGCAATTAACCCTCACTAAAGGGAGAAGTGGACGAAGCACGCCAGT-3’

5’-CCAAGCCTTCTAATACGACTCACTATAGGGAGATCCACGTTGTCTTTGCGCCC-3’

Cri-eve (#251)

5’-CAGAGATGCAATTAACCCTCACTAAAGGGAGAAGCAACACCGCCACAATCACCA-3’

5’-CCAAGCCTTCTAATACGACTCACTATAGGGAGATCAACGGCTTCTCTGGCGTCAC-3’

Mab-CG7997 (#252)(cloned into pTOPO vector for probe synthesis)

5’-GCTGCTAGAATAGCCCAAACCGCC-3’

5’-ACGCAGAGCTCCTTTGACGG-3’

Synthesis of probes was previously described (Rafiqi et al., 2008, 2010). T3 and T7 promoters are underlined in the forward and reverse primers respectively. # gives the probe collection number. RNAi was performed as described (Rafiqi et al., 2008, 2010). The following primers were used to synthesize dsRNA

Mab-doc:

5’-CCAAGCCTTCTAATACGACTCACTATAGGGAGAGACGAGGATGGCGAGTACTG-3’

5’-CAGAGATGCATAATACGACTCACTATAGGGAGAGTTCCCACCAATGGTTGTGC-3’

Mab-doc2:

5’-CCAAGCCTTCTAATACGACTCACTATAGGGAGATGAGTGGTGTGGATATCGCG-3’

5’-CAGAGATGCATAATACGACTCACTATAGGGAGAAGCAAGGACAGTGTGACCAT-3’

Mab-cv-2:

5’-CAGAGATGCATAATACGACTCACTATAGGGAGAACGGCGCAAATCCGACTGTTGT-3’

5’-CCAAGCCTTCTAATACGACTCACTATAGGGAGAAACGCAGAGTGGAGCCGCTT-3’

T7 promoters are underlined. *Mab-hnt, Mab-egr,* and *Mab-dpp* dsRNA were synthesized from PCR template created from clone #851, #1061, and #918 respectively with primer pair #1485 and #1486. *Mab-zen* dsRNA was synthesized from PCR template created from clone #154 with primer pair #1151 and #1152. *Mab-cad* dsRNA was synthesized by a former lab member, Steffen Lemke, from PCR template created from clone #414 with primer pair #539 and #540.

To create the template for capped *Mab-doc, Mab-hnt, Mab-eve* and *Mab-dpp* mRNA, complete ORFs were PCR-amplified from embryonic cDNA using primers with attB recombination sites attached at the 5’ ends. The following primers were used:

Mab-hnt

5’-GGGGACAAGTTTGTACAAAAAAGCAGGCTACCATGCTTCATGCAACCAACC-3’

5’-GGGGACCACTTTGTACAAGAAAGCTGGGTCTACTTCTCAACACCCAAGAACTTG-3’

Mab-doc

5’-GGGGACAAGTTTGTACAAAAAAGCAGGCTAAAATGATTACCATGAATGAATTAGTG-3’

5’-GGGGACCACTTTGTACAAGAAAGCTGGGTCTAACATTGCGCAACACCCAAAA-3’

Mab-eve

5’-GGGGACAAGTTTGTACAAAAAAGCAGGCTAAAATGCAAGGATACAGAAACTACA-3’

5’-GGGGACCACTTTGTACAAGAAAGCTGGGTTTAGGCCTCACTCTCTGTCTT-3’

Mab-dpp

5’-GGGGACAAGTTTGTACAAAAAAGCAGGCTAAAATGCGCGCATGGCTT-3’

5’-GGGGACCACTTTGTACAAGAAAGCTGGGTTCATCGACATCCACATCCAAC-3’

The attB recombination sites are underlined. ORFs were first cloned into an entry vector which is then recombined into a destination vector, which was modified from the pSP35T (Amaya et al., 1991) using Gateway® Cloning (Life Technology). Capped mRNAs were prepared using SP6 polymerase with the mMessage mMachine Kit (#AM1340 Ambion).

5.3) Injection and fixation of Megaselia embryos

For microinjection, embryos were collected and aligned on a glass slide along a 0.2-mm glass capillary, briefly desiccated, and covered with halocarbon oil (Sigma H8773) at room temperature as described (Rafiqi et al., 2011). For heat fixation, embryos were desiccated for 15-20 minutes. However, for chemical fixation, the embryos were desiccated for ~30 minutes for better devitellinization efficiency. Desiccations were done on bench without using any desiccants and container in room temperature. Stages of the embryos were defined according to (Wotton et al., 2014). Embryos were injected before the syncytial blastoderm stage (~1:30-2:30 hours at 18˚C after egg deposition) unless otherwise specified. Oil was removed from the injected embryos by tilting the slide and letting it run off. Additional oil was removed by gently washing the embryos in a stream of heptane. In case of heat fixation (see Protocol 2 in the appendix), I used a squirt bottle containing deionized water to wash the embryos into a 50-mL conical tube. Water was removed by decantation and the fixing solution was added to the tube. In case of chemical fixation (see Protocol 3 in the appendix), I used a squirt bottle containing solution of 0.7%

NaCl and 0.05% Triton X-100 to wash the embryos into a 50-mL conical tube. Embryos were transferred to an Eppendorf tube and detergent was removed by washing in 0.7% NaCl solution three times before adding the fixing solution. After fixation, injected embryos were manually devitellinized as described (Rafiqi et al., 2011) before in situ hybridization and immunostaining.

5.4) In situ hybridization, immunohistochemistry, and pMad quantification

The following procedures for RNA in situ hybridization (see Protocol 4-6 in the appendix), immunostaining (see Protocol 7-8 in the appendix), and combined in situ hybridization and immunostaining (see Protocol 9 in the appendix) were done as described (Rafiqi et al., 2012). The primary antibodies used were: monoclonal mouse anti-Biotin, (1:400, #1297597 Roche), polyclonal rabbit anti-FITC (1:400, #A889 Molecular Probes), monoclonal mouse anti-DIG (1:400, #1333062 Roche), and polyclonal sheep anti-DIG (1:400, #1333089 Roche). The secondary antibodies used were: Alexa Fluor® 488 goat anti-mouse (1:400, #A-11029 Invitrogen), Alexa Fluor® 488 donkey anti-mouse (1:200, #A-21202 Invitrogen), Cy3-conjugated donkey anti-rabbit (1:400, #711-165-152 Jackson ImmunoResearch) and Cy5-conjugated donkey anti-sheep, (1:400, #713-175-147 Jackson ImmunoResearch). AP-conjugated anti-DIG (#11093274910 Roche)/anti-BIOTIN (#11426303001 Roche)/anti-FITC (#1426338 Roche) were used at 1:1000 dilutions for single staining, followed by NBT/BCIP substrate reaction. pMad was detected with a monoclonal rabbit antibody against Smad3 phosphorylated on Serine 423 and Serine 425 (1:250, #1880-1 Epitomics). For RNA *in situ* hybridization, Megaselia embryos were heat fixed, while for immunostaining, they were fixed by formaldehyde except for quantification

(see below). For two-color and three-color fluorescent *in situ* hybridization, confocal scans were done with a Zeiss LSM510 laser-scanning microscope. All subsequent image quantification and analysis of confocal micrographs were done in ImageJ (Schneider et al., 2012). To quantify pMad staining intensity, embryos were stained with pMad as described (Rafiqi et al., 2012). To preserve better morphology for quantification, heat fixation was used instead of formaldehyde fixation. Embryos at early gastrulation were staged after the initiation of the cephalic furrow and before the dorsal-most point of the proctodeum reached 20% of total egg length measured from the posterior pole. The quantification of pMad staining in injected Megaselia embryos followed the Drosophila protocol (Gavin-Smyth et al., 2013). To determine whether there was a significant reduction of pMad intensity in *Mab-egr* RNAi embryos compared to wild type, a Wilcoxon rank sum test was performed in R [R Core Team (2012). R: A language and environment for statistical computing. R Foundation for Statistical Computing, Vienna, Austria. http://www.R-project.org].

5.5) Construction of gene trees

Amino acid sequences of *Doc* homologs were retrieved from National Center for Biotechnology Information:(*Aedes aegypti*; *Aae-docA XP_001648597.1* and *Aae-docB XP_001663692.1*), (*Anopheles gambiae*; *Aga-docA XP_315924.3* and *Aga-docB EAA11871.5*), (*Drosophila melanogaster*; *Doc1* AAF50328.2, *Doc2* AAF50329.1 and *Doc3* AAF50331.1), (*Drosophila pseudoobscura*; *Dps-Doc1 EAL31211.1, Dps-Doc2 EAL31212.2,* and *Dps-Doc3 EAL31210.1*), (*Drosophila grimshawi*; *Dgr-Doc1 EDV96918.1, Dgr-Doc2 EDV96917.1* and *Dgr-Doc3 EDV96915.1*). Full-length protein alignments were created using the MUSCLE

program with default parameters (Edgar, 2004). The best amino acid substitution model was estimated using AIC in ProtTest 3 (Darriba et al., 2011) and the LG model was chosen. Maximum likelihood trees were calculated using PhyML 3 (Criscuolo, 2011). Bootstrap values were based on 1000 replicas.

5.6) Transcriptome profiles of Drosophila and Megaselia

I have studied the Megaselia gene regulatory network using a candidate gene approach and have focused on genes that are conserved in Drosophila. However, the extraembryonic gene regulatory network could also involve recruitment of new genes. In order to examine genes that are not conserved, a system-wide approach is required. A previous study that compares microarray data of embryonic development between the malaria mosquito *Anopheles gambiae* and Drosophila identified species-specific gene clusters based on temporal discordances (Papatsenko et al., 2011). One of these clusters contains genes that are expressed specifically in the mosquito serosa and is likely important for serosa cuticle synthesis. This study suggests a system-wide approach can help to identify gene clusters that reflect developmental differences between dipteran species.

I extracted total RNA from single Megaselia and Drosophila embryos at nine and ten different developmental stages, respectively (one Megaselia sample was lost) (**Fig. 5**), based on protocols provided by Michael Ludwig at the University of Chicago and Susan Lott's lab at the University of California-Davis (see Protocol 10 in the appendix). In collaboration with another member of our laboratory (Jeff Klomp), we sequenced the transcriptomes of single Megaselia and Drosophila embryos at nine and ten different

developmental stages, respectively (one Megaselia sample was lost) (**Fig. 5**). The sequence data were processed and assembled as described in a previous paper (Klomp et al., 2015) with some modification in the annotation step which is described as following: Annotation was conducted in three steps. First, orthology searches were completed for the largest ORF in every transcriptome contig of Megaselia in the Drosophila annotated databases using the alignment algorithm in tBLASTn, and a maximum e-value of 0.01. For a given Megaselia contig, the BLAST hits from the reference databases were merged if they existed within 20 basepairs of each other. In the second step, the largest ORF from each remaining unannotated contig was searched in the NCBI protein reference sequence database (RefSeq, 04-24-2013) database using BLASTp. In the third step, the remaining unannotated contig nucleotide sequences were searched in the Drosophila annotated database using tBLASTx. Transcript annotations are provided in the assembled transcriptome fasta file with the Ensembl gene IDs, gene descriptions, and BLAST e-values. Transcript annotations using the RefSeq database are provided in standard RefSeq format with BLAST e-values. This resource was used to obtain initial information about the time course of expression of specific Megaselia genes (**Fig. 4.2 and 4.4**) and provides an entry point for identifying candidate expression differences between Megaselia and Drosophila genes.

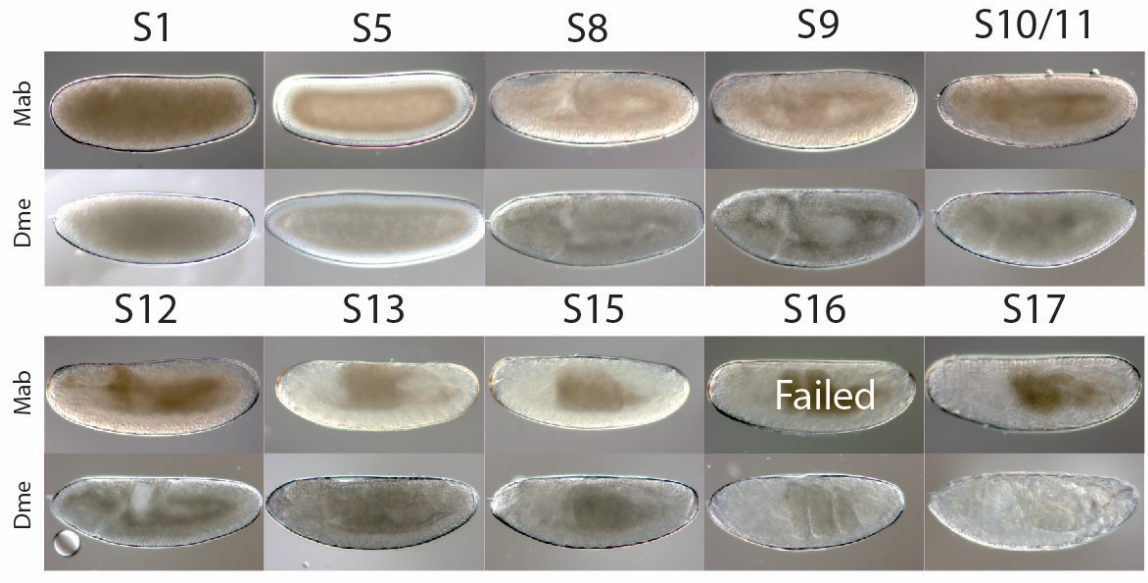

Figure 5: Images of Drosophila and Megaselia embryos that were sequenced.

Wild-type Drosophila and Megaselia embryos at ten different time points. Except for stage 16 Megaselia embryos, all were sequenced successfully.

Lateral views with dorsal up and anterior left.

Appendix) Supplemental Information

A.1) Expression patterns of potential amnion markers

In order to study amnion development, the expression patterns of several potential amnion markers were examined, including *Mab-egr*, *Mab-cv2, Mab-CG7997, Mab-CG6234* and *Mab-srp,* which all show amnioserosa-specific expression in Drosophila. *Mab-CG7997* did not show any staining from blastoderm to germ band extension stage (**Fig. 6.1A**), suggesting that it may not have any role in extraembryonic tissue specification although this may be an artifact and needs to be confirmed by further experiments. *Mab-srp* is expressed in vitellophages, anterior and posterior midgut primordia, and cephalic mesoderm primordium (**Fig. 6.1B**), similar to Drosophila (Abel et al., 1993; Rehorn et al., 1996; Sam et al., 1996; Spahn et al., 2014), however, no expression was detected on the dorsal side, suggesting that it may not be involved in extraembryonic tissues specification in Megaselia.

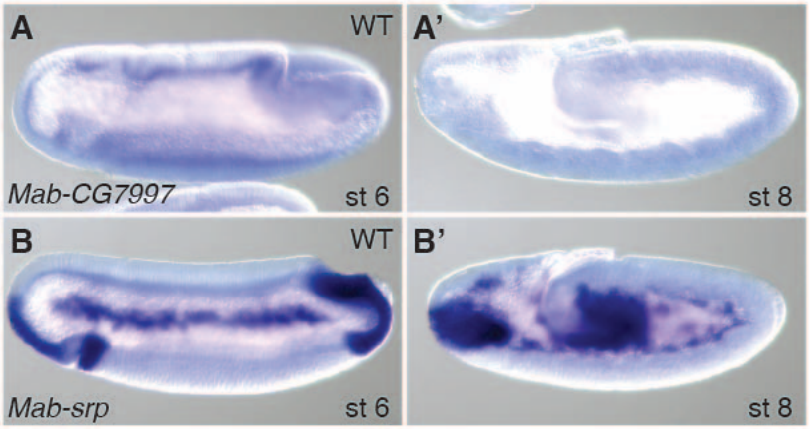

Figure 6.1: Expression patterns of potential amnion markers.

A-B, *Mab-CG7997* expression in Megaselia embryos at early gastrulation (**A**), early germ band extension (**A'**). *Mab-srp* expression in Megaselia embryos at early gastrulation (**B**), early germ band extension (**B'**).

Lateral views with dorsal up and anterior left.

A.2) *Mab-eve* overexpression suppresses *Mab-zen* and *Mab-hnt*

It is suggested that the BMP gradient promotes serosa and amnion by repressing embryonic genes that inhibit extraembryonic cell fates on the dorsal side. *Mab-eve*, which is used as embryonic marker, is repressed by BMP signaling. When *Mab-eve* was overexpressed, *Mab-zen* expression, which indicates serosa fate, was inhibited in blastoderm embryos (**Fig. 6.2A-D**), suggesting that *Mab-eve* could be one of the embryonic genes that represses extraembryonic fate and consistent with the previous observation that ectopic dorsal *Mab-eve* expression following *Mab-doc/hnt* knockdown correlates with repression of *Mab-zen* (**Fig. 2.3.2**). Another gene, *Mab-hnt,* which indicates extraembryonic fates, was also eliminated by *Mab-eve* overexpression (**Fig. 6.2E**).

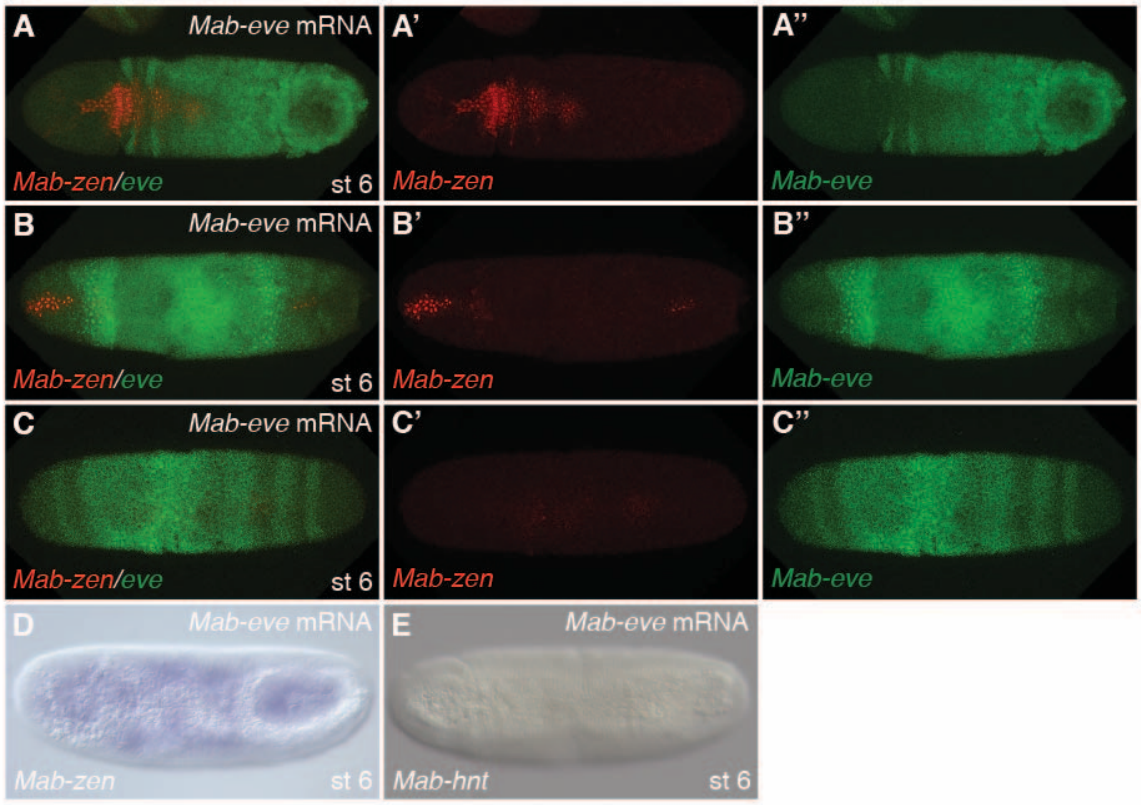

Figure 6.2: *Mab-eve* overexpression suppress *Mab-zen*.

A-C, *Mab-zen* and *Mab-eve* expression at early gastrulation after *Mab-eve* overexpression.

D-E, *Mab-zen* (**D**) and *Mab-hnt* expression (**E**) at early gastrulation after *Mab-eve* overexpression.

Dorsal views with anterior left.

A.3) Effect of *Mab-doc/doc2* and *Mab-hnt* RNAi on *Mab-ddc* expression

While essential for amnion specification, *Mab-doc/doc2* or *Mab-hnt* were not essential for serosa specification because *Mab-zen* expression was not affected following *Mab-doc/doc2* or *Mab-hnt* knockdown (**Fig. 2.3.2B-C**). However, *Mab-zen* expression was disrupted in *Mab-doc/hnt* knockdown embryos, suggesting that serosa specification was defective when both genes were disrupted. To examine whether serosa is disrupted at late developmental stage by knockdown of *Mab-doc/doc2* or *Mab-hnt* activity, I examined *Megaselia dopa decarboxylase* (*Mab-ddc*) expression, which specifically expresses in the serosa during germ band extension (Rafiqi et al., 2010). While *Mab-ddc* was not affected in most of the embryos following *Mab-doc/doc2* or *Mab-hnt* RNAi (92%, n=62 and 89%, n=90, respectively), similar to the control (91%, n=68), *Mab-ddc* expression was greatly reduced following *Mab-doc/hnt* RNAi and only some embryos retained normal expression (28%, n=74)(**Fig. 6.3**). Later stages were not examined because the serosa is easily lost during devintellinization after serosa expansion, making analysis difficult. These results are consistent with previous experiments, suggesting that *Mab-doc/doc2* or *Mab-hnt* alone is not essential for serosa specification. However, when both genes were knocked down, the serosa was reduced, probably because BMP signaling was greatly reduced.

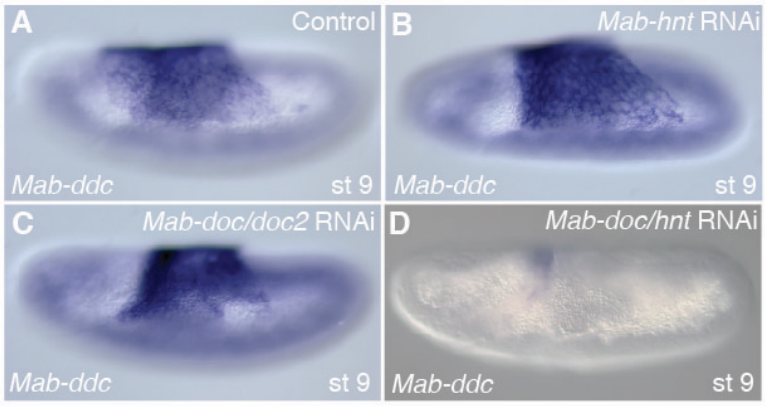

Figure 6.3: Effect of *Mab-doc* and *Mab-hnt* RNAi on *Mab-ddc* expression.

A-D, *Mab-ddc* expression at germ band extension in control embryo (**A**), after *Mab-hnt* knockdown (**B**), *Mab-doc/doc2* knockdown (**C**), or *Mab-doc/hnt* knockdown (**D**). Lateral views with dorsal up and anterior left.

A.4) *tkv-a* induces *Mab-zen* and *Mab-hnt* expression and represses *Mab-eve* expression

BMP signaling is required for *Mab-zen* and *Mab-hnt* expression and represses *Mab-eve* expression as knockdown of BMP signaling suppress *Mab-zen* and *Mab-hnt* expression and derepresses *Mab-eve* stripes on the dorsal side (Rafiqi et al., 2012) (**Fig. 2.2.2**). To determine whether BMP signaling is also sufficient for activating expression of *Mab-zen* and *Mab-hnt*, and for repressing *Mab-eve*, it was ectopically expressed by injecting embryos with mRNA of constitutively active Thickvein (*tkv-a*). Following *tkv-a* injection, both *Mab-zen* and *Mab-hnt* domain was expanded while *Mab-eve* was repressed near the injection site (**Fig. 6.4**), suggesting that BMP signaling is sufficient to drive *Mab-zen* and *Mab-hnt* expression and inhibit *Mab-eve* expression. Interestingly, *Mab-hnt* domain was slightly broader than the *Mab-zen* domain, suggesting a lower activation threshold for *Mab-hnt*. Distal to the injection site, however, endogenous *Mab-zen* and *Mab-hnt* expression was lost while *Mab-eve* strips became circumferential. This is consistent with the hypothesis that a positive feedback circuit downstream of BMP signaling promotes local receptor-ligand interactions.

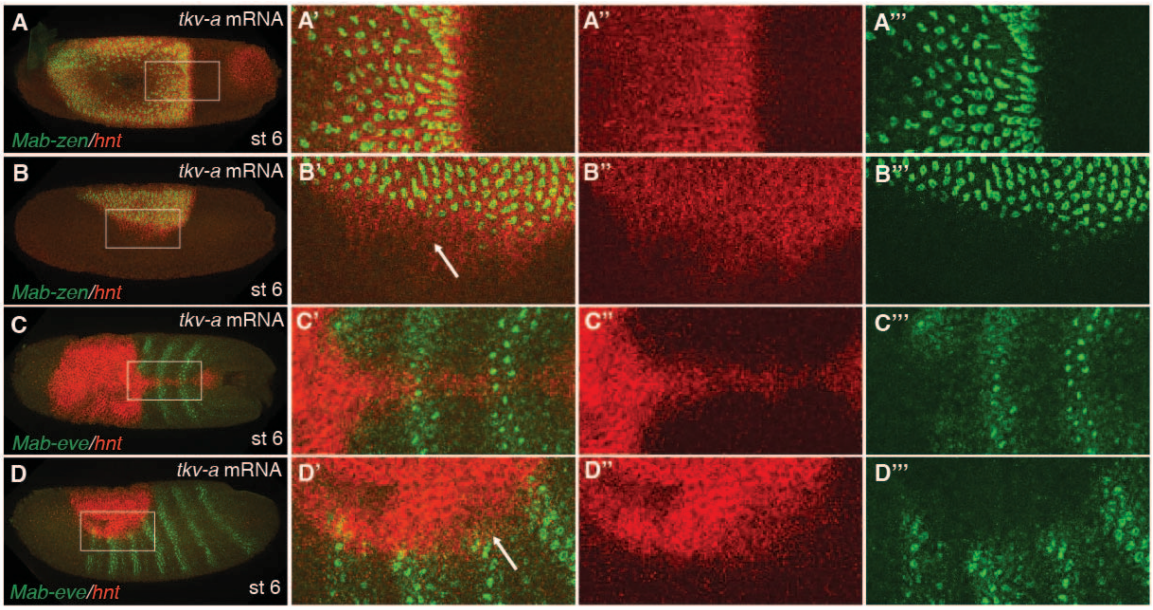

Figure 6.4: *tkv-a* induces *Mab-zen* and *Mab-hnt* but represses *Mab-eve* expression.

A-D, *Mab-zen* and *Mab-hnt* (**A-B**, enlargement **A'-B'**,**A''-B''**,**A'''-B'''**), or *Mab-eve* and *Mab-hnt* (**C-D**, enlargement **C'-D'**,**C''-D''**,**C'''-D'''**) expression in early gastrula embryo after *tkv-a* mRNA injection. Arrow (**B'**), *Mab-hnt* domain is slightly broader than *Mab-zen* domain. Arrow (**D'**), *Mab-hnt* domain slighly overlap with *Mab-eve* domain.

A, **C**, Dorsal views with anterior left. **B**, **D**, Lateral views with dorsal up and anterior left.

A.5) *Mab-doc* induces *Mab-zen* and *Mab-hnt* expression but represses *Mab-eve* expression

Mab-doc was shown to promote BMP signaling (**Fig. 2.3.6A,B**). Following *Mab-doc* mRNA injection, *Mab-zen* and *Mab-hnt* domains were expanded, and *Mab-eve* was repressed near the injection site (**Fig. 6.5**). Distal to the injection site, endogenous *Mab-zen* and *Mab-hnt* expression was lost while *Mab-eve* strips became circumferential, similar to the results described in section 6.4.

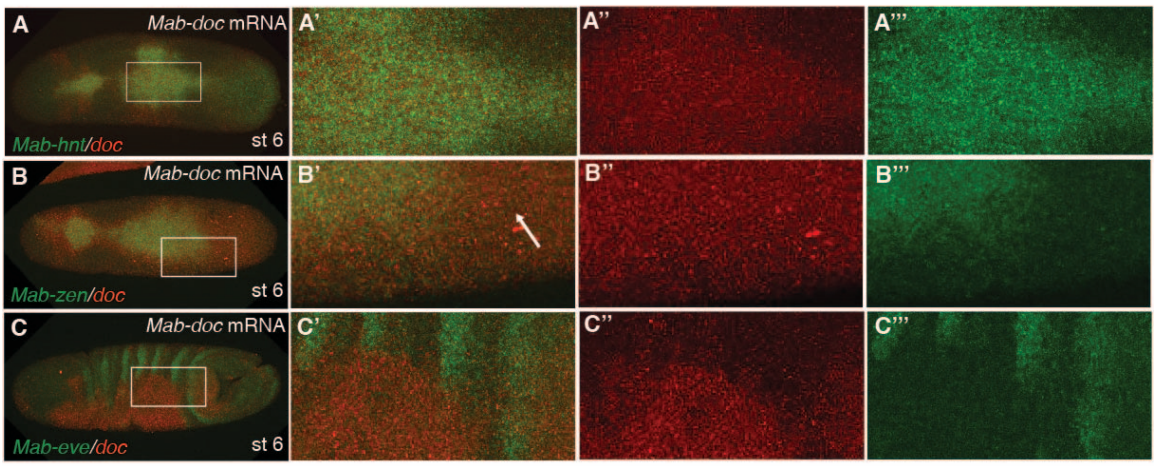

Figure 6.5: *Mab-doc* induces *Mab-zen* and *Mab-hnt* but represses *Mab-eve* expression.

A-C, *Mab-hnt* and *Mab-doc* (**A**, enlargement **A'**,**A''**,**A'''**), *Mab-zen* and *Mab-doc* (**B**, enlargement **B'**,**B''**,**B'''**), or *Mab-eve* and *Mab-doc* (**C**, enlargement **C'**,**C''**,**C'''**) expression in early gastrula embryo after *Mab-doc* overexpression. Arrow, *Mab-doc* domain is broader than *Mab-zen* domain.

Dorsal views with anterior left.

A.6) *Mab-ftz*, *Mab-run* and *Mab-h* expression

The pair rule gene *Mab-eve* is repressed in the serosa and later the amnion by BMP signaling. To study whether other pair rule genes are also repressed on the dorsal side, expression of Megaselia homologs of *fushi tarazi* (*Mab-ftz*), *runt* (*Mab-run*), and *hairy* (*Mab-h*) were examined. While all of them show dorsal repression during early gastrulation, the gap in these three genes seems to be narrower compared to *Mab-eve* (**Fig. 6.6.1-6.6.3**). When *Mab-ftz* was double-stained with *Mab-zen* at early gastrulation, their domains were confluent, in contrast to *Mab-eve*, which is repressed in the amnion (**Fig. 6.6.1E**). Furthermore, *Mab-ftz* stripes extend more toward the dorsal side compared to *Mab-eve* stripes (**Fig. 6.6.1F**). This suggests that *Mab-ftz* is repressed in serosa, but not in amnion.

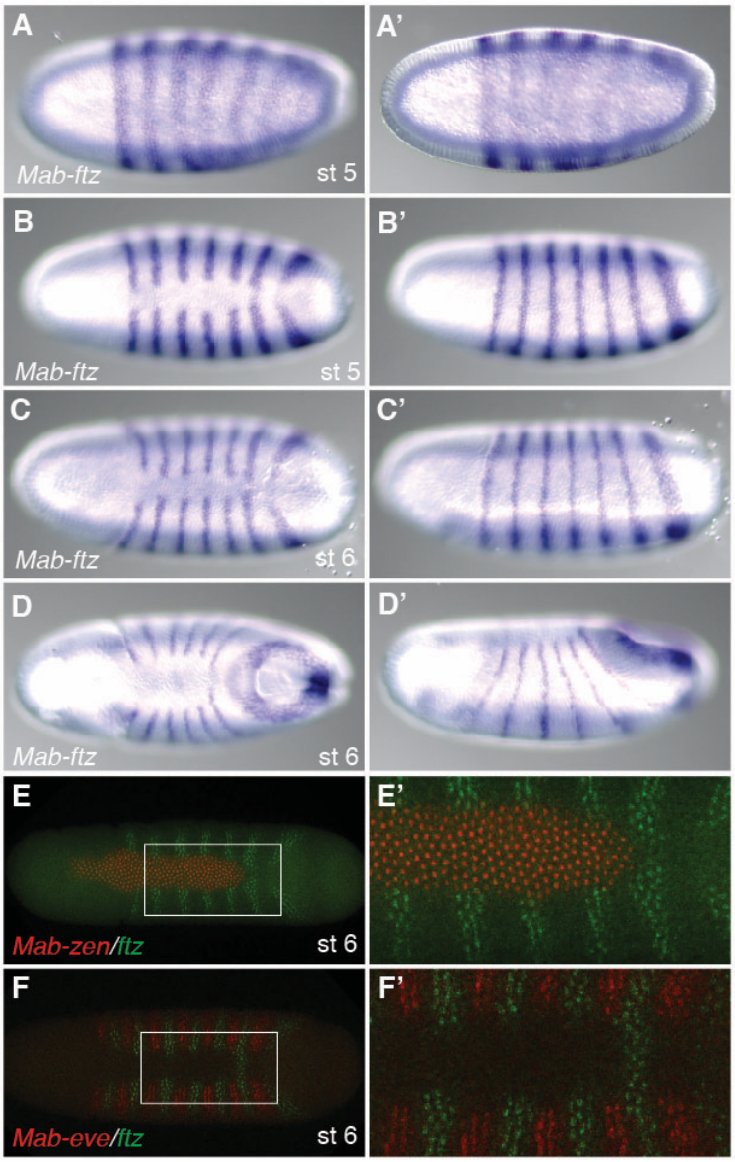

Figure 6.6.1: Expression profile of *Mab-ftz*.

A-D, *Mab-ftz* expression in Megaselia embryos during blastoderm cellularization (**A**,**B**) and early gastrulation (**C**,**D**).

E-F, *Mab-zen* and *Mab-ftz* (**E**, enlargement **E'**), and *Mab-eve* and *Mab-ftz* (**F**, enlargement **F'**) expression in early gastrula wild-type embryo.

A-F, Dorsal views with anterior left. **A'-D'**, Lateral views with dorsal up and anterior left.

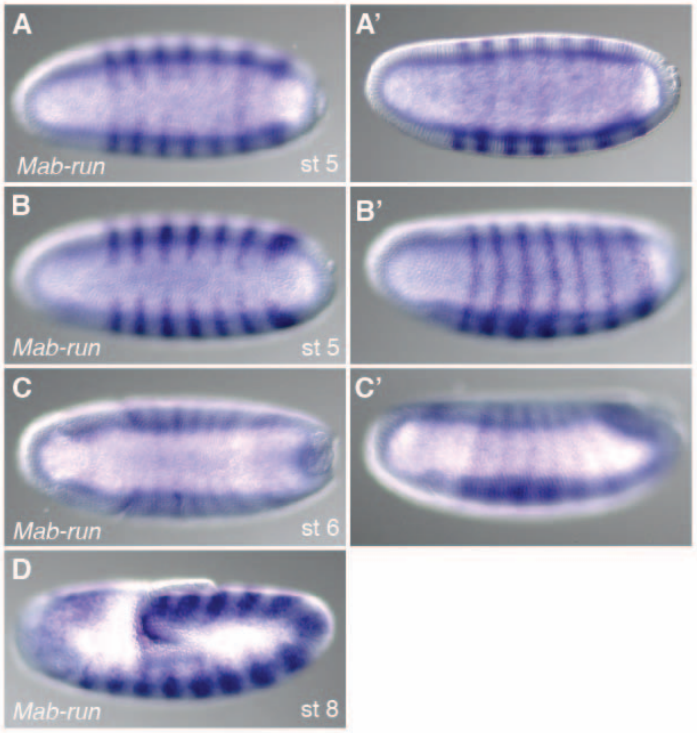

Figure 6.6.2: Expression profile of *Mab-run*.

A-D, *Mab-run* expression in Megaselia embryos during blastoderm cellularization (**A**,**B**), early gastrulation (**C**), and early germ band extension (**D**).

A-C, Dorsal views with anterior left. **A'-C'**, **D**, Lateral views with dorsal up and anterior left.

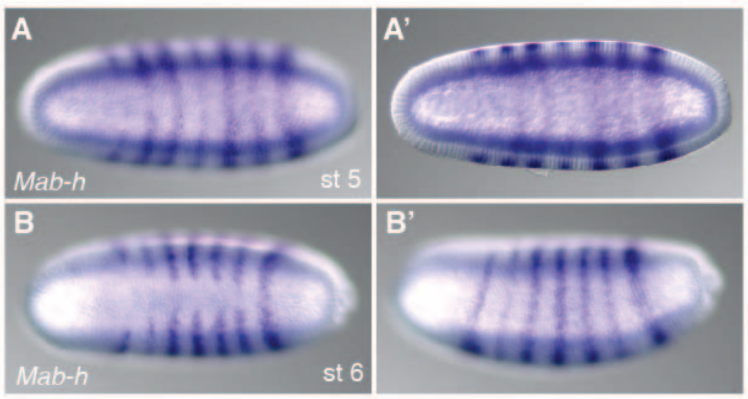

Figure 6.6.3: Expression profile of *Mab-h*.

A-B, *Mab-h* expression in Megaselia embryos during blastoderm cellularization (**A**) and early gastrulation (**B**).

A, **B**, Dorsal views with anterior left. **A'**, **B'**, Lateral views with dorsal up and anterior left.

A.7) *Mab-cad* RNAi does not affect amnion differentiation

Mab-cad is expressed in the amnion of Megaselia embryo at cellular blastoderm and early gastrulation stage (**Fig. 6.7A-B**) (Stauber et al., 2008). However, knockdown of *Mab-cad* does not affect *Mab-egr* expression in stage 11/12 embryos (99%, n=76), compared to control (97%, n=96) (**Fig. 6.7C-D**). This does not support the hypothesis that *Mab-cad* is required for amnion development. However, this also does not exclude the possibility that *Mab-cad* functions redundantly with other factors (for example: *Mab-doc, Mab-hnt*) to promote amnion development or the existence of unknown compensatory mechanism.

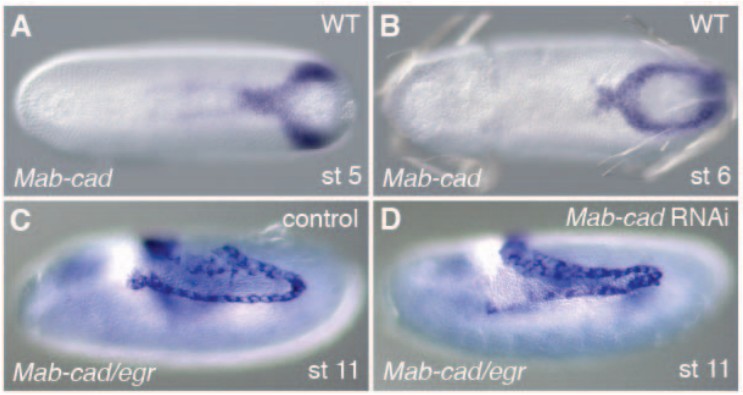

Figure 6.7: *Mab-cad* is not required for amnion differentiation.

A-B, *Mab-cad* expression in wild-type embryo at cellular blastoderm (**A**) or early gastrulation stage (**B**) (Data from Stauber et al., 2008).

C-D, *Mab-egr* and *Mab-cad* expression at germ band extension in control embryo (**C**) and after *Mab-cad* knockdown (**D**).

A, **B**, Dorsal views with anterior left. **C**, **D**, Lateral views with dorsal up and anterior left.

A.8) Protocols 1-10

Protocol 1

Basic Maintenance of M. abdita Cultures

(based on Rafiqi, Megaselia abdita: culturing and egg collection, Cold Spring Harb Protoc. 2011 Apr 1; 2011(4))

For *M. abdita* cultures, it is sufficient to start new bottles every 3 wk. We routinely maintain cultures of three phase-shifted generations (each shifted by a week), each of which comprises 24 bottles.

1. Culture M. abdita in standard Drosophila bottles (8oz round bottom bottle, Genesee Scientific, cat. 32-129F), supplemented with moist cotton (which helps to retain moisture) and a protein-rich fish food diet. Maintain the cultures in an environmentally controlled chamber (insectary) set at 25˚C and 50%–60% relative humidity on a 16/8-h day/night cycle, with the beginning of the dark cycle in the morning at 8-9 am. This setting for the light/dark transition allows egg collections in the morning because egg deposition peaks shortly (10–30 min) after the beginning of the dark cycle.

2. Every generation, transfer the culture to fresh bottles. (I routinely do the transfer on Wednesday)

i. Add 10 g ± 0.5 g of cotton and ample deionized water to each fresh culture bottle. Firmly compress the cotton at the bottom and remove excess liquid. Cotton compression is important to ensure that the cotton remains at the bottom of the culture bottle when inverting it during later handling.

ii. Add 4–5 g (3 spoons) of fish food mix per bottle and shake the bottle in upright position to level the surface. Wet the food with deionized water from a squirt bottle. Food should be wet, but water should not run out when inverting the vial.

iii. Anesthetize flies of the previous generation with CO2. Mix flies from eight to 12 bottles before redistributing them into the new bottles. Add 50–80 flies to each new bottle. Mixing flies from multiple bottles minimizes inbreeding. Typically, one-quarter to one-third of the offspring is used to maintain the culture (i.e., to start the next generation). I typically use 2-3 old bottles per new bottle. I keep a total of 24 bottles per generation (12 bottles/tray, 2 trays).

Reagent

Fish food mixture. Mix one part Spirulina Flake Food (Aquatic Eco-Systems, Inc., cat. no. ZSF5) with two parts Slow Sinking Powder (Aquatic Eco-Systems, Inc. cat. no. F1A) by weight. (Possible Replacement: Aquatic Eco-Systems, cat.no. ZM1, Both ingredients contain 45% protein.)

Procotol 2

Heat fixation of Megaselia embryos

(Modified from Wieschaus, E. and C. Nüsslein-Volhard. 1986. Looking at embryos. In Drosophila, a practical approach (ed. D.B. Roberts), pp. 199-226. IRL Press, Oxford. Edited by Chun Wai Kwan, Based on Matteen Rafiqi March 2008.)

A1. Embryo Collection (wild type)

1. Collect embryos with water in a meshed cage and wash 2-3 times with water.
2. Dechorionate embryos in bleach 25% for 90 second. Add bleach in a glass dish and dip the cage in it, swirl occasionally (preferably watch under scope to check for the extent of dechorionation.
3. Wash thoroughly with water (~1 min) to remove bleach.
4. Transfer to a 50 ml falcon tube using water and bush.
5. Decant water while swiveling the tube so that the embryos stick to the walls of the tube, alternatively pipette out water carefully.

A2. Embryo Collection (injected embryos)

6. Same as steps 1-3.
7. Transfer and line up the embryos on a slide and perform injection.
8. To collect the injected embryos, tilt the slides with injected embryos and let the oil runs off.
9. Wash the embryos with around 2 ml of heptane per slide to remove additional oil.
10. Wash the embryos into a 50-ml conical tube using deionized water.
11. Decant water while swiveling the tube so that the embryos stick to the walls of the tube, alternatively pipette out water carefully.

B. Fixation (Heat)

12. Freshly prepare 20 ml of Fixing solution I with the following composition

    19.3 ml of MilliQ water
    500 µl of NaCl (28%)
    200 µl of Triton X 100 (5%)

13. Heat in a microwave briefly (17 ~ 20 sec) to boil (it turns turbid and has bubbles on surface).
14. Immediately pour the heated fixative I to the falcon tube. Flip the tube up and down and rotate (with lid closed) so that all embryos get heated fixative I.
15. Add 30 ml of Mili Q water to the tube. Let floating embryos sink to the bottom of the tube.
16. Remove 30 ml of the solution and push embryos still sticking to the wall by pipetting with remaining solution.
17. Transfer heat fixed embryos to a fresh 1.5 ml tube and remove solution.
18. Add 1 ml of Mili Q water and quickly remove water. (Embryos can explode if they stay too long in hypotonic solution) This step is critical for devitellinization rate.
19. Add 600 ul of Heptane. Add 600 ul of MeOH and immediately shake intensely (fast motion) for 20 ~ 40 seconds. (You need to be very fast at this step for effective devitellinization.)
20. Let embryos settle and remove heptane and wash embryos 3 times with methanol.

D. Fixation (Formaldehyde) [This is a postfix and improves quality of storage and in situs]

21. Add fixative II (865 ul of 3:1 PBS:MeOH + 135 ul of 37% formaldehyde) and incubate in rotator for 25 minutes.
22. Remove fixative.
23. Repeat step 12 and 13.
24. Store embryos in MeOH at -20˚C.

C. Devitellinization (manual) [Required only if the vitelline membrane is still on]

25. Transfer embryos to a bath of methanol in a small agar plate.
26. Tease out the vitelline layer using tungsten needles under a scope.

<u>Solutions</u>

Dechorionation Solution: Commercial Bleach 25% (diluted with water)

Fixing Solution I: NaCl 7% + Triton-X100 0.5% [this is 10x]

Fixing Solution II: 1x PBT/MeOH (3:1) **+** 5% Formaldehyde

Methanol; Heptane; PBS; Water

Protocol 3

Formaldehyde fixation of Megaselia embryos

(Edited by Chun Wai Kwan, Based on Matteen Rafiqi's protocol.)

A1. Embryo Collection (wild type)

1. Collect embryos with water in a meshed cage and wash 2-3 times with water.
2. Dechorionate embryos in bleach 25% for 90 second. Add bleach in a glass dish and dip the cage in it, swirl occasionally (preferably watch under scope to check for the extent of dechorionation.
3. Wash thoroughly with water (~1 min) to remove bleach.
4. Transfer the embryos to a 1.5 ml tube.

A2. Embryo Collection (injected embryos)

5. Same as steps 1-3.
6. Transfer and line up the embryos on a slide and perform injection.
7. To collect the injected embryos, tilt the slides with injected embryos and let the oil runs off.
8. Wash the embryos into a 50-mL conical tube with solution of 0.7% NaCl and 0.05% Triton X-100
9. Transfer the embryos into a 1.5 ml tube and wash 3 times with 0.7% NaCl.

B. Fixation (Chemical)

10. Make mixture of fixative (mix by vortexing) and pour into a tube with embryos

    Fix mix:
    433 µl of PEMS : Methanol 3:1
    67.5 µl of Formaldehyde (37%)
    500 µl n-Heptane

11. Incubate on the wheel for 25 minutes
12. Remove all liquid
13. Add 500 µl of Heptane
14. Add 600 µl of Methanol and immediately shake for 20~40 seconds
15. Remove all solution and wash with Methanol 3 times (can be stored at – 20 C)

Solution

1X PEMS:

100 mM PIPES

2 mM MgSO4

1 mM EGTA

Protocol 4

Single histochemical (AP-NBT/BCIP) in situ hybridization protocol for *Megaselia abdita*

(Edited by Chun Wai Kwan, Based on Matteen Rafiqi's protocol.)

Dehydration and Clearing of Embryos

1. Wash 3x in Ethanol
2. Wash 1x in Xylene/Ethanol (1/1)
3. On wheel 1 hr in Xylene/Ethanol (3/1)
4. Wash 1x in Xylene/Ethanol (1/1)
5. Wash 3x in Ethanol
6. Wash 3x in Methanol
7. Wash embryos in PBT:MeOH (1:1)
8. Wash 3 times with PBT
9. Wash 2 times 20 minutes in PBT

Proteinase K Treatment And Postfix

10. Prepare ProteinaseK solution, 0.08 U/ml and incubate embryos with diluted proteinase-K on ice for 1 hour
    (10 mg/ml stock with 20 U/mg [Invitrogen 25530-015]:0.4 µl in 1 ml PBT)
11. Wash 3x in ice cold PBT
12. Post fix with 25' PBT + 5% Formaldehyde, with mild shaking
    (37% Formaldehyde [Fisher BP531-500]: 865 µl PBT + 135 µl Formaldehyde)
13. Wash 3x in PBT
14. Wash on rocker/rotator twice 5' in PBT

Probe Hybridization

15. Wash for 10' in PBT/HYB (1/1)
16. Wash for 2' in HYB (400 µl)
17. Prehybridize 1 hr at 56 °C in HYB (400 µl)
18. Prepare 30-100 µl of HYB (depends on amount of embryos) (In most case, I mixed 1 µl of probe with 29 µl HYB). Heat probe at 80 °C for 5 minutes, remove prehybridization

solution and add heated probe to prehybridized embryos. Hybridize overnight with probe at 56 °C.

Post Hybridization (next morning)

19. Warm HYB to 56 °C (30' in water bath)
20. Remove probe and store the probe at -20 C for re-use
21. Posthybridize 2x 30' in pre-warmed HYB at 56 °C (400 µl)
22. Wash 5' in PBT/HYB (1:1) at room temperature (as for all following steps)
23. Wash 4x 15' in PBT

Antibody Incubation and 1st AP (Alkaline Phoasphatase) Reaction

24. Rock 1x PBTriton+10% goat serum (GS), 30'
25. Incubate with **1/1000 dilution of AP-conjugated anti-DIG/BIOTIN/FITC** in 5%GS in PBT for 2 hr
26. Wash 3x PBT
27. Rock 4x PBT, 15'
28. Prepare AP-Buffer (1.5 ml/sample)

a.	final conc.	stock	10 ml	1.5 ml	3ml
NaCl	100 mM	2 M	500 µl	75	150
MgCl	50 mM	2 M	250 µl	37.5	75
Tris pH 9.5	100 mM	1 M	1000 µl	150	300
Tween-20	0.1%	10%	100 µl	15	30
Water			8.15 ml	611X2	2.445ml

29. On rocker/rotator 2x 5' in AP-Buffer
30. Prepare NBT/BCIP solution (500 µl/sample)

		stock	1 ml
NBT	Roche 1 383 213	100 mg/ml	3.5 µl
BCIP	Roche 1 383 221	50 mg/ml	3.5 µl

31. Incubate embryos with 500 µl of NBT/BCIP solution in the dark

Stop Staining

32. Wash 3x with PBT
33. Wash 1x in PBT/EtOH (1/1) (optional: 33-35)
34. Rock 3x 10' in 100% EtOH
35. Wash 1x in PBT/EtOH (1/1)
36. Wash 2x with PBS

37. Remove PBT and add PBS/Glycerol (1:1). Let embryos settle

38. Transfer to 70% glycerol in PBS and store at 4°C

Solutions:

PBS, 10X

NaCl	80 g
KCl	2.0 g
Na_2HPO_4	14.4 g
KH_2PO_4	2.4 g
H_2O	ad 800 ml

adjust pH to 7.4 (HCl)

H_2O	ad 1 L

autoclave

PBT, 1X

PBS

0.1% Triton X-100

AP-buffer (10 ml)

NaCl (2M)	500 µl
MgCl (2M)	250 µl
Tris-HCl (1M), pH 9.5	1 ml
Tween-20 (10% stock, diluted in MilliQ water)	100 µl

HYB

50% formamide, Sigma Ultra minimus 99% GC (Sigma, F-5786)

5x SSC (final conc., stock is 20x)

5 mg/ml torula yeast RNA (Sigma, R-6625)

50 µg/ml Heparin (Sigma H 1027, 140 USP units/mg – serves as RNAse inhibitor)

0.1% Tween 20 (pipet from stock 1:10 dilution in H_2O_{MILLIQ})

pH 5.0-6.0 (test aliquot with pH-strip, normally not necessary to adjust)

Protocol 5

Double fluorescent in situ hybridization protocol for *Megaselia abdita*

(Edited by Chun Wai Kwan, Based on Matteen Rafiqi's protocol.)

Dehydration And Clearing of Embryos

1. Wash 3x in Ethanol
2. Wash 1x in Xylene/Ethanol (1/1)
3. On wheel 1 hr in Xylene/Ethanol (3/1)
4. Wash 1x in Xylene/Ethanol (1/1)
5. Wash 3x in Ethanol
6. Wash 3x in Methanol
7. Wash 1x in PBT/Methanol (1/1)
8. Wash 3x in PBT
9. Wash on rocker/rotator 5' in PBT

Proteinase K Treatment And Postfix

10. Prepare ProteinaseK solution, 0.08 U/ml and incubate embryos with diluted proteinase-K on ice for 1 hour
    (10 mg/ml stock with 20 U/mg [Invitrogen 25530-015]: 0.4 µl in 1 ml PBT)
11. Wash 3x in ice cold PBT
12. Post fix with 25' PBT + 5% Formaldehyde, with mild shaking
    (37% Formaldehyde [Fisher BP531-500]: 865 µl PBT + 135 µl Formaldehyde)
13. Wash 3x in PBT
14. Wash on rocker/rotator twice 5' in PBT

Probe Hybridization

15. Wash for 10' in PBT/HYB (1/1)
16. Wash for 2' in HYB (400 µl)
17. Prehybridize 1 hr at 56 °C in HYB (400 µl)
18. Prepare 30-100 µl of HYB (depends on amount of embryos) (In most case, I mixed 3 µl of probe with 27 µl HYB). Heat probe at 80 °C for 5 minutes, remove prehybridization solution and add heated probe to prehybridized embryos. Hybridize overnight with probe at 56 °C.

Post Hybridization (next morning)

19. Warm HYB to 56 °C (30' in water bath)
20. Remove probe and store the probe at -20 C for re-use.
21. Posthybridize 2x 30' in pre-warmed HYB at 56 °C (400 µl)
22. Wash 5' in PBT/HYB (1:1) at room temperature (as for all following steps)
23. Wash 4x 15' in PBT

Antibody Incubations

24. Remove PBT, add 4-5 drops of image iT ® FX Signal Enhancer (I36933 Invitrogen)
25. Rock 30'
26. Wash 1x in PBT
27. Incubate with shaking for 30' in PBT + 10% goat serum (G9023 Sigma)
28. Prepare antibody solutions

    1:400 dilutions (monoclonal mouse anti-Biotin, 1297597 Roche

    OR monoclonal mouse anti-DIG, 1333062 Roche

    + polyclonal rabbit anti-FITC, A889 Molecular Probes)

    in PBT + 5% goat serum
39. Incubate with antibody for 2 hr.
30. Wash 3x in PBT
31. Wash 4x 15' in PBT
32. Incubate with 1:400 dilutions

    (Alexa Fluor® 488 goat anti-mouse, A-11029 Invitrogen

    Cy3-conjugated donkey anti-rabbit, 711-165-152 Jackson ImmunoResearch)

    in PBT + 5% goat serum for 1hr
33. Wash 3x in PBT
34. Wash 4x 15' in PBT

Stop Staining

35. Wash 2x with PBS
36. Transfer to 50% glycerol in PBS and let the embryos settle
37. Transfer to 70% glycerol in PBS and store at 4°C

Protocol 6

Triple fluorescent in situ hybridization protocol for *Megaselia abdita*

(Edited by Chun Wai Kwan, Based on Matteen Rafiqi's protocol.)

Dehydration And Clearing of Embryos

1. Wash 3x in Ethanol
2. Wash 1x in Xylene/Ethanol (1/1)
3. On wheel 1 hr in Xylene/Ethanol (3/1)
4. Wash 1x in Xylene/Ethanol (1/1)
5. Wash 3x in Ethanol
6. Wash 3x in Methanol
7. Wash 1x in PBT/Methanol (1/1)
8. Wash 3x in PBT
9. Wash on rocker/rotator 5' in PBT

Proteinase K Treatment And Postfix

10. Prepare ProteinaseK solution, 0.08 U/ml and incubate embryos with diluted proteinase-K on ice for 1 hour
    (10 mg/ml stock with 20 U/mg [Invitrogen 25530-015]: 0.4 µl in 1 ml PBT)
11. Wash 3x in ice cold PBT
12. Post fix with 25' PBT + 5% Formaldehyde, with mild shaking
    (37% Formaldehyde [Fisher BP531-500]: 865 µl PBT + 135 µl Formaldehyde)
13. Wash 3x in PBT
14. Wash on rocker/rotator twice 5' in PBT

Probe Hybridization

15. Wash for 10' in PBT/HYB (1/1)
16. Wash for 2' in HYB (400 µl)
17. Prehybridize 1 hr at 56 °C in HYB (400 µl)
18. Prepare 30-100 µl of HYB (depends on amount of embryos) (In most case, I mixed 3 µl of probe with 27 µl HYB). Heat probe at 80 °C for 5 minutes, remove prehybridization solution and add heated probe to prehybridized embryos. Hybridize overnight with probe at 56 °C.

Post Hybridization (next morning)

19. Warm HYB to 56 °C (30' in water bath)
20. Remove probe and store the probe at -20 C for re-use.
21. Posthybridize 2x 30' in pre-warmed HYB at 56 °C (400 µl)
22. Wash 5' in PBT/HYB (1:1) at room temperature (as for all following steps)
23. Wash 4x 15' in PBT

Antibody Incubations

24. Remove PBT, add 4-5 drops of image iT ® FX Signal Enhancer (I36933 Invitrogen)
25. Rock 30'
26. Wash 1x in PBT
27. Incubate with shaking for 30' in PBT + 10% donkey serum (017-000-001 Jackson ImmunoResearch)
28. Prepare antibody solutions

    1:400 dilutions (monoclonal mouse anti-Biotin, 1297597 Roche

    + polyclonal rabbit anti-FITC, A889 Molecular Probes

    + polyclonal sheep anti-DIG, 1333089 Roche)

    in PBT + 5% donkey serum
39. Incubate with antibody for 2 hr.
30. Wash 3x in PBT
31. Wash 4x 15' in PBT
32. Incubate with 1:400 dilutions

    (Alexa Fluor® 488 donkey anti-mouse, A-21202 Invitrogen **(1:200 dilution is used instead)**

    Cy3-conjugated donkey anti-rabbit, 711-165-152 Jackson ImmunoResearch

    Cy5-conjugated donkey anti-sheep, 713-175-147 Jackson ImmunoResearch)

    in PBT + 5% donkey serum for 1hr
33. Wash 3x in PBT
34. Wash 4x 15' in PBT

Stop Staining

35. Wash 2x with PBS

36. Transfer to 50% glycerol in PBS and let the embryos settle
37. Transfer to 70% glycerol in PBS and store at 4°C

Protocol 7

pMad histochemical immunostaining protocol for *Megaselia abdita*

(Edited by Chun Wai Kwan, Based on Matteen Rafiqi's protocol.)

Proteinase K digestion

1. Wash embryos in PBT:MeOH (1:1)
2. Wash 3 times with PBT
3. Rock 5 minutes in PBT
4. Prepare Proteinase K solution: 2 ul of proteinase K (20 U/mg) in 5 ml of PBT
5. Incubate embryos in Proteinase K solution for 2 minutes at room temperature.
6. Wash 3 times in PBT
7. Rock 5 minutes in PBT
8. Post fix with 4 % Formaldehyde in PBT for 25 minutes on the wheel (100 µl Formaldehyde + 825 µl PBT)
9. Wash 3 times with PBT
10. Wash 2 times 20 minutes in PBT

1st Antibody Incubation and 2nd Antibody Incubations

11. Rock 1x PBT+10% goat serum (GS), 30'
12. Rock with **1/1000 dilution of Rabbit-anti-pMad (Ed Laufer) or 1/250 of anti-Smad3 (1880-1, Epitomics/ ab52903, abcam)** in PBT+5%GS, 2 hours or over night at 4 ^{o}C
13. Wash 3x PBT
14. Rock 4x PBT, 15'
15. Incubate with **1/1000 dilution of Biotin-anti-rabbit (BA-1000, Vector)** in 5%GS in PBT for 90' or 2 hours
16. Wash 3x PBT
17. Rock 4x PBT, 15'
18. Rock 1x PBT+5%GS, 30'
19. Rock with **1/2000 AP-anti-Biotin (11426303001, Roche) in PBT+5%GS**, 60'
20. Wash 3x PBT

21. Rock 4x PBT, 15’
22. Rock 2x AP-buffer, 5’
23. Proceed with **NBT/BCIP reaction**
24. 1ml AP + 3.5µl NBT + 3.5µl BCIP (keep dark and check 20-30 minutes
    a. Alternatively: use 2.5 µl of NBT and 2.5µl of BCIP in 5 ml and incubate at 4 ^{o}C for up to 20 hrs.)
25. **Stop staining** reaction by washing 3x with PBT
26. Wash in 50% EtOH in PBT
27. Rock 3x with 100% EtOH, 10’
28. Wash in 50% EtOH in PBT
29. Wash 3x with PBT
30. Wash 2x with PBS
31. Remove PBS and add PBS/Glycerol (1:1). Let embryos settle
32. Transfer to 70% glycerol in PBS and store at 4°C

Protocol 8

pMad fluorescent immunostaining protocol for *Megaselia abdita*

(Edited by Chun Wai Kwan, Based on Matteen Rafiqi's protocol.)

Proteinase K digestion

1. Wash embryos in PBT:MeOH (1:1)
2. Wash 3 times with PBT
3. Rock 5 minutes in PBT
4. Incubate injected embryos in a 1:1000 solution of Wheat Germ Agglutinin (WGA) conjugated to Alexa633 dye in PBT (Invitrogen) for 15 minutes at RT
5. Wash injected embryos 5 times 3 minutes each
6. Mix with unmarked control embryos in the same tube
7. Prepare Proteinase K solution: 2 ul of proteinase K (20 U/mg) in 5 ml of PBT
8. Incubate embryos in Proteinase K solution for 2 minutes at room temperature
9. Wash 3 times in PBT
10. Rock 5 minutes in PBT
11. Post fix with 4 % Formaldehyde in PBT for 25 minutes on the wheel (100 µl Formaldehyde + 825 µl PBT)
12. Wash 3 times with PBT
13. Wash 2 times 20 minutes in PBT

1st Antibody Incubation and 2nd Antibody Incubations

14. Remove PBT, add 4-5 drops of image iT ® FX Signal Enhancer (Invitrogen, Cat no. I36933)
15. Rock 30'
16. Wash 1x in PBT
17. Rock 1x PBT+10% goat serum (GS), 30'
18. Rock with **1/1000 dilution of Rabbit-anti-pMad (Ed Laufer) or 1/250 of anti-Smad3 (1880-1, Epitomics/ ab52903, abcam)** in PBT+5%GS, 2 hours or over night at 4 ^{o}C
19. Wash 3x PBT
20. Rock 4x PBT, 15'

21. Incubate with **1/400 dilution of Cy3-anti-rabbit (711-165-152, Jackson ImmunoResearch)** in 5%GS in PBT for 1 hour
22. Wash 3x PBT
23. Rock 4x PBT, 15’
24. Wash 2x with PBS
25. Transfer to 50% glycerol in PBS and let the embryos settle
26. Transfer to 70% glycerol in PBS and store at 4°C

Protocol 9

In situ hybridization (*Mab-zen+Mab-eve*) + immunostaining (pMad) protocol for *Megaselia abdita*

(Edited by Chun Wai Kwan, Based on Matteen Rafiqi's protocol.)

Dehydration and Clearing of Embryos

1. Wash 3x in Ethanol
2. Wash 1x in Xylene/Ethanol (1/1)
3. On wheel 1 hr in Xylene/Ethanol (3/1)
4. Wash 1x in Xylene/Ethanol (1/1)
5. Wash 3x in Ethanol
6. Wash 3x in Methanol
7. Wash embryos in PBT:MeOH (1:1)
8. Wash 3 times with PBT
9. Rock 5 minutes in PBT

Proteinase K Treatment And Postfix

10. Prepare Proteinase K solution: 2 ul of proteinase K (20 U/mg) in 5 ml of PBT
11. Incubate embryos in Proteinase K solution for 2 minutes at room temperature.
12. Wash 3 times in PBT
13. Rock 5 minutes in PBT
14. Post fix with 4 % Formaldehyde in PBT for 25 minutes on the wheel
    (100 µl Formaldehyde + 825 µl PBT)
15. Wash 3 times with PBT
16. Wash 2 times 20 minutes in PBT

Probe Hybridization

17. Wash for 10' in PBT/HYB (1/1)
18. Wash for 2' in HYB (400 µl)

19. Prehybridize 1 hr at 56 °C in HYB (400 µl)
20. Prepare 30 µl of HYB with 2 µl of **DIG-*Mab-zen* probe (#241)** +1 µl of **BIO-*Mab-eve* probe (#013)**
21. Heat probe at 80 °C for 5 minutes
22. Remove prehybridization solution and add heated probe to prehybridized embryos
23. Incubate overnight with probe at **56 °C**

Post Hybridization (next morning)

24. Warm HYB to 56 °C (30' in water bath)
25. Remove probe (and store at -20 C for re-use)
26. Posthybridize 2x 30' in pre-warmed HYB at 56 °C
27. Wash 5' in PBT/HYB (1:1) at RT (as for all following steps)
28. Wash 4x 15' in PBT

Immunocytochemistry and Staining

29. Remove PBT, add 4-5 drops of image iT ® FX Signal Enhancer (Invitrogen, Cat no. I36933)
30. Rock 30'
31. Wash 1x in PBT
32. Rock 1x PBTriton+10% goat serum (GS), 60'
33. Rock with **1/250 of anti-Smad3 (1880-1, Epitomics/ ab52903, abcam), 1:400 dilutions (monoclonal mouse anti-Biotin, 1297597 Roche + monoclonal mouse anti-DIG, 1333062 Roche)** in PBT+5%GS, 3 hours or over night at 4 °C
34. Wash 3x PBT
35. Rock 4x PBT, 15'
36. Incubate with **1:400 dilutions (Alexa Fluor® 488 goat anti-mouse, A-11029 Invitrogen, Cy3-conjugated donkey anti-rabbit, 711-165-152 Jackson ImmunoResearch)** in PBT + **1:000 dilution of DAPI,** 5% goat serum for 1hr
37. Wash 3x PBT
38. Rock 4x PBT, 15'

Stop Staining

39. Wash 2x with PBS
40. Transfer to 50% glycerol in PBS and let the embryos settle
41. Transfer to 70% glycerol in PBS and store at 4°C

Protocol 10

Extracting RNA from single embryos for sequencing

(Based on Michael Ludwig and Susan Lott's protocol.)

Trizol step:

1. Prepare fresh Trizol-glycogen solution. Final concentration of glycogen in Trizol should be 200-150 µg/ml. Aliquot 40 µl into each 1.5 ml tube.

2. Remove chorions, by exposing embryos to 25% bleach for 90 seconds. Rinse thoroughly.

3. Transfer embryos onto glass slide, remove excess water with a Kimwipe.

4. Cover embryos with Halocarbon oil 27. Don't add a lot.

5. Investigate and document stage under dissecting or compound microscope.

6. Transfer embryo to a clean piece of parafilm on agar plate to remove excess oil.

7. Place a 2 µl drop of Trizol-glycogen solution next to the embryo, and gently roll the embryo with the side of the needle into the drop. Use the needle to poke the embryo, the embryo will burst and therefore dissolve faster. The embryo should dissolve in 5-10 minutes. I do this all under a dissecting microscope. Be careful working with the needle, as embryos can stick, and at the wrong angle, you can end up losing solution (with RNA in it!) into the needle due to capillary action. I tend to use a piece of parafilm big enough for several embryos, and place the next embryo in the drop and poke it while the prior one is dissolving.

8. Take 5 µl of the Trizol-glycogen solution and add to the drop with the dissolved embryo, and transfer all of it back to the tube where you took the 5 µl from. Let each tube with individual embryo stay at room temp for at least 10 minutes.

9. Transfer the tubes with embryos to a -80 freezer. You can keep them there a month or two.

Phenol-chloroform extraction:

10. Take the tubes with embryos from -80 freezer and thaw the Trizol-glycogen solution in RT for 5-10 min.

11. Add 8 µl of chloroform to each tube. Vortex vigorously for 15 sec and spin at 12,000 X g for 15 min at 4˚C. (Two phases are visible, DNA and protein are in lower phase while RNA is in upper one)

12. Transfer the upper phase (~20-22 µl) to a new tube and add 20 µl of phenol-chloroform. (Lower phase can be discarded if DNA is not required)

13. Vortex vigorously for 15 sec. Let the tube stand for 5 min. Spin at 12,000 X g for 15 min at 4˚C.

14. Transfer the upper phase (~18-20 µl) to a new tube and add 18 µl of isopropanol. Mix well by hand and let it stand for 20 min to precipitate RNA.

15. Spin at 12,000 X g for 15 min at 4˚C. A pellet should be visible.

16. Remove the supernatant and add 100 µl of 75% ethanol (First wash).

17. Spin at 12,000 X g for 15 min at 4˚C. Remove the supernatant and add 100 µl of 75% ethanol (Second Wash). RNA pellet can be kept in 75% ethanol at -20˚C for a couple of days (optional).

18. Spin at 12,000 X g for 15 min at 4˚C. Remove the supernatant and let it stand for few minutes to dry the pellet.

19. Dissolve the pellet in 5 µl of RNase-free water and incubate in 55˚C for 10 min to allow complete dissolution. The sample is now ready to be sent for quality check and library construction.

Reagents:

2% agar plate
Hypodermic Needles, Gauge x L: 27G x 1.5 in. (Fisher, #14-840-99)
Halocarbon oil 27 (Sigma, H8773)
Trizol Reagent (Invitrogen, 15596-026)
Ultrapure Glycogen (Invitrogen, 10814-010)
Chloroform (Fisher, BP1145-1)
Phenol-chloroform (Sigma, P2069-100ML)
Isopropanol (Fisher, BP2618-500)
Ethanol (Fisher, BP2818-500)
RNase-free water (Gibco, 10977-015)

References

Abel, T., Michelson, A.M., and Maniatis, T. (1993). A Drosophila GATA family member that binds to Adh regulatory sequences is expressed in the developing fat body. Dev. Camb. Engl. *119*, 623–633.

Abzhanov, A., Protas, M., Grant, B.R., Grant, P.R., and Tabin, C.J. (2004). Bmp4 and morphological variation of beaks in Darwin's finches. Science *305*, 1462–1465.

Amaya, E., Musci, T.J., and Kirschner, M.W. (1991). Expression of a dominant negative mutant of the FGF receptor disrupts mesoderm formation in Xenopus embryos. Cell *66*, 257–270.

Andersen, D.S., Colombani, J., Palmerini, V., Chakrabandhu, K., Boone, E., Röthlisberger, M., Toggweiler, J., Basler, K., Mapelli, M., Hueber, A.-O., et al. (2015). The Drosophila TNF receptor Grindelwald couples loss of cell polarity and neoplastic growth. Nature *522*, 482–486.

Biehs, B., Francois, V., and Bier, E. (1996). The Drosophila short gastrulation gene prevents Dpp from autoactivating and suppressing neurogenesis in the neuroectoderm. Genes Dev. *10*, 2922–2934.

Bier, E., and De Robertis, E.M. (2015). EMBRYO DEVELOPMENT. BMP gradients: A paradigm for morphogen-mediated developmental patterning. Science *348*, aaa5838.

Bullock, S.L., Stauber, M., Prell, A., Hughes, J.R., Ish-Horowicz, D., and Schmidt-Ott, U. (2004). Differential cytoplasmic mRNA localisation adjusts pair-rule transcription factor activity to cytoarchitecture in dipteran evolution. Dev. Camb. Engl. *131*, 4251–4261.

Burke, R., and Basler, K. (1996). Dpp receptors are autonomously required for cell proliferation in the entire developing Drosophila wing. Dev. Camb. Engl. *122*, 2261–2269.

Callahan, S.M., and Buikema, W.J. (2001). The role of HetN in maintenance of the heterocyst pattern in Anabaena sp. PCC 7120. Mol. Microbiol. *40*, 941–950.

Campbell, G., and Tomlinson, A. (1999). Transducing the Dpp morphogen gradient in the wing of Drosophila: regulation of Dpp targets by brinker. Cell *96*, 553–562.

Campos-Ortega, J., and Hartenstein, V. (1997). The embryonic development of Drosophila melanogaster (Berlin ;New York: Springer).

Caroti, F., Urbansky, S., Wosch, M., and Lemke, S. (2015). Germ line transformation and in vivo labeling of nuclei in Diptera: report on Megaselia abdita (Phoridae) and Chironomus riparius (Chironomidae). Dev. Genes Evol. *225*, 179–186.

Casanueva, M.O., and Ferguson, E.L. (2004). Germline stem cell number in the Drosophila ovary is regulated by redundant mechanisms that control Dpp signaling. Dev. Camb. Engl. *131*, 1881–1890.

Chen, Y., and Schier, A.F. (2002). Lefty proteins are long-range inhibitors of squint-mediated nodal signaling. Curr. Biol. CB *12*, 2124–2128.

Conley, C.A., Silburn, R., Singer, M.A., Ralston, A., Rohwer-Nutter, D., Olson, D.J., Gelbart, W., and Blair, S.S. (2000). Crossveinless 2 contains cysteine-rich domains and is required for high levels of BMP-like activity during the formation of the cross veins in Drosophila. Dev. Camb. Engl. *127*, 3947–3959.

Criscuolo, A. (2011). morePhyML: improving the phylogenetic tree space exploration with PhyML 3. Mol. Phylogenet. Evol. *61*, 944–948.

Darriba, D., Taboada, G.L., Doallo, R., and Posada, D. (2011). ProtTest 3: fast selection of best-fit models of protein evolution. Bioinforma. Oxf. Engl. *27*, 1164–1165.

Decotto, E., and Ferguson, E.L. (2001). A positive role for Short gastrulation in modulating BMP signaling during dorsoventral patterning in the Drosophila embryo. Dev. Camb. Engl. *128*, 3831–3841.

Dorfman, R., and Shilo, B.Z. (2001). Biphasic activation of the BMP pathway patterns the Drosophila embryonic dorsal region. Dev. Camb. Engl. *128*, 965–972.

Doyle, H.J., Kraut, R., and Levine, M. (1989). Spatial regulation of zerknüllt: a dorsal-ventral patterning gene in Drosophila. Genes Dev. *3*, 1518–1533.

Economou, A.D., Ohazama, A., Porntaveetus, T., Sharpe, P.T., Kondo, S., Basson, M.A., Gritli-Linde, A., Cobourne, M.T., and Green, J.B.A. (2012). Periodic stripe formation by a Turing mechanism operating at growth zones in the mammalian palate. Nat. Genet. *44*, 348–351.

Edgar, R.C. (2004). MUSCLE: multiple sequence alignment with high accuracy and high throughput. Nucleic Acids Res. *32*, 1792–1797.

Ferguson, E.L., and Anderson, K.V. (1992). Decapentaplegic acts as a morphogen to organize dorsal-ventral pattern in the Drosophila embryo. Cell *71*, 451–461.

Flores-Benitez, D., and Knust, E. (2015). Crumbs is an essential regulator of cytoskeletal dynamics and cell-cell adhesion during dorsal closure in Drosophila. eLife *4*.

Frank, L.H., and Rushlow, C. (1996). A group of genes required for maintenance of the amnioserosa tissue in Drosophila. Dev. Camb. Engl. *122*, 1343–1352.

Gavin-Smyth, J., Wang, Y.-C., Butler, I., and Ferguson, E.L. (2013). A genetic network conferring canalization to a bistable patterning system in Drosophila. Curr. Biol. CB *23*, 2296–2302.

Gierer, A., and Meinhardt, H. (1972). A theory of biological pattern formation. Kybernetik *12*, 30–39.

Goltsev, Y., and Papatsenko, D. (2009). Time warping of evolutionary distant temporal gene expression data based on noise suppression. BMC Bioinformatics *10*, 353.

Goltsev, Y., Fuse, N., Frasch, M., Zinzen, R.P., Lanzaro, G., and Levine, M. (2007). Evolution of the dorsal-ventral patterning network in the mosquito, Anopheles gambiae. Dev. Camb. Engl. *134*, 2415–2424.

Gorman, M.J., Kankanala, P., and Kanost, M.R. (2004). Bacterial challenge stimulates innate immune responses in extra-embryonic tissues of tobacco hornworm eggs. Insect Mol. Biol. *13*, 19–24.

Hamada, H., Watanabe, M., Lau, H.E., Nishida, T., Hasegawa, T., Parichy, D.M., and Kondo, S. (2014). Involvement of Delta/Notch signaling in zebrafish adult pigment stripe patterning. Dev. Camb. Engl. *141*, 318–324.

Harris, M.P., Williamson, S., Fallon, J.F., Meinhardt, H., and Prum, R.O. (2005). Molecular evidence for an activator-inhibitor mechanism in development of embryonic feather branching. Proc. Natl. Acad. Sci. U. S. A. *102*, 11734–11739.

Hilbrant, M., Horn, T., Koelzer, S., and Panfilio, K.A. (2016). The beetle amnion and serosa functionally interact as apposed epithelia. eLife *5*.

Horn, T., and Panfilio, K.A. (2016). Novel functions for Dorsocross in epithelial morphogenesis in the beetle Tribolium castaneum. Dev. Camb. Engl. *143*, 3002–3011.

Huang, X., Dong, Y., and Zhao, J. (2004). HetR homodimer is a DNA-binding protein required for heterocyst differentiation, and the DNA-binding activity is inhibited by PatS. Proc. Natl. Acad. Sci. U. S. A. *101*, 4848–4853.

Igaki, T., and Miura, M. (2014). The Drosophila TNF ortholog Eiger: emerging physiological roles and evolution of the TNF system. Semin. Immunol. *26*, 267–274.

Igaki, T., Kanda, H., Yamamoto-Goto, Y., Kanuka, H., Kuranaga, E., Aigaki, T., and Miura, M. (2002). Eiger, a TNF superfamily ligand that triggers the Drosophila JNK pathway. EMBO J. *21*, 3009–3018.

Inaba, M., Yamanaka, H., and Kondo, S. (2012). Pigment pattern formation by contact-dependent depolarization. Science *335*, 677.

Jacobs, C.G.C., and van der Zee, M. (2013). Immune competence in insect eggs depends on the extraembryonic serosa. Dev. Comp. Immunol. *41*, 263–269.

Jacobs, C.G.C., Rezende, G.L., Lamers, G.E.M., and van der Zee, M. (2013). The extraembryonic serosa protects the insect egg against desiccation. Proc. Biol. Sci. *280*, 20131082.

Jacobs, C.G.C., Spaink, H.P., and van der Zee, M. (2014). The extraembryonic serosa is a frontier epithelium providing the insect egg with a full-range innate immune response. eLife *3*.

Jacobs, C.G.C., Braak, N., Lamers, G.E.M., and van der Zee, M. (2015). Elucidation of the serosal cuticle machinery in the beetle Tribolium by RNA sequencing and functional analysis of Knickkopf1, Retroactive and Laccase2. Insect Biochem. Mol. Biol. *60*, 7–12.

Jazwinska, A., Rushlow, C., and Roth, S. (1999). The role of brinker in mediating the graded response to Dpp in early Drosophila embryos. Dev. Camb. Engl. *126*, 3323–3334.

Jiménez-Guri, E., Huerta-Cepas, J., Cozzuto, L., Wotton, K.R., Kang, H., Himmelbauer, H., Roma, G., Gabaldón, T., and Jaeger, J. (2013). Comparative transcriptomics of early dipteran development. BMC Genomics *14*, 123.

Jiménez-Guri, E., Wotton, K.R., Gavilán, B., and Jaeger, J. (2014). A staging scheme for the development of the moth midge Clogmia albipunctata. PloS One *9*, e84422.

Kanda, H., Igaki, T., Kanuka, H., Yagi, T., and Miura, M. (2002). Wengen, a member of the Drosophila tumor necrosis factor receptor superfamily, is required for Eiger signaling. J. Biol. Chem. *277*, 28372–28375.

Kawase, E., Wong, M.D., Ding, B.C., and Xie, T. (2004). Gbb/Bmp signaling is essential for maintaining germline stem cells and for repressing bam transcription in the Drosophila testis. Dev. Camb. Engl. *131*, 1365–1375.

Klomp, J., Athy, D., Kwan, C.W., Bloch, N.I., Sandmann, T., Lemke, S., and Schmidt-Ott, U. (2015). Embryo development. A cysteine-clamp gene drives embryo polarity in the midge Chironomus. Science *348*, 1040–1042.

Kondo, S., and Miura, T. (2010). Reaction-diffusion model as a framework for understanding biological pattern formation. Science *329*, 1616–1620.

Kosman, D., Mizutani, C.M., Lemons, D., Cox, W.G., McGinnis, W., and Bier, E. (2004). Multiplex detection of RNA expression in Drosophila embryos. Science *305*, 846.

Lamka, M.L., and Lipshitz, H.D. (1999). Role of the amnioserosa in germ band retraction of the Drosophila melanogaster embryo. Dev. Biol. *214*, 102–112.

Lecuit, T., Brook, W.J., Ng, M., Calleja, M., Sun, H., and Cohen, S.M. (1996). Two distinct mechanisms for long-range patterning by Decapentaplegic in the Drosophila wing. Nature *381*, 387–393.

Li, H., Qi, Y., and Jasper, H. (2013). Dpp signaling determines regional stem cell identity in the regenerating adult Drosophila gastrointestinal tract. Cell Rep. *4*, 10–18.

Liang, H.-L., Nien, C.-Y., Liu, H.-Y., Metzstein, M.M., Kirov, N., and Rushlow, C. (2008). The zinc-finger protein Zelda is a key activator of the early zygotic genome in Drosophila. Nature *456*, 400–403.

Marcon, L., Diego, X., Sharpe, J., and Müller, P. (2016). High-throughput mathematical analysis identifies Turing networks for patterning with equally diffusing signals. eLife *5*.

Marques, G., Musacchio, M., Shimell, M.J., Wunnenberg-Stapleton, K., Cho, K.W., and O'Connor, M.B. (1997). Production of a DPP activity gradient in the early Drosophila embryo through the opposing actions of the SOG and TLD proteins. Cell *91*, 417–426.

Michon, F., Forest, L., Collomb, E., Demongeot, J., and Dhouailly, D. (2008). BMP2 and BMP7 play antagonistic roles in feather induction. Dev. Camb. Engl. *135*, 2797–2805.

Minami, M., Kinoshita, N., Kamoshida, Y., Tanimoto, H., and Tabata, T. (1999). brinker is a target of Dpp in Drosophila that negatively regulates Dpp-dependent genes. Nature *398*, 242–246.

Monteiro, A. (2015). Origin, development, and evolution of butterfly eyespots. Annu. Rev. Entomol. *60*, 253–271.

Mou, C., Jackson, B., Schneider, P., Overbeek, P.A., and Headon, D.J. (2006). Generation of the primary hair follicle pattern. Proc. Natl. Acad. Sci. U. S. A. *103*, 9075–9080.

Müller, P., Rogers, K.W., Jordan, B.M., Lee, J.S., Robson, D., Ramanathan, S., and Schier, A.F. (2012). Differential diffusivity of Nodal and Lefty underlies a reaction-diffusion patterning system. Science *336*, 721–724.

Nakamasu, A., Takahashi, G., Kanbe, A., and Kondo, S. (2009). Interactions between zebrafish pigment cells responsible for the generation of Turing patterns. Proc. Natl. Acad. Sci. U. S. A. *106*, 8429–8434.

Nakamura, T., Mine, N., Nakaguchi, E., Mochizuki, A., Yamamoto, M., Yashiro, K., Meno, C., and Hamada, H. (2006). Generation of robust left-right asymmetry in the mouse embryo requires a self-enhancement and lateral-inhibition system. Dev. Cell *11*, 495–504.

Nellen, D., Burke, R., Struhl, G., and Basler, K. (1996). Direct and long-range action of a DPP morphogen gradient. Cell *85*, 357–368.

Newman, S.A., and Frisch, H.L. (1979). Dynamics of skeletal pattern formation in developing chick limb. Science *205*, 662–668.

Niepielko, M.G., Hernáiz-Hernández, Y., and Yakoby, N. (2011). BMP signaling dynamics in the follicle cells of multiple Drosophila species. Dev. Biol. *354*, 151–159.

Niepielko, M.G., Ip, K., Kanodia, J.S., Lun, D.S., and Yakoby, N. (2012). Evolution of BMP signaling in Drosophila oogenesis: a receptor-based mechanism. Biophys. J. *102*, 1722–1730.

Nunes da Fonseca, R., von Levetzow, C., Kalscheuer, P., Basal, A., van der Zee, M., and Roth, S. (2008). Self-regulatory circuits in dorsoventral axis formation of the short-germ beetle Tribolium castaneum. Dev. Cell *14*, 605–615.

Painter, K.J., Hunt, G.S., Wells, K.L., Johansson, J.A., and Headon, D.J. (2012). Towards an integrated experimental-theoretical approach for assessing the mechanistic basis of hair and feather morphogenesis. Interface Focus *2*, 433–450.

Panfilio, K.A. (2008). Extraembryonic development in insects and the acrobatics of blastokinesis. Dev. Biol. *313*, 471–491.

Panfilio, K.A. (2009). Late extraembryonic morphogenesis and its zen(RNAi)-induced failure in the milkweed bug Oncopeltus fasciatus. Dev. Biol. *333*, 297–311.

Papatsenko, D., Levine, M., and Goltsev, Y. (2011). Clusters of temporal discordances reveal distinct embryonic patterning mechanisms in Drosophila and anopheles. PLoS Biol. *9*, e1000584.

Pennetier, D., Oyallon, J., Morin-Poulard, I., Dejean, S., Vincent, A., and Crozatier, M. (2012). Size control of the Drosophila hematopoietic niche by bone morphogenetic protein signaling reveals parallels with mammals. Proc. Natl. Acad. Sci. U. S. A. *109*, 3389–3394.

Rafiqi, A.M., Lemke, S., Ferguson, S., Stauber, M., and Schmidt-Ott, U. (2008). Evolutionary origin of the amnioserosa in cyclorrhaphan flies correlates with spatial and temporal expression changes of zen. Proc. Natl. Acad. Sci. U. S. A. *105*, 234–239.

Rafiqi, A.M., Lemke, S., and Schmidt-Ott, U. (2010). Postgastrular zen expression is required to develop distinct amniotic and serosal epithelia in the scuttle fly Megaselia. Dev. Biol. *341*, 282–290.

Rafiqi, A.M., Lemke, S., and Schmidt-Ott, U. (2011). The Scuttle Fly Megaselia abdita (Phoridae): A Link between Drosophila and Mosquito Development. Cold Spring Harb. Protoc. *2011*, pdb.emo143 pdb.emo143.

Rafiqi, A.M., Park, C.-H., Kwan, C.W., Lemke, S., and Schmidt-Ott, U. (2012). BMP-dependent serosa and amnion specification in the scuttle fly Megaselia abdita. Dev. Camb. Engl. *139*, 3373–3382.

Raspopovic, J., Marcon, L., Russo, L., and Sharpe, J. (2014). Modeling digits. Digit patterning is controlled by a Bmp-Sox9-Wnt Turing network modulated by morphogen gradients. Science *345*, 566–570.

Rehorn, K.P., Thelen, H., Michelson, A.M., and Reuter, R. (1996). A molecular aspect of hematopoiesis and endoderm development common to vertebrates and Drosophila. Dev. Camb. Engl. *122*, 4023–4031.

Reim, I., Lee, H.H., and Frasch, M. (2003). The T-box-encoding Dorsocross genes function in amnioserosa development and the patterning of the dorsolateral germ band downstream of Dpp. Dev. Camb. Engl. *130*, 3187–3204.

Rezende, G.L., Martins, A.J., Gentile, C., Farnesi, L.C., Pelajo-Machado, M., Peixoto, A.A., and Valle, D. (2008). Embryonic desiccation resistance in Aedes aegypti: presumptive role of the chitinized serosal cuticle. BMC Dev. Biol. *8*, 82.

Risser, D.D., and Callahan, S.M. (2009). Genetic and cytological evidence that heterocyst patterning is regulated by inhibitor gradients that promote activator decay. Proc. Natl. Acad. Sci. U. S. A. *106*, 19884–19888.

Ross, J.J., Shimmi, O., Vilmos, P., Petryk, A., Kim, H., Gaudenz, K., Hermanson, S., Ekker, S.C., O'Connor, M.B., and Marsh, J.L. (2001). Twisted gastrulation is a conserved extracellular BMP antagonist. Nature *410*, 479–483.

Rushlow, C., and Levine, M. (1990). Role of the zerknüllt gene in dorsal-ventral pattern formation in Drosophila. Adv. Genet. *27*, 277–307.

Rushlow, C., Frasch, M., Doyle, H., and Levine, M. (1987a). Maternal regulation of zerknullt: a homoeobox gene controlling differentiation of dorsal tissues in Drosophila. Nature *330*, 583–586.

Rushlow, C., Doyle, H., Hoey, T., and Levine, M. (1987b). Molecular characterization of the zerknullt region of the Antennapedia gene complex in Drosophila. Genes Dev. *1*, 1268–1279.

Rushlow, C., Colosimo, P.F., Lin, M.C., Xu, M., and Kirov, N. (2001). Transcriptional regulation of the Drosophila gene zen by competing Smad and Brinker inputs. Genes Dev. *15*, 340–351.

Sam, S., Leise, W., and Hoshizaki, D.K. (1996). The serpent gene is necessary for progression through the early stages of fat-body development. Mech. Dev. *60*, 197–205.

Sawala, A., Scarcia, M., Sutcliffe, C., Wilcockson, S.G., and Ashe, H.L. (2015). Peak BMP Responses in the Drosophila Embryo Are Dependent on the Activation of Integrin Signaling. Cell Rep. *12*, 1584–1593.

Schier, A.F. (2009). Nodal morphogens. Cold Spring Harb. Perspect. Biol. *1*, a003459.

Schmidt-Ott, U., and Kwan, C.W. (2016). Morphogenetic functions of extraembryonic membranes in insects. Curr. Opin. Insect Sci. *13*, 86–92.

Schneider, C.A., Rasband, W.S., and Eliceiri, K.W. (2012). NIH Image to ImageJ: 25 years of image analysis. Nat. Methods *9*, 671–675.

Scuderi, A., and Letsou, A. (2005). Amnioserosa is required for dorsal closure in Drosophila. Dev. Dyn. Off. Publ. Am. Assoc. Anat. *232*, 791–800.

Serpe, M., Umulis, D., Ralston, A., Chen, J., Olson, D.J., Avanesov, A., Othmer, H., O'Connor, M.B., and Blair, S.S. (2008). The BMP-binding protein Crossveinless 2 is a short-range, concentration-dependent, biphasic modulator of BMP signaling in Drosophila. Dev. Cell *14*, 940–953.

Sharma, R., Beermann, A., and Schröder, R. (2013). The dynamic expression of extraembryonic marker genes in the beetle Tribolium castaneum reveals the complexity of serosa and amnion formation in a short germ insect. Gene Expr. Patterns GEP *13*, 362–371.

Shen, W., Chen, X., Cormier, O., Cheng, D.C.-P., Reed, B., and Harden, N. (2013). Modulation of morphogenesis by Egfr during dorsal closure in Drosophila. PloS One *8*, e60180.

Sheth, R., Marcon, L., Bastida, M.F., Junco, M., Quintana, L., Dahn, R., Kmita, M., Sharpe, J., and Ros, M.A. (2012). Hox genes regulate digit patterning by controlling the wavelength of a Turing-type mechanism. Science *338*, 1476–1480.

Shimell, M.J., Ferguson, E.L., Childs, S.R., and O'Connor, M.B. (1991). The Drosophila dorsal-ventral patterning gene tolloid is related to human bone morphogenetic protein 1. Cell *67*, 469–481.

Shiratori, H., and Hamada, H. (2006). The left-right axis in the mouse: from origin to morphology. Dev. Camb. Engl. *133*, 2095–2104.

Sick, S., Reinker, S., Timmer, J., and Schlake, T. (2006). WNT and DKK determine hair follicle spacing through a reaction-diffusion mechanism. Science *314*, 1447–1450.

Spahn, P., Huelsmann, S., Rehorn, K.-P., Mischke, S., Mayer, M., Casali, A., and Reuter, R. (2014). Multiple regulatory safeguards confine the expression of the GATA factor Serpent to the hemocyte primordium within the Drosophila mesoderm. Dev. Biol. *386*, 272–279.

Srinivasan, S., Rashka, K.E., and Bier, E. (2002). Creation of a Sog morphogen gradient in the Drosophila embryo. Dev. Cell *2*, 91–101.

Stauber, M., Jäckle, H., and Schmidt-Ott, U. (1999). The anterior determinant bicoid of Drosophila is a derived Hox class 3 gene. Proc. Natl. Acad. Sci. U. S. A. *96*, 3786–3789.

Stauber, M., Lemke, S., and Schmidt-Ott, U. (2008). Expression and regulation of caudal in the lower cyclorrhaphan fly Megaselia. Dev. Genes Evol. *218*, 81–87.

Tautz, D., and Pfeifle, C. (1989). A non-radioactive in situ hybridization method for the localization of specific RNAs in Drosophila embryos reveals translational control of the segmentation gene hunchback. Chromosoma *98*, 81–85.

Turing, A.M. (1952). The Chemical Basis of Morphogenesis. Philos. Trans. R. Soc. Lond. B Biol. Sci. *237*, 37–72.

Umulis, D.M., and Othmer, H.G. (2012). The importance of geometry in mathematical models of developing systems. Curr. Opin. Genet. Dev. *22*, 547–552.

Umulis, D.M., Shimmi, O., O'Connor, M.B., and Othmer, H.G. (2010). Organism-scale modeling of early Drosophila patterning via bone morphogenetic proteins. Dev. Cell *18*, 260–274.

Vargas, H.C.M., Farnesi, L.C., Martins, A.J., Valle, D., and Rezende, G.L. (2014). Serosal cuticle formation and distinct degrees of desiccation resistance in embryos of the mosquito vectors Aedes aegypti, Anopheles aquasalis and Culex quinquefasciatus. J. Insect Physiol. *62*, 54–60.

Wang, Y.C., and Ferguson, E.L. (2005). Spatial bistability of Dpp-receptor interactions during Drosophila dorsal-ventral patterning. Nature *434*, 229–234.

Wiegmann, B.M., Trautwein, M.D., Winkler, I.S., Barr, N.B., Kim, J.-W., Lambkin, C., Bertone, M.A., Cassel, B.K., Bayless, K.M., Heimberg, A.M., et al. (2011). Episodic radiations in the fly tree of life. Proc. Natl. Acad. Sci. U. S. A. *108*, 5690–5695.

Wolpert, L. (1968). The French Flag Problem: A contribution to the discussion on pattern development and regulation. In Towards a Theoretical Biology. An IUBS Symposium, C.H. Waddington, ed. (Edinburgh University Press), pp. 125–133.

Wolpert, L. (1969). Positional information and the spatial pattern of cellular differentiation. J. Theor. Biol. *25*, 1–47.

Wolpert, L. (1971). Positional information and pattern formation. Curr. Top. Dev. Biol. *6*, 183–224.

Wotton, K.R., Jiménez-Guri, E., García Matheu, B., and Jaeger, J. (2014). A staging scheme for the development of the scuttle fly Megaselia abdita. PloS One *9*, e84421.

Xie, T., and Spradling, A.C. (1998). decapentaplegic is essential for the maintenance and division of germline stem cells in the Drosophila ovary. Cell *94*, 251–260.

Xie, T., and Spradling, A.C. (2000). A niche maintaining germ line stem cells in the Drosophila ovary. Science *290*, 328–330.

Xu, M., Kirov, N., and Rushlow, C. (2005). Peak levels of BMP in the Drosophila embryo control target genes by a feed-forward mechanism. Dev. Camb. Engl. *132*, 1637–1647.

Yamanaka, H., and Kondo, S. (2014). In vitro analysis suggests that difference in cell movement during direct interaction can generate various pigment patterns in vivo. Proc. Natl. Acad. Sci. U. S. A. *111*, 1867–1872.

Yip, M.L., Lamka, M.L., and Lipshitz, H.D. (1997). Control of germ-band retraction in Drosophila by the zinc-finger protein HINDSIGHT. Dev. Camb. Engl. *124*, 2129–2141.

Yoon, H.S., and Golden, J.W. (1998). Heterocyst pattern formation controlled by a diffusible peptide. Science *282*, 935–938.

Zecca, M., Basler, K., and Struhl, G. (1995). Sequential organizing activities of engrailed, hedgehog and decapentaplegic in the Drosophila wing. Dev. Camb. Engl. *121*, 2265–2278.

van der Zee, M., Berns, N., and Roth, S. (2005). Distinct functions of the Tribolium zerknullt genes in serosa specification and dorsal closure. Curr. Biol. CB *15*, 624–636.

van der Zee, M., Stockhammer, O., von Levetzow, C., Nunes da Fonseca, R., and Roth, S. (2006). Sog/Chordin is required for ventral-to-dorsal Dpp/BMP transport and head formation in a short germ insect. Proc. Natl. Acad. Sci. U. S. A. *103*, 16307–16312.

Zhang, Y., Tomann, P., Andl, T., Gallant, N.M., Huelsken, J., Jerchow, B., Birchmeier, W., Paus, R., Piccolo, S., Mikkola, M.L., et al. (2009). Reciprocal requirements for EDA/EDAR/NF-kappaB and Wnt/beta-catenin signaling pathways in hair follicle induction. Dev. Cell *17*, 49–61.

Zúñiga, A., Hödar, C., Hanna, P., Ibáñez, F., Moreno, P., Pulgar, R., Pastenes, L., González, M., and Cambiazo, V. (2009). Genes encoding novel secreted and transmembrane proteins are temporally and spatially regulated during Drosophila melanogaster embryogenesis. BMC Biol. *7*, 61.